

Journal of Organometallic Chemistry, 404 (1991) 213-324
 Elsevier Sequoia S.A., Lausanne
 JOM 20577AS

Annual Survey of Ruthenium and Osmium for the Year 1988*

Michael G. Richmond

Center for Organometallic Research and Education,
 Department of Chemistry, University of North Texas,
 Denton, TX 76203

I. Dissertations	214
II. Mononuclear Complexes	216
(a) Organometallic Porphyrins	216
(b) Halides	219
(c) Hydrides	219
(d) Phosphines	222
(e) Carbonyls	227
(f) Sulfur and Oxygen Ligands	229
(g) Nitrogen Ligands	234
(h) Alkenyl and Alkylidene Complexes	259
(i) π -Complexes	261
III. Binuclear Complexes	265
(a) Homonuclear Complexes	265
(b) Heteronuclear Complexes	271
IV. Polynuclear Complexes	271
(a) Trinuclear Clusters	271
1. Simple and Hydrocarbon Ligands	271
2. Phosphine Ligands	279
3. Nitrogen Ligands	285
4. Sulfur Ligands	287
(b) Tetranuclear Clusters	288
(c) Pentanuclear Cluster	291
(d) Hexanuclear Clusters	292
(e) Higher Nuclearity Clusters	293
(f) Mixed-Metal Clusters	294
1. Clusters Containing Main Group Atoms	294
2. Clusters Containing Other Metals	295
V. Miscellaneous Chemistry	302
(a) Heterogeneous and Supported Complexes	302
(b) CO and CO ₂ Reduction	305
(c) Oxidation Reactions	306
(d) Carbon-Carbon Bond Forming Reactions	309
(e) Hydrogen Production	309
VI. Acknowledgment	310
VII. References	310

*No reprints available.

References p. 310

I. Dissertations

Eleven dissertations dealing with nitrogen-substituted ruthenium and osmium complexes have been published. Ruthenium(II) mononuclear and polynuclear complexes based on 2,2'-bipyrimidine and 2,3-bis(2'-pyridyl)pyrazine have been prepared and examined in connection with water splitting chemistry.¹ The reaction of potassium osmate with 2,4-bis-hydroxymethylpropamido-2,4-dimethyl-3-pentanone (H_4 -HMPA-DMP) gives the osmium oxo complex $Os(VI)(\eta^4\text{-HMPA-DMP})(O)$.² Structural characterization and electrochemical studies involving the $Os(VI)/(IV)$ redox couple are reported. The synthesis of the new ruthenium oxo complexes $cis\text{-}[(bpy)_2(AsR_3)Ru(IV)(O)](ClO_4)_2$ has been described.³ The use of these oxo complexes in kinetic and mechanistic oxidation studies of alcohols, olefins, sulfides, sulfoxides, and free phosphines is reported. The processes controlling excited state decay in several ruthenium(II) and osmium(II) polypyridyl complexes have been examined,⁴ along with the synthesis, electrochemistry, and photophysics of various tris(substituted-bipyridyl) $Ru(II)$ complexes being described.⁵ The photochemistry and photophysics of mononuclear and covalently linked polynuclear ruthenium(II) bipyridyl complexes have also been examined.⁶ Cis and trans osmium complexes of the form $[(bpy)_2Os(CO)R]^+$ (where $R = H, Me, Et, Ph, benzyl, \text{ or } Cl$) have been prepared and their photochemistry and photophysical properties reported.⁷ The synthesis and characterization of sundry ruthenium "picnic-basket" porphyrins have been reported.⁸ These complexes exhibit reversible dinitrogen and dioxygen binding; the latter complex being characterized by NMR and IR spectroscopy. Results dealing with $[Ru(NH_3)_5H_2O]^{+2}$ modified metalloproteins and the kinetics of electron transfer associated with these ruthenium modified systems have been presented.⁹ Two reports have appeared that describe the reactivity

of unsaturated ligands¹⁰ and carbon hydrogen bond activation in aromatic nitrogen heterocycles¹¹ with pentaammineosmium(II).

Polynuclear ruthenium and osmium complexes accounted for twelve dissertations in 1988. The photochemistry and phosphine-phosphite substitution chemistry of (fulvalene)diruthenium(tetracarbonyl) has been presented.¹² Ethylene extrusion from (μ -ethanediyl)octacarbonyldiosmium and preparation and reactivity of the osmacyclobutane complex $(\text{CH}_2\text{CH}_2\text{CH}_2)\text{Os}(\text{CO})_4$ have been reported.¹³ The reactivity of the triruthenium ketylidene cluster $[\text{PPN}]_2[\text{Ru}_3(\text{CO})_6(\mu_2\text{-CO})_3(\mu_3\text{-CCO})]^{14}$ and the reactions of $\text{Os}_4(\text{CO})_{12}(\mu_3\text{-S})$ with CO, Me_2NH , acetylene, and H_2 have been reported.¹⁵ The catalytic hydrogenation of olefins using the isocyanato clusters $[\text{Ru}_3(\text{NCO})(\text{CO})_{10}]^{-1}$ and $[\text{Os}_3(\text{NCO})(\text{CO})_{11}]^{-1}$ was reported¹⁶ with ligand transformations and catalytic transalkylation of tertiary amines using osmium carbonyl clusters providing a second example of cluster-mediated substrate activation.¹⁷ The substitutional reactivity of the trimetallic clusters $\text{Ru}_3(\text{CO})_{12}$ and $\text{Os}_3(\text{CO})_{12}$ is contrasted with the corresponding mononuclear analogues and substitution reactions with the mixed-metal clusters $\text{Fe}_2\text{Ru}(\text{CO})_{12}$, $\text{FeRu}_2(\text{CO})_{12}$, $\text{Fe}_2\text{Os}(\text{CO})_{12}$ have been published.¹⁸ A detailed study concerning the kinetics of ^{13}C exchange, effects of ion pairing in $[\text{HRu}_3(\text{CO})_{11}]^{-1}$ and $[\text{HOs}_3(\text{CO})_{11}]^{-1}$ and their role in the water-gas shift reaction has appeared.¹⁹ Sequential reductive elimination of three C-H bonds from $(\mu\text{-H})_3\text{Ru}_3(\text{CO})_9(\mu_3\text{-CX})$ has been reported to give CH_3X .²⁰ Homogeneous and oxide-supported polynuclear ruthenium and osmium complexes were the subject of solid-state ^{13}C NMR analysis²¹ and an investigation using a specially designed NMR probe capable of analyzing compounds from -40 to 100 °C and pressures up to 4000 psi has appeared.²² The use of Diffuse Reflectance FTIR spectroscopy (DRIFTS) to

investigate surface-supported ruthenium carbonyl clusters active in CO₂ methanation has been described.²³

Other dissertations abstracted include the investigation of [1.1]ferro-ruthenocenophane,²⁴ structure analysis of Os(ethylene)₂(C₆Me₆),²⁵ and the geometric isomerization and 1-hexene hydrogenation exhibited by complexes based on RuCl₂(CO)₂P₂.²⁶ Finally, ruthenium complexes possessing π -bound thiophene and benzo[b]thiophenes have been reported along with their reactions with hydride, methoxide, in homogeneous solution and deuterium exchange in heterogeneous reaction studies.²⁷

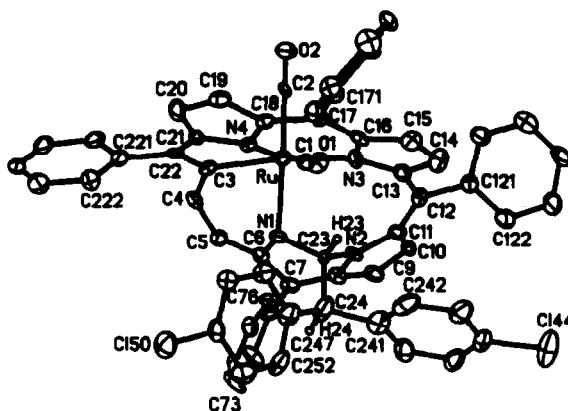
II. Mononuclear Complexes

(a) Organometallic Porphyrins

The synthesis and characterization of a new sterically protected ruthenium porphyrin has been reported. The tetraaryl porphyrins are synthesized in moderate to good yields from the high-dilution coupling of selected $\alpha,\alpha,\alpha,\alpha$ -tetrakis(o-aminophenyl)porphyrin derivatives with isophthaloyl chloride, followed by reaction with Ru₃(CO)₁₂. The resulting ruthenium porphyrins possess a rigid superstructure with a cavity being defined by the appended superstructure. The regiochemistry for CO coordination has been reported along with equilibration studies involving axial coordination of CO and pyridine.²⁸ A subsequent study has reported the reversible binding of dinitrogen and dioxygen to those same ruthenium porphyrin complexes. The ligated N₂ and O₂ complexes have been characterized spectroscopically and a transient pentacoordinate ruthenium is the active species that binds these molecules within the protected cavity. Based on IR measurements, an O-O band at 1103 cm⁻¹ suggests that dioxygen is reduced by one electron and is coordinated as a superoxide ion.²⁹

The reaction of Ru₃(CO)₁₂ with the N,N'-vinyl-bridged porphyrin based on tetraphenylporphyrin, TPP, affords three

products. The major product in boiling DMF is the carbene complex $\text{TPPRu}=\text{C}=\text{C}(\text{p-C}_6\text{H}_4\text{Cl})_2$, with N,N' -bridged $[\text{TPPC}=\text{C}(\text{p-C}_6\text{H}_4\text{Cl})_2]\text{Ru}(\text{CO})_2$ and $[\text{TPPCHCH}(\text{p-C}_6\text{H}_4\text{Cl})_2]\text{Ru}(\text{CO})_2$ being formed in THF. The latter porphyrin requires the presence of the noncoordinating base 1,8-bis(dimethylamino)naphthalene for formation. These latter two porphyrin complexes maintain intact N,N' -carbene bridges and display insertion of the ruthenium into a pyrrole C-N bond. All complexes were characterized spectroscopically in addition to a X-ray structure of $[\text{TPPC}=\text{C}(\text{p-C}_6\text{H}_4\text{Cl})_2]\text{Ru}(\text{CO})_2$ being reported.³⁰



Oxidation of several para-substituted porphyrins based on TPP and octaethylporphyrin (OEP), prepared from $\text{Os}_3(\text{CO})_{12}$ and H_2TTP or H_2OEP , to give dioxoosmium(VI) complexes, $\text{Os}(\text{p-X-TPP})(\text{O})_2$ and $\text{Os}(\text{OEP})(\text{O})_2$ is reported. In each case a stable osmium(IV) intermediate has been observed and spectroscopically characterized. The X-ray crystal structure of $[\text{Os}(\text{p-Me-TPP})(\text{O})_2] \cdot 2\text{THF}$ is also presented.³¹

Several dinitrogen complexes have been synthesized from the tetramesitylporphyrin (TMP) complex $\text{Ru}(\text{TMP})\text{CO}$. Photolysis of this monocarbonyl porphyrin in coordinating solvents such as MeCN, or

THF, gives the corresponding bis-solvates, $\text{Ru}(\text{TMP})\text{L}_2$. The analogous complexes $\text{Ru}(\text{TMP})(\text{DMF})_2$ and $\text{Ru}(\text{TMP})(\text{Et}_2\text{O})_2$ were prepared from $\text{Ru}(\text{TMP})$ in benzene. The former complex could not be synthesized via the photochemical route due to the photocatalyzed decarbonylation of DMF to dimethylamine. Reaction of $\text{Ru}(\text{TMP})\text{L}_2$ with N_2 led to $\text{Ru}(\text{TMP})\text{L}(\text{N}_2)$ and a X-ray structure was obtained for $\text{Ru}(\text{TMP})\text{THF}(\text{N}_2)$. The bis-dinitrogen complex $\text{Ru}(\text{TMP})(\text{N}_2)_2$ is obtained from the highly reactive $\text{Ru}(\text{TMP})$ complex in the solid state upon exposure to N_2 .³²

$[\text{Ru}(\text{OEP})]_2$ reacts with the thioethers undecyl methyl sulfide (DecMeS) and Ph_2S to give low-spin complexes with the formula $\text{Ru}(\text{OEP})\text{L}_2$. Both bis(thioether) complexes have been structurally characterized by X-ray diffraction analysis and display an α -band that is rather hypsochromically shifted, suggesting the presence of only weak π -backbonding. $\text{Ru}(\text{OEP})(\text{DecMeS})_2$ catalyzes the slow autoxidation of DecMeS (excess) to the sulfoxide (mainly) and more rapidly with in situ air generated H_2O_2 .³³

Other papers dealing with porphyrin complexes include a study of the reaction of nitrosobenzene with $\text{Ru}(\text{OEP})(\text{CO})(\text{EtOH})$ to give $\text{Ru}(\text{OEP})(\text{PhNO})_2$ or $\text{Ru}(\text{OEP})(\text{PhNO})\text{L}$ (where $\text{L} = \text{pyridine}, \text{CO}, \text{H}_2\text{O},$ or PPh_3) depending on the reaction conditions,³⁴ a resonance Raman investigation of the backbonding in $\text{Os}(\text{OEP})\text{L}_2$ (where $\text{L} = \text{pyridine}$ or NH_3 ; $\text{L}_2 = \text{CO/pyridine}$) has appeared,³⁵ CO addition to $\text{Ru}(\text{OEP})\text{L}_2$ and $\text{Ru}(\text{TPP})\text{L}_2$ (where $\text{L} = \text{DMF}, \text{MeCN}, \text{aniline},$ or substituted benzonitriles) has been examined and the first-order rate constants for the loss of para and meta $\text{XC}_6\text{H}_5\text{CN}$ from $\text{Ru}(\text{OEP})\text{L}_2$ reported.³⁶ Oxidation of $\text{Ru}(\text{TTP})(\text{CO})$ and $\text{Ru}(\text{OEP})(\text{CO})$ yields the corresponding π -cation radicals that are shown to give well-resolved, hyperfine shifted NMR spectra; the non-Curie law behavior for $\text{Ru}(\text{TTP})(\text{CO})\cdot^+\text{Br}^-$ arises from a thermal equilibrium between the ${}^2\text{A}_{2u}$

= ${}^2A_{1u}$ π -cation radical states.³⁷ The redox properties of $Ru[(O-NH_2)TPP]L_2$ (where L = CO, pyridine, MeCH and THF) along with the electrocatalysis of O_2 has been reported.³⁸ Axial-ligand control on the photophysics associated with $Ru(TPP)L(CO)$ and $Ru(OEP)L(CO)$ (where L = EtOH, piperidine, DMSO, or pyridine) has allowed for a comparison and reactivity evaluation of the metalloporphyrin (π, π^*) and (d, π^*) excited states.³⁹ Finally, the deactivation of the lowest excited triplet state, ${}^3(\pi, \pi^*)$, in $Ru(\text{porphyrin})L(CO)$ complexes is shown to occur, in part, via a metal-to-ring (d, π^*) charge-transfer excited state which lies at higher energy.⁴⁰

(b) Halides

The reaction of osmium sponge with fluorine gas at 300 °C gave OsF_6 which was then isolated by low temperature in inert-gas matrices and subjected to IR spectroscopic analysis.⁴¹ *Trans*- $RuCl_2(DMSO)_4$ and *cis*- $RuBr_2(DMSO)_4$ have been prepared and their structures determined by X-ray diffraction analysis. DMSO dissociation along with the use of these complexes as anticancer agents against Lewis lung carcinomas is presented.⁴² The preparation and X-ray diffraction results for $OsBr_4(AsPh_3)_2$ ⁴³ and $(OsX_6)(PPh_3H)_2$ (where X = Cl or Br)⁴⁴ have appeared.

The dichlorocarbene complex $OsCl_2(=CCl_2)(CO)(PPh_3)_2$ reacts with the nucleophiles HE^- (where E = O, S, Se, or Te) to give the chalcocarbonyl complex $OsCl_2(CO)(CE)(PPh_3)_2$. Substitution of H_2E for HE^- also yields the corresponding chalcocarbonyl complex except when H_2Te is used. X-Ray diffraction analyses are reported for the thio, seleno, and telluro analogues with the establishment of an increasing trans-influence in the order $CO < CS \leq CSe < CTe$.⁴⁵

(c) Hydrides

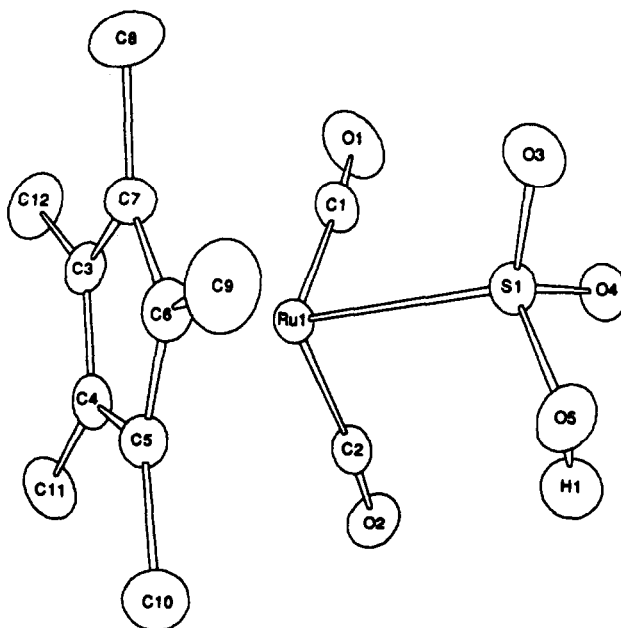
The hydrides $RuH_2(PPh_3)_4$ and $OsH_4(PPh_3)_3$ react with sulphonic

acids RSO_3H (where $\text{R} = \text{CH}_3$ or CF_3) in boiling benzene to yield $[\text{MH}(\eta^6\text{-C}_6\text{H}_6)\text{PPh}_3)_2](\text{O}_3\text{SR})$ as air-stable solids while the latter hydride affords $[\text{OsH}_3(\text{PPh}_3)_4](\text{O}_3\text{SR})$ in EtOH solvent.⁴⁶

Monosubstituted alkynes $\text{R}'\text{C}\equiv\text{CH}$ (where $\text{R} = n\text{-C}_3\text{H}_7$, Me_3C , Ph , or CO_2Me) have been reported to react with the ruthenium hydride complexes $\text{HRu}(\text{CO})\text{Cl}(\text{Me}_2\text{Hpz})(\text{PR}_3)_2$ (where $\text{R} = \text{Ph}$ or *p*-tolyl; $\text{Me}_2\text{Hpz} = 3,5\text{-dimethylpyrazole}$) to give alkenylpyrazole complexes $\text{Ru}(\text{CO})\text{Cl}(\text{CH}=\text{CHR}')(\text{Me}_2\text{Hpz})(\text{PR}_3)_2$ through *cis* alkyne insertion into the Ru-H bond. Double insertion was observed with dimethyl acetylenedicarboxylate to give $\text{Ru}(\text{CO})\text{Cl}[\text{MeO}_2\text{C}=\text{C}(\text{CO}_2\text{Me})\text{C}(\text{CO}_2\text{Me})=\text{CHCO}_2\text{Me}](\text{PR}_3)_2$ while phenyl acetylene afforded unusual metallocycles of the form $\text{Ru}[\overline{\text{NH}=\text{C}(\text{Ph})\text{OC}}-\text{CHPh}](\text{CO})\text{Cl}(\text{PR}_3)_2$. The reaction between methyl propionate and $\text{HRu}(\text{CO})\text{Cl}(\text{Me}_2\text{Hpz})(\text{PPh}_3)_2$ besides yielding the insertion product as the major complex also gives as a minor product the bicarbonate complex $\text{Ru}(\text{CO})(\text{MeO}_2\text{C}=\text{CHCO}_2\text{Me})(\text{HCO}_3)(\text{PPh}_3)_2$. Spectroscopic data and X-ray structures are presented.⁴⁷

The reaction between dimethyl acetylenedicarboxylate and $(\eta^5\text{-C}_5\text{H}_5)\text{Ru}(\text{PPh}_3)_2\text{H}$ has been reinvestigated and it has been shown that the product of initial *cis* alkyne insertion rearranges into the *trans* isomer. Chelation of one of the carbomethoxy ester groups follows upon PPh_3 dissociation. The use of ^1H and ^{13}C NMR chemical shifts are shown to be an unreliable guide for vinyl stereochemistry assignment.⁴⁸

SO_2 insertion into $(\eta^5\text{-C}_5\text{Me}_5)\text{Ru}(\text{CO})_2\text{H}$ has been shown to give $(\eta^5\text{-C}_5\text{Me}_5)\text{Ru}(\text{CO})_2\text{SO}_3\text{H}$. Use of isotopically enriched S^{18}O_2 reveals that the additional oxygen atom is derived from a second S^{18}O_2 molecule via oxygen abstraction from the unstable first insertion product, $(\eta^5\text{-C}_5\text{Me}_5)\text{Ru}(\text{CO})_2\text{S}^{18}\text{O}_2\text{H}$. Infrared spectral data and characterization by X-ray diffraction analysis is included.⁴⁹



The fluorocarbon acid $\text{H}_2\text{C}(\text{SO}_2\text{CF}_3)_2$ has been reacted with several ruthenium and osmium hydride/acetate complexes in order to probe for selective hydrogen or acetic acid elimination upon protonation. $(\text{Ph}_3\text{P})_2\text{Ru}(\text{CO})\text{H}(\text{OAc})$ gives the binuclear complex $[(\text{Ph}_3\text{P})_4\text{Ru}_2(\text{CO})_2(\mu\text{-H})_2(\mu\text{-OAc})][\text{CH}(\text{SO}_2\text{CF}_3)_2]$ while $(\text{Ph}_3\text{P})_3\text{RuH}(\text{OAc})$ in toluene yields the cationic toluene complex $[(\pi\text{-toluene})\text{RuH}(\text{PPh}_3)_2][\text{CH}(\text{SO}_2\text{CF}_3)_2]$ upon treatment with $\text{H}_2\text{C}(\text{SO}_2\text{CF}_3)_2$. The osmium complex $(\text{Ph}_3\text{P})_3\text{OsH}(\text{OAc})$ reacts with $\text{H}_2\text{C}(\text{SO}_2\text{CF}_3)_2$ in toluene giving $[(\text{Ph}_3\text{P})_3\text{Os}(\eta^2\text{-H}_2)(\eta^2\text{-OAc})][\text{CH}(\text{SO}_2\text{CF}_3)_2]\cdot\text{toluene}$. The $\eta^2\text{-H}_2$ ligand was not clearly resolved in the X-ray structure, but a ^1H spin-lattice relaxation study and the value of J_{HD} in the HD analogue ($J = 13.7$ Hz) support the presence of coordinated hydrogen. Upon treatment with acetonitrile, elimination of acetic acid is observed along with formation of mer-trans- $[(\text{Ph}_3\text{P})_3\text{OsH}(\text{MeCN})_2][\text{CH}(\text{SO}_2\text{CF}_3)_2]$.⁵⁰

Five papers have appeared concerning the use of spin-lattice

relaxation times, T_1 , in determining the nature of ancillary bound dihydrogen and/or dihydride ligands in mononuclear ruthenium and osmium complexes. T_1 values for several ruthenium hydride complexes have been measured. The complex $\text{RuH}_4(\text{PPh}_3)_3$ displayed a T_1 value of 0.050 s at ca. 291 K reinforcing the presence of both dihydride (M-H, classical) and coordinated molecular hydrogen [M-(H₂), non-classical].⁵¹ The complex $\text{RuH}_6(\text{PCy}_3)_2$ has been reformulated as *cis, cis, trans*- $\text{Ru}(\text{H}_2)_2(\text{H})_2(\text{PCy}_3)_3$, a complex that contains two ($\eta^2\text{-H}_2$) groups and two terminal Ru-H bonds. The new assignment is supported by a short, temperature-dependent T_1 value for the rapidly exchanging hydrogen ligands. The same complex readily loses three moles of hydrogen to give the first dinuclear complex $\text{Ru}_2(\text{H}_2)(\text{H})_4(\text{PCy}_3)_4$ possessing an $\eta^2\text{-H}_2$ ligand.⁵² *Trans*- $[\text{Os}(\eta^2\text{-H}_2)(\text{H})(\text{Ph}_2\text{PCH}_2\text{CH}_2\text{PET}_2)_2](\text{BF}_4)$ reveals two distinct, high-field proton resonances at low temperature consistent with an octahedral structure where the $\eta^2\text{-H}_2$ ligand is *trans* to the terminal hydride. The isotopomer *trans*- $[\text{Os}(\eta^2\text{-HD})(\text{D})(\text{Ph}_2\text{PCH}_2\text{CH}_2\text{PET}_2)_2](\text{BF}_4)$, prepared by heating the protio complex under D_2 , displays one of the smallest $^1\text{J}(\text{H},\text{D})$ values (19 Hz) reported to date. The T_1 value of the $\eta^2\text{-H}_2$ ligand in this complex indicates that the H-H bond length in the aryl/alkyl phosphine ($\text{Ph}_2\text{PCH}_2\text{CH}_2\text{PET}_2$) is shorter than that calculated from T_1 measurements in the corresponding dialkyl phosphine ($\text{Et}_2\text{PCH}_2\text{CH}_2\text{PET}_2$).^{53,54}

The complexes *trans*- $[\text{Os}(\eta^2\text{-H}_2)(\text{H})(\text{meso-tetraphos})]^+1$ and *trans*- $[\text{Os}(\eta^2\text{-H}_2)(\text{H})(\text{rac-tetraphos})]^+1$ [where tetraphos = $\text{Ph}_2\text{P}(\text{CH}_2\text{CH}_2\text{PPh})_2\text{CH}_2\text{CH}_2\text{PPh}_2$] have been prepared and the T_1 values measured and compared to the above $\text{Ph}_2\text{PCH}_2\text{CH}_2\text{PET}_2$ analogues.⁵⁵

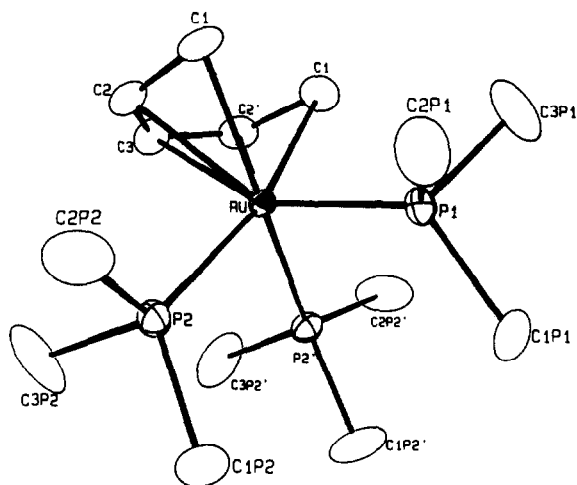
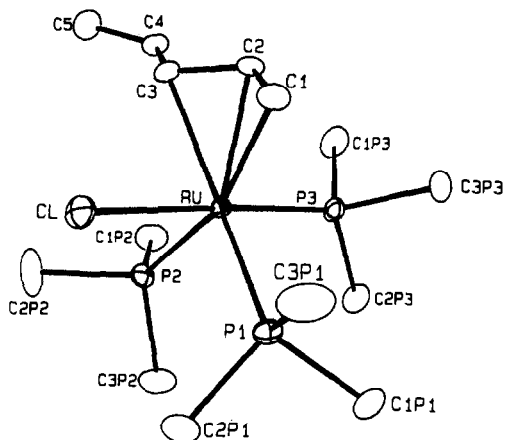
(d) Phosphines

Treatment of $(\eta^5\text{-C}_5\text{H}_5)\text{Ru}(\text{diphos})\text{I}$ with methyl trifluoromethane

sulfonate gives the iodomethane complex $[(\eta^5\text{-C}_5\text{H}_5)\text{Ru}(\text{diphos})\text{IME}](\text{CF}_3\text{SO}_3)$ in high yield. This new complex has been fully characterized by ^1H , ^{13}C , and ^{31}P NMR spectroscopies; the iodomethane ligand does not exchange with free iodomethane in solution based on ^1H NMR measurements. The reactivity of this complex was examined in methylation reactions with the enamine 1-(N-pyrrolidine)cyclohexene and the trimethylsilyl enol ether of cyclohexanone. Both substrates reacted in moderate to high yield to give the corresponding product of C-alkylation as the major product.⁵⁶

The axially dissymmetric phosphines (R)- and (S)-2,2'-bis(diphenylphosphino)-1,1'-binaphthyl [i.e., (R)- or (S)-BINAP] have been reacted with $[\text{RuCl}_2(\text{COD})]_x$ in the presence of added RCO_2Na to yield the ruthenium(II) complexes $\text{Ru}(\text{O}_2\text{CR})_2[(\text{R})\text{- or }(\text{S})\text{-BINAP}]$ (where R = Me or t-Butyl). The X-ray crystal structure of $\text{Ru}[\text{O}_2\text{CC}(\text{CH}_3)_3]_2[(\text{S})\text{-BINAP}]$ indicates that the complex has a Λ structure, while the BINAP-containing seven-membered chelate ring is observed to adopt a δ conformation. Structural comparison with the known $[\text{Rh}\{(\text{R})\text{-BINAP}\}(\text{norbornadiene})](\text{ClO}_4)$ complex and results of efficient asymmetric hydrogenation reactions are presented.⁵⁷

Pentadienyltributyltin reacts with $\text{RuCl}_2(\text{PPh}_3)_3$ to yield $(\eta^5\text{-pentadienyl})\text{RuCl}(\text{PPh}_3)_2$. This complex serves as a precursor to other pentadienyl complexes. Addition of PMe_3 or PMe_2Ph (3 equiv.) to the above complex leads to $(\eta^3\text{-pentadienyl})\text{RuCl}(\text{PR})_3$ with the $\eta^3\text{-pentadienyl}$ ligand adopting a W-shaped syn geometry. Halide abstraction using AgO_3SCF_3 or MeO_3SCH_3 affords the cationic complex $[(\eta^5\text{-pentadienyl})\text{Ru}(\text{PR}_3)_3](\text{O}_3\text{SCF}_3)$. Variable-temperature ^{31}P NMR measurements reveal that the $\eta^5\text{-pentadienyl}$ complexes equilibrate the ancillary phosphines via rotation of the pentadienyl group relative to the metal-ligand framework.⁵⁸

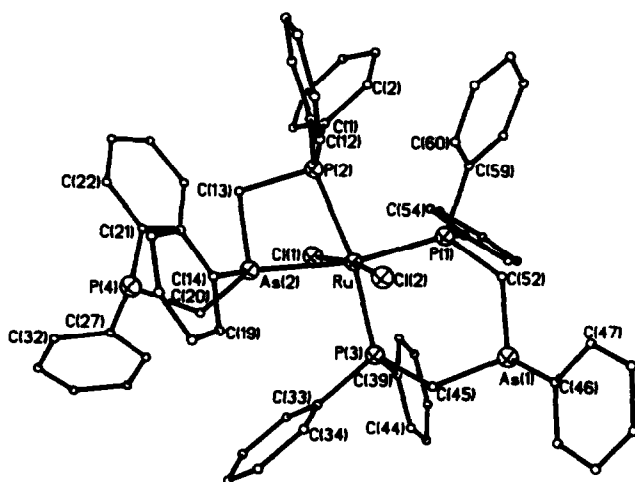


The transition-metal diphosphane complex $(\eta^5\text{-C}_5\text{Me}_5)\text{Ru}(\text{CO})_2\text{P-PR}$ (where $\text{R} = 2,4,6\text{-t-Bu}_3\text{C}_6\text{H}_2$) reacts with the sulfur ylide $(\text{Me})_2\text{S}(\text{O})=\text{CH}_2$ to give the diphosphirane complex $(\eta^5\text{-C}_5\text{Me}_5)\text{Ru}(\text{CO})_2\overline{\text{PCH}_2}\text{PR}$. Use of diphenylsulfonium cyclopropanide yields the first example of a 1,2-diphosphaspiro[2.2]pentane complex $(\eta^5\text{-C}_5\text{Me}_5)\text{Ru}(\text{CO})_2\overline{\text{PC}(\text{CH}_2\text{CH}_2)}\text{PR}$ which has been fully characterized.⁵⁹

Several ruthenium(II) complexes based on $\text{RuCl}_2(\text{CO})_2\text{P}_2$ (where $\text{P} = \text{Bz}_3\text{P}, \text{Ph}_3\text{P}, \text{Ph}_2\text{MeP}, \text{PhMe}_2\text{P},$ or Me_3P) have been prepared and

fully characterized. The initially formed complex has all ligand pairs trans (ttt) and is observed to thermally isomerize to the isomeric complex where all ligand pairs are cis (ccc). Kinetic measurements indicate a rate-determining loss of CO with the phosphine's cone angle and basicity influencing the rate of isomerization. The ΔS^\ddagger and ΔV^\ddagger values are both consistent with the proposed dissociation process for the ttt \rightarrow ccc isomerization.⁶⁰ A report dealing with the solid-phase thermal isomerization of these same ruthenium(II) complexes using differential scanning calorimetry has also appeared.⁶¹

The labile solvent complex $\text{Ru}(\text{DMSO})_4\text{Cl}_2$ reacts with bis[(diphenylphosphino)methyl]phenylarsine (dpma) giving $\text{Ru}(\text{dpma})\text{Cl}_2$ which has been characterized by X-ray diffraction analysis. The ruthenium is six-coordinate with trans chloride ligands. One of the dpma ligands is bound through the two phosphines while the other dpma ligand is bound through one phosphorus and arsine atom, presumably due to steric factors associated with the dpma ligand. An autocorrelated ^{31}P NMR spectrum recorded at -60°C suggests the presence of an additional isomer in solution having cis chloride ligands.⁶²



Reaction of $\text{Ru}(\text{DMSO})_4\text{Cl}_2$ with the tripod ligand $\text{MeC}(\text{CH}_2\text{PPh}_2)_3$ (triphos) gives the dinuclear complex $[\text{Ru}_2(\mu_2\text{-Cl})_3(\text{triphos})_2]\text{Cl}$ while $\text{MeC}(\text{CH}_2\text{AsPPh}_2)_3$ (triars) allows isolation of the mononuclear intermediate $\text{RuCl}_2(\text{DMSO})(\text{triars})$. This latter complex dimerizes to $[\text{Ru}_2(\mu_2\text{-Cl})_2(\text{triars})_2]\text{Cl}$ upon dissolution in MeOH. Chloride ligand abstraction using AgO_3SCF_3 in MeCN produces $[\text{Ru}(\text{MeCN})_3(\text{tripod})](\text{CF}_3\text{SO}_3)_2$ while use of DMSO solvent and temperatures above 100°C lead to $[\text{Ru}(\text{DMSO})_3(\text{tripod})](\text{CF}_3\text{SO}_3)_2$. The DMSO/tripod complex reacts readily with CO to give the dicarbonyl triflate complex $[\text{Ru}(\text{CF}_3\text{SO}_3)(\text{CO})_2(\text{tripod})](\text{CF}_3\text{SO}_3)$.⁶³

New ruthenium(II) 2,2',2''-terpyridine (trpy) complexes possessing trans spanning diphosphine ligands have been prepared and cationic complexes of the form $[\text{Ru}(\text{trpy})(\text{P-P})\text{Cl}](\text{ClO}_4)$ [where P-P = diphenyl-P-benzyl-N(Me)₂-(CH₂)_n-N(Me)₂-benzyl-P-diphenyl; N = 5 or 6] isolated. Spectral characterization, conductance and cyclic voltammetry studies of the ruthenium(III)/ruthenium(II) redox couple of all new complexes are reported along with comparison to related complexes.⁶⁴

Two reports have appeared concerning the reduction and functionalization of $\text{RuCl}_2(\text{PP}_3)$ [where $\text{PP}_3 = \text{P}(\text{CH}_2\text{CH}_2\text{CH}_2\text{PMe}_2)_3$]. Treatment with LiAlH_4 leads to the dihydride $\text{RuH}_2(\text{PP}_3)$ which reacts with CO_2 to give the formate complex $\text{RuH}(\text{O}_2\text{CH})(\text{PP}_3)$. C-H bond activation of benzene occurs when the dihydride complex is photolyzed. The coordinatively unsaturated $d^8\text{-ML}_4$ fragment $\text{Ru}(\text{PP}_3)$ reacts by an oxidative addition reaction with the benzene solvent. This aryl/hydride product has been characterized by X-ray diffraction analysis.⁶⁵ Related C-H bond activation products have been obtained from the sodium amalgam reduction of $\text{RuCl}_2(\text{PP}_3)$ in the presence of benzene, toluene, and o- or m-xylene. Toluene C-H bond activation occurs at the meta position to give two isomers characterized by a syn or anti meta-methyl/RuH disposition. X-Ray

crystal structures for all the C-K bond activation products are reported.⁶⁶

The reaction of the bidentate ligand diphenylphosphinoacetic acid (POH) with ruthenium(II) and (III) complexes is described. $\text{Ru}(\text{Cl}_2)(\text{PPh}_3)_3$ reacts with POH (3 equiv.) to give $\text{Ru}(\text{PO})_2(\text{POH})$ and $\text{Ru}(\text{PO})_2(\text{PPh}_3)$ when 2 equiv of POH are used. POH reacts with $\text{Ru}(\text{DMSO})_4\text{Cl}_2$ (2:1 ratio) to yield a complex of composition $\text{HRu}(\text{PO})_2\text{Cl}(\text{DMSO})$ while a 3:1 ratio of POH to $\text{Ru}(\text{DMSO})_4\text{Cl}_2$ affords $\text{HRu}(\text{PO})_3$. $\text{RuCl}_3 \cdot 3\text{H}_2\text{O}$ reacts with POH resulting in the formation of the bridged dimer $\{\text{Ru}(\text{PO})_2\text{Cl}\}_2$. All complexes have been characterized spectroscopically (^1H and ^{31}P NMR) and by EPR and electrochemical measurements.⁶⁷

The aminophosphine ligand $(\text{Ph}_2\text{PCH}_2\text{CH}_2)_3\text{N}$ (TPEA) reacts with $\text{RuCl}_2(\text{PPh}_3)_3$ and $\text{Ru}(\text{DMSO})_4\text{Cl}_2$ to give the chelated complexes $\text{RuCl}_2(\text{TPEA})$ and $\text{RuCl}_2(\text{DMSO})(\text{TPEA})$, respectively. Depending on the reaction conditions, $\text{RuX}_3(\text{TPEA})$ or $[\text{RuX}_2(\text{AsPh}_3)(\text{TPEA})](\text{X})$ can be obtained from the reaction of TPEA with $\text{RuX}_3(\text{AsPh}_3)_2\text{MeOH}$ (where X = Cl or Br).⁶⁸

Electronic spectra and resonance Raman behavior of several $\text{RuCl}_2(\text{PPh}_3)_2(\text{x-py})_2$ complexes (where x-py = substituted pyridine) have been published. The electronic spectra display two intense charge-transfer bands which are assigned to the $d_{xz} \rightarrow \pi^*$ and $d_{xy} \rightarrow \text{X}$ electronic transitions while the resonance Raman spectra reveal the presence of three charge-transfer excited states involving the Ru-pyridine chromophor.⁶⁹

(e) Carbonyls

The photochemistry of $\text{Ru}(\text{CO})_4(\eta^2\text{-diene})$ (where diene = 1,4-pentadiene, 3-methyl-1,4-pentadiene, 1,5-hexadiene, or 1,6-heptadiene) and the thermal chemistry of $\text{Ru}(\text{CO})_3(\text{ethylene})_2$ with these dienes are reported. The thermal isomerization of

$\text{Ru}(\text{CO})_3(\eta^4\text{-1,4-pentadiene})$ to $\text{Ru}(\text{CO})_3(\eta^4\text{-1,3-pentadiene})$ proceeds with a half-life of ca. 2 min at room temperature. Photolysis of $\text{Ru}(\text{CO})_4(\eta^2\text{-1,4-pentadiene})$ at 77 K yields both $\text{Ru}(\text{CO})_3(\eta^4\text{-1,4-pentadiene})$ (~75%) and $\text{HRu}(\text{CO})_3(\eta^3\text{-C}_5\text{H}_7)$ (~25%). The latter product is observed to thermally isomerize to $\text{Ru}(\text{CO})_3(\eta^4\text{-1,3-pentadiene})$ above 198 K. The complex $\text{Ru}(\text{CO})_3(\eta^4\text{-1,5-hexadiene})$ is stable for several hours at room temperature while photolysis of $\text{Ru}(\text{CO})_4(\eta^2\text{-1,6-heptadiene})$ in the presence of added 1,6-heptadiene affords only the bis(olefin) complex $\text{Ru}(\text{CO})_3(\eta^2\text{-1,6-heptadiene})_2$.⁷⁰

The mechanism of carbonyl insertion in the complexes $\text{cis-RuMeX}(\text{CO})_2(\text{PMe}_3)_2$, (where X = I or CN) has been examined. Studies using ^{13}CO with natural abundance $\text{cis-RuMeX}(\text{CO})_2(\text{PMe}_3)_2$, ^{12}CO with isotopically enriched $\text{cis-RuMeX}(^{13}\text{CO})_2(\text{PMe}_3)_2$, and ^{13}CO with selectively labeled $\text{cis-RuMeX}(^{12}\text{CO})(^{13}\text{CO})(\text{PMe}_3)_2$ indicate that these reactions proceed via methyl group migration to a cis carbonyl group and not by CO migration to the methyl site.⁷¹

Reaction of the cyclopentadienone complex $(\eta^4\text{-Ph}_4\text{C}_4\text{CO})\text{Ru}(\text{CO})_3$ with Et_2NH at room temperature gives the amine complex $(\eta^4\text{-Ph}_4\text{CCO})\text{Ru}(\text{CO})_2(\text{Et}_2\text{NH})$ which has been characterized spectroscopically and by X-ray diffraction analysis. The same amine complex was also isolated using Et_3N at 140 °C.⁷²

$\text{Os}(\text{CO})_5$ has been the subject of a gas-phase electron diffraction study which shows that $\text{Os}(\text{CO})_5$ possesses D_{3h} symmetry. Corrections for three-atom multiple scattering are reported to improve the fit of the experimental data, but little improvement of the parameter values is observed.⁷³

The synthesis and spectral characterization of several ruthenium(II) complexes of the form $\text{RuCl}_2(\text{CO})_2\text{L}_2$ (where L = naphthisoxazole, 2-aminobenzthiazole, allylthiourea, thioacetamide, or $\text{P}(\text{OPh})_3$) have been described.⁷⁴

Hexabromoosmium(IV) reacts with PPh_3 in refluxing acetic acid/acetic anhydride to yield $\text{OsBr}_2(\text{CO})_2(\text{PPh}_3)_2$. X-Ray diffraction analysis reveals that the osmium atom adopts an octahedral coordination with three disordered Br/CO atoms/molecule, and a single ordered CO molecule possessing trans PPh_3 groups.⁷⁵

(f) Sulfur and Oxygen Ligands

The isomerization kinetics for the conversion of *cis*- $\text{Os}(\eta^4\text{-CHBA-DCB})(\text{OPPh}_3)_2$ (where CHBA-DCB = 1,2-bis-3,5-dichloro-2-hydroxybenzamido-4,5-dichlorobenzene) to the corresponding *trans* isomer has been examined and is shown to be first order in metal complex and zero order in OPPh_3 . An intramolecular twist mechanism is favored based on the absence of rate suppression using hydroquinone or 2-mercaptoethanol and a lack of $\text{OP}(\text{p-tolyl})_3$ incorporation in the final product. The equilibrium constant between *cis*- and *trans*- $\{\text{Os}(\eta^4\text{-CHBA-DCB})(\text{OPPh}_3)_2\}^{+1}$ and the kinetics for the conversion of the *cis* cation to the *trans* cation are reported. The activation parameters and their mechanistic significance are discussed and comparisons made between the neutral and cationic reactions.⁷⁶

Synthesis and reactivity studies of the stable η^2 -thioxophosphane complex $\text{Os}(\text{CO})_2(\text{PPh}_3)_2(\eta^2\text{-PHS})$ are reported. X-ray diffraction analysis shows that the two PPh_3 groups are oriented in a *trans* fashion and that the phosphorus and sulfur atoms of the η^2 -thioxophosphane group are coplanar with the two CO groups.⁷⁷

Reaction of $\text{K}_2\text{Ru}(\text{NO})\text{Cl}_5$ with substituted aromatic thiolate anions affords complexes with the composition $\{\text{Ru}\{\text{SR}\}_4\{\text{NO}\}\}^{-1}$ (where $\text{R} = 2,3,5,6\text{-Me}_4\text{C}_6\text{H}$, $2,6\text{-Me}_2\text{C}_6\text{H}_3$, or $2,4,6\text{-i-Pr}_3\text{C}_6\text{H}_2$). The isopropyl derivative reacts with MeOH, DMSO, or MeCN via solvent displacement of the nitrosyl group to give $\text{Ru}(\text{SR})_4\text{L}$. $\text{Ru}(\text{SR})_4(\text{MeOH})$ readily loses MeOH under vacuum to give $\text{Ru}(\text{SR})_4$. X-Ray structural analysis

reveals a pentacoordinated ruthenium atom formed by four thiolate groups and methine C-H activation of one of the ortho isopropyl groups. The methyl derivatives react slowly at room temperature in MeOH to yield a dimeric complex through a C-H bond activation process. For the thiolate ligand $R = 2,3,5,6\text{-Me}_4\text{C}_6\text{H}$, the resulting dimer $[(\text{Ru}(\mu_2\text{-S-CH}_2\text{-}3,5,6\text{-Me}_3\text{C}_6\text{H})(\text{S-}2,3,5,6\text{-C}_6\text{H})(\text{NO}))_2(\mu_2\text{-S-}2,3,5,6\text{-Me}_4\text{C}_6\text{H})]^{-1}$ does not possess a Ru-Ru bond as judged by a X-ray diffraction study where a Ru-Ru distance in excess of 3.3 Å was observed.⁷⁸

A comprehensive NMR kinetic study of water exchange with $[\text{Ru}(\text{H}_2\text{O})_6]^{+3}$, $[\text{Ru}(\text{H}_2\text{O})_6]^{+2}$, and $[\text{Ru}(\text{MeCN})_6]^{+2}$ has been reported.¹⁷ NMR measurements were employed with the former two aquo complexes while ^1H NMR spectroscopy was used to assess MeCN exchange in the latter complex. From the kinetic parameters in the ruthenium(II) systems, solvent exchange is shown to proceed by an interchange I mechanism. The ruthenium(III) complex displays exchange from both $[\text{Ru}(\text{H}_2\text{O})_6]^{+3}$ and the monohydroxyl complex $[\text{Ru}(\text{H}_2\text{O})_5\text{OH}]^{+2}$. The kinetics for exchange support an associative interchange I_a for water on $[\text{Ru}(\text{H}_2\text{O})_6]^{+3}$ and an I mechanism on the deprotonated $[\text{Ru}(\text{H}_2\text{O})_5\text{OH}]^{+2}$. The results of exchange are compared to other di- and trivalent transition-metal complexes.⁷⁹

The kinetics of aquation and anation reactions have been studied using $[\text{RuCl}_4(\text{H}_2\text{O})_2]^{-1}$, $\text{RuCl}_3(\text{H}_2\text{O})_3$, $[\text{RuCl}_2(\text{H}_2\text{O})_4]^{+1}$, and $[\text{RuCl}(\text{H}_2\text{O})_5]^{+2}$. The dependence on hydronium ion concentration and KCl concentration on the kinetics is reported along with possible mechanisms and computed rate constants for all reaction steps.⁸⁰

Treatment of $\text{mer-OsCl}_2(\text{N}_2)(\text{PMe}_2\text{Ph})_3$ with $\text{Me}_2\text{NCS}_2^-$ leads to loss of dinitrogen and formation of $\text{mer/fac-OsCl}(\text{Me}_2\text{NCS}_2)(\text{PMe}_2\text{Ph})_3$ or $\text{cis-Os}(\text{Me}_2\text{NCS}_2)_2(\text{PMe}_2\text{Ph})_2$ depending on the conditions employed and the nature of the regeneration. Reaction of $\text{mer-OsX}_2(\text{N}_2)(\text{PMe}_2\text{Ph})_3$ (where X = Cl or Br) with monodentate thiolates RS^- (where R = CF_3 ,

Me, Ph, or C_6F_5) at room temperature gives the product of only halide displacement $mer-OsX(RS)(N_2)(PMe_2Ph)_3$. A X-ray structure of $mer-OsCl(C_6F_5)N_2(PMe_2Ph)_3$ reveals the presence of an octahedral osmium atom with *trans* dinitrogen and chloride ligands.⁸¹

The electrophilic imino-oxo- λ^4 -sulphane 4-MeC₆H₄SO₂NSO reacts with $OsCl(NO)(ethylene)(PPh_3)_2$ to give $OsCl(NO)(PPh_3)_2(4-MeC_6H_4SO_2NSO)$ in quantitative yield. Hydrolysis of the sulphane complex yields the corresponding sulfur dioxide complex $OsCl(NO)(PPh_3)_2(SO_2)$ while reaction with H_2S/HS^- gives the disulfur complex $OsCl(NO)(PPh_3)_2(S_2)$. The latter derivative is readily oxidized with meta-chloroperoxybenzoic acid to give the disulfur monoxide complex $OsCl(NO)(PPh_3)_2(S_2O)$.⁸²

Zinc amalgam reduction of tris(β -diketonato)ruthenium(III) complexes [where β -diketonato = acetylacetonate {acac}, 1,1,1-trifluoro-2,4-pentanedionate {tfac}, 1,1,1,3,3,3-hexafluoro-2,4-pentanedionate {hfac}, or 2,2,6,6-tetramethyl-3,5-heptanedionate {dpm}] in acetonitrile leads to diacetonitrile-bis(β -diketonato)ruthenium(II) complexes. Reduction of mixed-ligand β -diketonato complexes reveals that the more electron-donating β -diketonato ligand is displaced by two acetonitrile ligands. The synthetic usefulness of these solvated ruthenium(II) complexes is shown by the preparation of known and new mixed-ligand β -diketonato ruthenium(III) complexes RuL_2L' .⁸³

The $Ru(hfac)_3^{0/-1}$ self-exchange has been examined by 1H NMR measurements in a variety of solvents and as a function of pressure up to 200 MPa. Data analysis using the Stranks-Rush-Marcus relationship reveals that the kinetics for electron transfer are influenced primarily by solvent reorganization with a minor contribution originating from internal reorganization within the ruthenium complexes. The effect of pressure on the 1H line width and chemical shift of $Ru(acac)_3$ in similar solvents is also reported.⁸⁴

A report dealing with the crystal structure and absolute configuration of (+)^{CD}₂₇₅ - Ru(acac)₃ has appeared. The optical antipode was isolated from an enantiomeric mixture of Ru(acac)₃ using cellulose tris(phenylcarbamate) coated silica gel and is shown to possess a Δ configuration of D₃ symmetry with slight axial elongation.⁸⁵

o-Formylphenols and o-acylphenols react with ethanol-reduced RuCl₃ to give tris chelate ruthenium(III) complexes. The complex formed from salicylaldehyde has been crystallized and analyzed by X-ray diffraction analysis. The EPR data of these low-spin RuL₃ complexes display rhombic spectra with axial and rhombic distortion parameters of ~4500 and 1500 cm⁻¹ respectively. The redox chemistry of these complexes is reported along with the conversion of [Ru^{IV}L₃]⁺¹ to [Ru^{IV}L₂(MeCN)₂]⁺¹. The bis(acetonitrile) complex provides an entry point to other compounds based on the Ru^{II}L₂ fragment.⁸⁶

A voltammetric examination of the redox behavior of [Ru₄(OH)₁₂]⁺⁴ at a platinum rotating disk electrode has been reported. Oxidation leads to [Ru₄(OH)₁₂]⁺⁵ which is formulated as a tetrameric Ru(4.25) species. The oxidation process is independent of the solution acidity which suggests that hydroxyl oxidation is unlikely. The ruthenium(4.25) complex is reduced by water in 1.0 M HClO₄ by an undetermined photochemical process.⁸⁷

Reactions with the thioether dithiolato complex Ru(PPh₃)₂(dtttd) [where dtttd = 2,2'-ethylenedithiobis(thiophenolate)] and the amino dithiolato complex Ru(PPh₃)₂(bmae) [where bmae = 2,2'-ethylenediiminobis(thiophenolate)] are described. PPh₃ substitution is observed by CO in Ru(PPh₃)₂(dtttd) at room temperature to give Ru(CO)(PPh₃)₂(dtttd) whereas the bmae complex is unreactive. The bmae complex is shown to yield Ru(CO)(PPh₃)(bmae)

and $\text{Ru}(\text{CO})_2(\text{bmae})$ at elevated temperatures or through a base-induced deprotonation of the amine functionality.⁸⁸

$\text{Ru}(\text{CO})(\text{dpttd})$ (where $\text{dpttd} = 2,2'$ -[thiobis(ethylenethio)]bis(thiophenolate)} has been shown to react with bis(2-bromoethyl)sulfide at elevated temperature to give, via loss of an o-benzenedithiolate group, the new ligand containing complex $\text{Ru}(\text{Bzo-S-S})(\text{CO})_2$ (where $\text{Bzo-S-S} = \text{trithiodbenzo}(9\text{-crown-3})$). This new complex has been characterized spectroscopically and by X-ray diffraction analysis.⁸⁹

A X-ray diffraction study reveals intermolecular stacking of the N-bound tetracyanoethylene (tcne) ligands in $\text{Os}(\text{S}_2\text{PMe}_2)(\text{PPh}_3)(\text{tcne})$ which was prepared by reacting tcne with $\text{Os}(\text{S}_2\text{PMe}_2)(\text{PPh}_3)_2$. In contrast, $\text{Os}(\text{S}_2\text{PPh}_2)(\text{PPh}_3)(\text{tcne})$ displays no such intermolecular contacts in the solid state. The spectra, electrochemical and coulometric properties of these complexes are reported and compared with known charge-transfer complexes.⁹⁰

An in-depth examination of all bond-isomeric hexakis[thiocyanato(N)-thiocyanato(S)]osmium(III) and (IV) complexes has appeared. Included here is the preparation, redox behavior, vibrational and electronic spectral analysis of all complexes discussed.^{91,92}

The chemistry associated with several ruthenium hydroxides and alkoxides has been partially reviewed in a comprehensive review of the late transition metals.⁹³

Kinetic and equilibrium measurements have been reported for the redox reaction between the dioxo complex $[\text{Ru}_3(\text{NH}_3)_4(\text{O})_2]^{+7}$ and Fe^{II} salts.⁹⁴ The electronic spectrum of the dioxo complex $[\text{Os}(\text{O})_2(\text{CN})_4]^{-2}$ exhibits five distinct band systems at 10 K. Band assignments and singlet-triplet distances are discussed.⁹⁵ A report dealing with the crystal structure and electronic properties of $[\text{Ru}(\text{O})_3(\text{OH})_2]^{-2}$ has appeared. The three oxo groups are observed

to reside in the equatorial plane giving rise to an overall trigonal-bipyramidal geometry and idealized D_{3h} symmetry.⁹⁶ The redox properties of several trans-dioxoosmium(VI) Schiff-base complexes have been reported. The X-ray structure of trans-[Os^{VI}(O)₂(3-t-Bu-saltmen)] [where 3-t-Bu-saltmen = N,N'-(1,1,2,2-tetramethylethylene)bis(3-tert-butylsalicylideneamino)] is also presented.⁹⁷ The X-ray structure and spectral properties of the μ -oxo complex [Ru₂(μ -O)(μ -OAc)₂(pyridine)₆]⁺² have been reported. The redox properties and the relationship of this ruthenium dimer to the iron-containing protein methemerythrin are discussed.⁹⁸

Two reports dealing with the synthesis and reactivity of μ -peroxo bis(ethylenediaminetetraacetate)ruthenium(IV) complexes have been published. The μ -peroxo complexes are prepared using molecular oxygen or H₂O₂.^{99,100}

(g) Nitrogen Ligands

Several reports dealing with the chemistry associated with [Os(NH₃)₅L]⁺² complexes have appeared. For L = acetone, a redox-induced $\eta^1 \rightarrow \eta^2$ isomerization is observed upon one-electron reduction. The thermal rate constant for $\eta^2 \rightarrow \eta^1$ acetone conversion has been measured and the η^2 -coordination of acetone is shown to be 5.0 kcal/mol more stable than the η^1 -isomer. A variety of coordinated aldehydes and ketones have been examined and it is shown that the initially formed complex arises by η^2 -arene coordination. Linkage isomerization to the η^1 -coordinated carbonyl complex is readily observed upon oxidation to the osmium(III) complex.¹⁰¹ A similar linkage isomerization was also reported for [Os(NH₃)₅(η^2 -PhNH₂)]⁺² along with the isomerization rates and thermodynamic parameters.¹⁰² Substituent effects on η^2 -coordinated arene complexes in [Os(NH₃)₅L]⁺² complexes have been examined by variable-temperature NMR measurements. Tautomerization rates associated with 2,3- $\eta^2 = 5,6$ - η^2 exchange process have been

calculated for several substituted-benzene osmium(II) complexes. The stabilities of the corresponding osmium(III) complexes are also presented.¹⁰³

Benzene hydrogenation to cyclohexene under mild conditions using $[\text{Os}(\text{NH}_3)_5(\eta^2\text{-C}_6\text{H}_6)]^{+2}$ in the presence of palladium on carbon has appeared. The hydrogenation reaction proceeds through an osmium (II)→(III) redox couple.¹⁰⁴ The complex $\{[\text{Os}(\text{NH}_3)_5]_2(\eta^2:\eta^2\text{-}\mu\text{-C}_6\text{H}_6)\}^{+4}$ is unreactive due to steric crowding which prevents palladium coordination to the arene. Reaction of $[\text{Ru}(\text{NH}_3)_5]^{+2}$ with $[\text{Os}(\text{NH}_3)_5(\eta^2\text{-C}_6\text{H}_6)]^{+2}$ yields the mixed-metal $\eta^2:\eta^2\text{-}\mu\text{-arene}$ complex $[\text{Os}(\text{NH}_3)_5\text{-Ru}(\text{NH}_3)_5(\eta^2:\eta^2\text{-}\mu\text{-C}_6\text{H}_6)]^{+4}$, analogous to the above dimeric osmium arene.¹⁰⁵

New pyrazine bridged osmiumpentaamine complexes are described using $[\text{Os}(\text{NH}_3)_5\text{pz}]^{+2}$ (where pz = pyrazine) as the starting material.

The new complexes include $\{[\text{Os}(\text{NH}_3)_5(\text{pz})\text{Os}(\text{NH}_3)_5]_n\}^{+n}$ ($n = 4, 5, \text{ or } 6$), $[\text{Os}(\text{NH}_3)_4(\text{Cl})\text{Os}(\text{pz})\text{Os}(\text{NH}_3)_5]^{+n}$ ($n = 3, 4, \text{ or } 5$), $[\text{Os}(\text{NH}_3)_5\text{Os}(\text{pz})\text{Rh}(\text{NH}_3)_5]^{+n}$ ($n = 5 \text{ or } 6$), all of which are fully investigated by electrochemical and spectroscopic techniques. The chemistry associated with the pyrazine-bridged rutheniumpentaamine complexes $\{[\text{Ru}(\text{NH}_3)_5(\text{pz})\text{Ru}(\text{NH}_3)_5]_n\}^{+n}$ is described and compared to the osmium analogues.¹⁰⁶

The synthesis and redox properties of several new N-heterocyclic complexes of ruthenium and osmium of the form $[\text{M}(\text{NH}_3)_5(\text{N-heterocycle})]^{+2}$ have been reported. The method of choice for the preparation of these ruthenium(II) and osmium(II) complexes is through reduction of the corresponding metal (III) complex in nonaqueous solvents.¹⁰⁷

Treatment of $[\text{Os}(\text{NH}_3)_6]^{+2}$ with acetone gives the imine complex $[\text{Os}(\text{NH}_3)_5(\text{NHCMe}_2)]^{+2}$ through a redox-catalyzed condensation scheme

involving $[\text{Os}(\text{NH}_3)_6]^{+3}$. NMR measurements reveal the imine to be terminally coordinated, unlike the η^2 - π coordination observed with the isoelectronic acetone analogue.¹⁰⁸

An in-depth electrochemical and spectroscopic study of $[\text{Os}(\text{NH}_3)_5(\text{nitrite})]^{+2,+3}$ complexes has appeared.¹⁰⁹

The synthesis, linkage isomerization, and autoxidation kinetics have been examined for reductive acid complexes of pentamineruthenium(III). The ascorbate and tetramethylreductate complexes display either rhombic or axial EPR spectra depending on the degree of protonation along with magnetic susceptibilities consistent with Ru(III) species. The pH dependence on the redox processes is described.¹¹⁰ Ascorbic acid reduction of mononuclear and binuclear ruthenium(III) amine complexes is presented. The rate-determining reaction involves reaction between the ruthenium(III) complex and two ascorbate monoanions, followed by reaction of the ascorbate radical with the ruthenium(III) complex. The reactions have been analyzed using the Marcus-Sutin model for outer-sphere electron-transfer reactions to give the self-exchange rate constant of the ascorbate monoanion/ascorbate radical couple.¹¹¹

The rates of $[\text{Ru}(\text{NH}_3)_5(\text{pyridine})]^{+3}$ reduction by $[\text{Ti}(\text{C}_2\text{O}_4)]^{-1}$ have been measured and are observed to occur via an outer-sphere mechanism. Use of $[\text{Ru}(\text{OAc})_2(\text{C}_2\text{O}_4)_2]^{-1}$ as the oxidant leads to an inner-sphere mechanism with an observable Ru/Ti oxalate intermediate. The stability constants for $[\text{TiC}_2\text{O}_4]^{+1}$ and $[\text{Ti}(\text{C}_2\text{O}_4)]^{-1}$ are also reported.¹¹² The formation kinetics for the binuclear complex $[(\text{NH}_3)_5\text{Ru}^{\text{III}}\text{NCFe}^{\text{III}}(\text{CN})_5]^{-1}$ have been measured. The reaction proceeds through the rapid formation of the ion pair $[(\text{NH}_3)_5\text{RuOH}_2]^{+3}/[\text{Fe}(\text{CN})_6]^{-4}$ which is shown to be the precursor to the valence-trapped binuclear Ru/Fe complex. The intervalence absorbance band has been measured and a discussion is presented

dealing with the extent of electronic delocalization in this and related complexes.¹¹³ $[\text{Ru}(\text{NH}_3)_5(\text{olefin})]^{+2}$ and $[\text{Os}(\text{NH}_3)_5(\text{olefin})]^{+2}$ (where olefin = isobutylene, propene, 1,3-butadiene, 1,4-pentadiene, or 1,5-hexadiene) have been prepared and spectroscopically characterized. The redox potentials have been measured and are contrasted with other known complexes. Binuclear complexes based on 1,3-butadiene are obtained by reacting $[(\text{NH}_3)_5\text{M}(1,3\text{-butadiene})]^{+2}$ with $[(\text{NH}_3)_5\text{M}(\text{triflate})](\text{triflate})_2$ while the mixed-metal analogues are prepared similarly. In $[(\text{NH}_3)_5\text{M}(1,3\text{-butadiene})]^{+2}$, the uncoordinated olefin may be brominated using Br_2 while no reaction is observed in the binuclear complexes.¹¹⁴

The preparation of isothiocyano and isoselenocyano complexes based on pentaammineosmium(II) are reported. Reaction of $-\text{SCN}$ and $-\text{SeCN}$ with $[(\text{NH}_3)_5\text{Os}(\text{triflate})](\text{triflate})_2$ yields the respective N-bonded complexes as determined by vibrational spectroscopy.¹¹⁵ Finally, the crystal and molecular structure of the mixed-valence ruthenium dimer $[(\text{NH}_3)_3\text{RuBr}_3\text{Ru}(\text{NH}_3)_3](\text{Br}_4)$ has appeared.¹¹⁶

The synthesis and redox properties of $\text{trans}-[\text{Ru}(\text{NH}_3)_4\text{LL}']^{+2}$ complexes (where L, L' = pyridine, 4-picoline, isonicotinamide, 4-acetylpyridine, pyrazine, or pyrazinone) are reported along with the aqueous solution basicities of the coordinated pyrazine ligand in all the new complexes.¹¹⁷ In the complexes $\text{trans}-[\text{Ru}(\text{NH}_3)_4(\text{PR}_3)(\text{H}_2\text{O})]^{+2}$ (where R = Et, Bu, Ph, PhO, EtO, or BuO) the *trans-effect* and *trans-influence* on the aquation reaction in the presence of pyridine have been measured. Generalizations concerning the influence of π bonding on the *trans-influence* of the ancillary phosphine are discussed.¹¹⁸

A report dealing with the optical outer-sphere ligand to metal charge transfer (LMCT) in the ion pair $[\text{Ru}(\text{NH}_3)_6]^{+3}/[\text{Rh}(\text{CN})_6]^{-3}$ has appeared. Mixing these ions gives an increased $\text{UV}/\text{near-UV}$

absorption assigned to an outer-sphere LMCT from a Rh-cyanide to the Ru-amine.¹¹⁹

The nitrosyl complex $[\text{RuCl}_5(\text{NO})]^{-2}$ reacts with the macrocyclic amine ligand 1,4,8,11-tetramethyl-1,4,8,11-tetraazacyclotetradecane in the presence of hydrazine and acetonitrile to give trans- $[\text{Ru}^{\text{II}}(\text{macrocycle})(\text{N}_3)(\text{MeCN})]^{+1}$. The molecular structure of the azide complex has been determined and the measured Ru-N(acetonitrile) bond distance is contrasted to the analogous oxo complex trans- $[\text{Ru}^{\text{II}}(\text{macrocycle})(\text{O})(\text{MeCN})]^{+1}$.¹²⁰

A report on the electrocatalytic reduction of nitrite using the ethylenediaminetetraacetic acid (edta) complexes $[\text{Ru}^{\text{II}}(\text{Hedta})(\text{NO}^+)]$ and $[\text{Ru}^{\text{II}}(\text{Hedta})(\text{H}_2\text{O})]^{-1}$ has appeared. The nitrite reduction pattern is compared to known water-soluble iron porphines.¹²¹ The oxidation of $\text{Na}[\text{Ru}^{\text{II}}(\text{Hedta})(\text{H}_2\text{O})] \cdot 4\text{H}_2\text{O}$ by sodium persulfate leads to $\text{Ru}_2\text{O}(\text{Hedta})_2 \cdot x\text{H}_2\text{O}$ ($x = 15.4 \pm 0.4$). Cyclic voltammetric analysis suggests a bridging Ru-O-Ru structure. Use of $[\text{Ru}^{\text{II}}(\text{edta})]^{-2}$ gave similar results. The complexes $[\text{Ru}^{\text{II}}(\text{edta})]^{-2}$, $[\text{Ru}^{\text{II}}(\text{Hedta})(\text{H}_2\text{O})]^{-1}$, and $[\text{Ru}^{\text{II}}_2(\text{ttha})(\text{H}_2\text{O})_2]^{-2}$ (where ttha = triethylenetetraaminehexaacetic acid salt) are oxidized by either H_2O_2 or O_2 to give products of H_2O replacement by H_2O_2 . The EPR data and DMPO spin adduct EPR data of several $\text{LRu}^{\text{III}}(\text{O}_2^{-2})$ complexes (where L = edta⁻⁴, Hedta⁻³, or ttha⁻⁶) are reported along with the olefin epoxidation behavior exhibited by those complexes.¹²² The aquation of $[\text{Ru}(\text{edta})(\text{H}_2\text{O})]^{-1}$ using SCN^- , N_3^- , thiourea, and substituted thioureas has been examined as a function of pH, temperature, and pressure. A reaction involving an I_a mechanism is favored based on the pH dependence and activation parameters.¹²³

The autoxidation of the metal encapsulated complex $[\text{Ru}(\text{sar})]^{+2}$ (where sar = 3,6,10,13,16,19-hexaazabicyclo[6.6.6]eicosane) has been examined electrochemically and spectrophotometrically. The

rate of autoxidation is strongly pH dependent and a mechanism is presented that accounts for the rate differences at low and high pH. Analysis of the kinetic data has allowed evaluation of the acidity of the proton on the secondary nitrogen ($pK_a \approx 6.3$) in $[\text{Ru}(\text{sar})]^{+3}$.¹²⁴

Reaction of the tridentate ligand 1,4,7-triazacyclonane (tacn) with $[\text{Ru}(\text{DMF})_6]^{+2}$ gives $[\text{Ru}(\text{tacn})_2]^{+2}$. This ruthenium(II) complex has been fully characterized and its redox properties presented. The $\text{Ru}^{2+/3+}$ redox couple is fully reversible which has allowed the electron-self-exchange rate to be measured by NMR measurements. The large electron-self-exchange rate constant ($k_{\text{ex}} = 5 \times 10^4 \text{ M}^{-1} \text{ s}^{-1}$, $\mu = 0.1 \text{ M}$, $T = 23 \text{ }^\circ\text{C}$) has been used to assess the effect of strain in the tacn ligand on the exchange reactions and has been contrasted with other ruthenium amine complexes and cobalt and nickel redox couples.¹²⁵

$\text{Ru}(\text{CO})_4\text{I}_2$ reacts with $\text{Ag}(\text{tolN}_5\text{tol})$ [where $\text{tolN}_5\text{tol} = 1,5\text{-bis}(\text{p-tolyl})\text{pentazadiene}$] to give $[\text{Ru}(\text{CO})_3(\text{tolN}_5\text{tol})_2]_2$ which has been characterized crystallographically. Two pentazadienido ligands bridge the two $\text{Ru}(\text{CO})_3$ units by the N_1 and N_3 atoms. The pentazadienido ligands display planar N_5 zig-zag chains with an all-trans configuration.¹²⁶

Several new 1,3-diaryltriazenido complexes of ruthenium and osmium have been reported. The synthesis and spectral characterization of $[\text{Ru}(\text{ArNNNAr})(\text{CO})_3]_2$, $[\text{Ru}(\text{ArNNNAr})_2]_2$, $\text{cis-Ru}(\text{ArNNNAr})_2(\text{CO})_2$, $\text{MX}_2(\text{ArNNNAr})(\text{PPh}_3)_2$, and $\text{M}(\text{ArNNNAr})_3$ [where $\text{M} = \text{Ru}$ or Os ; $\text{X} = \text{Cl}$ or Br ; $\text{Ar} = \text{p-substituted aryl (H, Cl, or Me)}$] are described. The measured magnetic moments of the dimeric $[\text{Ru}(\text{ArNNNAr})_2]_2$ complex reveals ca. one unpaired electron per dimer, suggesting population of the spin states $\sigma^2\pi^4\delta^2\pi^*4$ and $\sigma^2\pi^4\delta^2\pi^*3\sigma^1$.¹²⁷ The ruthenium(II) and osmium(II) complexes $\text{MCl}_2(\text{PPh}_3)_3$ react rapidly with 1,3-diaryltriazenes under aerobic

conditions to yield the corresponding 1,3-diaryltriazenido complexes $MCl_2(ArN_3)(PPh_3)_2$. All of these complexes display measured magnetic moments consistent with a low spin d^5 Ru(III) or Os(III) center.¹²⁸

A report of optical outer-sphere metal-to-metal charge transfer in the ion pairs $[Pt(NH_3)_5Cl]^{+3}/[M(CN)_6]^{-4}$ (where M = Ru or Os) has appeared. The energetics associated with the optical MMCT are briefly discussed.¹²⁹

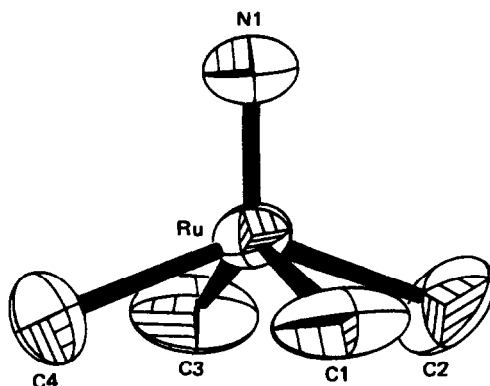
The interactions of the nucleosides adenosine, cytidine, guanosine and inosine with $[Ru(CO)_3Cl_2]_2$ and polymeric $[Ru(CO)_2Cl_2]_x$ have been reported. Depending on the Ru:nucleoside ratio, mono- and bis-nucleoside derivatives may be isolated. IR and NMR spectral data are presented.¹³⁰

A reactivity study of $[Ru_3(CO)_{10}(\mu_2-NO)]^{-1}$ has appeared. P-ligand substitution occurs rapidly at a nitrosyl-substituted ruthenium atom and complete ^{13}CO exchange is observed under mild conditions. The reaction of $PPN(NO_2)$ with $[Ru_3(CO)_{10}(\mu_2-NO)]^{-1}$ under CO gives $[Ru(CO)_3NO]^{-1}$ when photolyzed. This latter complex can also be synthesized using $PPN(NO_2)$ and $Ru(CO)_5$ as starting materials.¹³¹

$Li_2[Ru(^{13}CN)_5NO]$ has been synthesized at 90% isotopic enrichment and characterized spectroscopically. Attempts to determine the two-bond coupling $^2J(^{13}C_{ax}-Ru-^{13}C_{eq})$ using ^{13}C NMR spectroscopy were unsuccessful. The doubly labeled complex $Li_4[Ru(^{13}CN)_5(^{15}NO_2)]$, prepared from the nitrosyl complex and excess $Li(^{15}NO_2)$, revealed a two-bond coupling to the ^{15}N , $^2J(^{13}C_{ax}-Ru-^{15}NO_2)$ and $^2J(^{13}C_{eq}-Ru-^{15}NO_2)$. The reactivity of the nitrosyl with other nucleophiles is reported and compared with nitroprusside.¹³²

Three reports concerning the chemistry associated with nitrido complexes have appeared. Halide metathesis in trans-

$[\text{Os}(\text{N})(\text{CH}_2\text{SiMe}_3)\text{Cl}_2]^{-1}$ is observed using the silver salts Ag_2CO_3 , AgReO_4 , and AgSO_4 . The isolated carbonate, perrhenate, and sulfate complexes all possess a square-pyramidal structure with the nitrido group occupying the apical position.¹³³ Reaction of the anionic nitridoruthenium(IV) complex $[\text{Ru}(\text{N})(\text{OSiMe}_3)_4]^{-1}$ with AlMe_3 or $\text{Me}(\text{CH}_2\text{SiMe}_3)_2$ yields $[\text{Ru}(\text{N})(\text{Me})_4]^{-1}$ and $[\text{Ru}(\text{N})(\text{CH}_2\text{SiMe}_3)_4]^{-1}$, respectively. The X-ray structure of the tetramethyl derivative is reported and is shown to be square pyramidal with the methyl groups bent down below the plane of the ruthenium. The reactions of these anionic nitrido complexes with HCl , $\text{Au}(\text{PPh}_3)\text{Cl}$, and Lewis acids is described and contrasted with the related osmium analogues.¹³⁴ Several new nitridoosmium complexes with ancillary



sulfur ligands have been synthesized and characterized. $[\text{Os}(\text{N})(\text{CH}_2\text{SiMe}_3)_2\text{Cl}_2]^{-1}$ reacts readily with 1,2-ethanedithiol in the presence of Et_3N to give the osmium dithiolate complex $[\text{Os}(\text{N})(\text{CH}_2\text{SiMe}_3)_2(\text{SCH}_2\text{CH}_2\text{S})]^{-1}$. Reaction of the dichloro complex with thiocyanate gives $[\text{Os}(\text{N})(\text{CH}_2\text{SiMe}_3)_2(\text{SCN})_2]^{-1}$ which is shown to exhibit linkage isomerization. The major isomer possesses two N-bound thiocyanates while the minor isomer displays one thiocyanate and one isothiocyanate ligand. Both chlorides are

replaced upon reaction with 2-pyridine thiol to give the neutral dimer $[\text{Os}(\text{N})(\text{CH}_2\text{SiMe}_3)_2(\text{SC}_5\text{H}_4\text{N})]_2$. The 2-pyridine thiolato ligands are shown to chelate and bridge the two osmium centers by X-ray diffraction analysis.¹³⁵

The synthesis and X-ray structure of $\text{RuCl}(\text{8-quinolate})_2(\text{NO})$ have been reported. The chloride is shown to be cis to the nitrosyl group with the quinolate arranged with cis oxygens and trans nitrogen atoms.¹³⁶ Geometric isomerization in the related 2-methyl-8-quinolate complex $\text{RuX}(2\text{-mqm})_2(\text{NO})$ (where X = Cl or Br) has been observed upon optical excitation. The all trans- $\text{RuX}(2\text{-mqm})_2(\text{NO})$ complex has been prepared starting from either cis(O,O), cis(N,N)- or cis(O,O),trans(N,N)- $\text{RuX}(2\text{-mqm})_2(\text{NO})$.¹³⁷ The influence of the axial ligand in the oxidation of trans- $[\text{RuX}(\text{NO})(\text{py})_4]^{+2}$ (where X = Cl or OH) is discussed. Oxidation is shown to give the oxo complexes trans- $[\text{Ru}(\text{ONO})(\text{O})(\text{py})_4]^{+1}$ and trans- $[\text{RuCl}(\text{O})(\text{py})_4]^{+1}$ starting with the hydroxyl and chloride complexes, respectively.¹³⁸ The preparation and X-ray structure of cis- $[\text{OsCl}_4(\text{NO})(\text{NSCl})]^{-1}$ starting from $(\text{NSCl})_3$ and $\text{OsCl}_3(\text{NO})$ have appeared.¹³⁹

A study dealing with the preparation and properties of ruthenium nitrosyl/nitrite complexes with ancillary 2-(arylo)pyridine ligands (L) starting from the dinitro complex $\text{Ru}(\text{NO}_2)_2\text{L}_2$ has been published. Protonation of the dinitro complex $\text{Ru}(\text{NO}_2)_2\text{L}_2$ gives the nitrosyl/nitrite complex in high yield. IR analysis reveals the existence of a highly electrophilic nitrosyl ligand based on the observed νNO stretch at 1950 cm^{-1} . The redox chemistry and chemical reactivity toward hydroxide ion is described.¹⁴⁰ The stereospecific isomerization of trans- γ - $\text{Ru}(\text{azpy})_2\text{Cl}_2$ [where azpy = 2-phenylazo(pyridine)] into the α or β geometric isomers has been reported using hydroxide as a catalyst. The kinetics for the isomerization of the γ form into the β form and mechanistic interpretations are presented.¹⁴¹

The structure of $\text{mer-RuCl}_3(\text{MeCN})[1\text{-methyl-3-(2-pyridyl)-1,2,4-triazole}]$ has been solved. The heterocyclic complex is prepared by reacting RuCl_3 with the triazole in acetonitrile. The ORTEP diagram reveals that the MeCN ligand is trans to the pyridyl nitrogen.¹⁴² The chemistry and radiosensitizing activity of ruthenium(II) complexes with ancillary 4-nitroimidazole ligands has appeared. The new complexes have the general formula $\text{RuCl}_2(\text{DMSO})_2\text{L}_n$ (where L = 4-nitroimidazole derivative; n = 1 or 2) and the N-methyl-4-nitroimidazole derivative (n = 1) displays a higher sensitizing enhancement ratio relative to the free heterocycle and shows no in vitro cytotoxicity toward hypoxic tumor cell.¹⁴³

A new Schiff base complex without a π -acidic ligand has been synthesized. The ruthenium(III) complex $[\text{Ru}(\text{SB})\text{Cl}_2]^{-1}$ (where SB = Schiff base) has been prepared using $\text{MeC}(\text{O})\text{CH}_2\text{CR}=\text{NCHR}'\text{CH}_2\text{N}=\text{CRCH}_2\text{C}(\text{O})\text{Me}$ and the usual spectroscopic characterizations are reported along with XPS data.¹⁴⁴

Aryldiazonium cations react with $\text{RuH}_2[\text{P}(\text{OEt})_3]_4$ to give bis(aryldiazene)- and mono(aryldiazenido)ruthenium complexes. A low-precision X-ray structure of the bis(diazene) complex $[\text{Ru}(4\text{-MeC}_6\text{H}_4\text{N}=\text{NH})_2(\text{P}(\text{OEt})_3)_4]^{+2}$ reveals an octahedrally disposed ruthenium with cis diazene groups. The bis(diazene) complexes react with Et_3N to afford new pentacoordinate aryldiazenido complexes of the form $[\text{Ru}(\text{ArN}_2)(\text{P}(\text{OEt})_3)_4]^{+1}$. Protonation of the aryldiazenido complexes using HBF_4 and $\text{CF}_3\text{CO}_2\text{H}$ gives $[\text{Ru}(\text{ArN}=\text{NH})(\text{P}(\text{OEt})_3)_4]^{+2}$ and $[\text{Ru}(\text{CF}_3\text{CO}_2)(\text{ArN}=\text{NH})(\text{P}(\text{OEt})_3)_4]^{+1}$, respectively.¹⁴⁵

The results of EPR studies of irradiated single crystals of alkali halides doped with ruthenium and osmium cyanide complexes have been published.¹⁴⁶

The tripod ligands tris(2-pyridyl)amine, tris(2-pyridyl)methane and tris(2-pyridyl)phosphine have been reacted with $[\text{Ru}(\text{DMF})_6]^{+2}$ to give the respective bis(tripod)ruthenium(II)

complexes. All three complexes were examined by X-ray analysis, revealing an increased distortion from idealized D_{3d} symmetry as the bridgehead X-C(pyridyl) bond distance increases.¹⁴⁷

The electrochemistry of $[M(\text{bpy})_3]^{+2}$ (where $\text{bpy} = 2,2'$ -bipyridine; $M = \text{Ru}$ or Os) has been examined in liquid SO_2 at -70°C using ultramicrovoltammetric electrodes. $[\text{Ru}(\text{bpy})]^{+2}$ displays oxidation waves to the 3+, 4+, 5+ and 6+ species. The 3+ state corresponds to a metal-centered oxidation while the latter three states are derived from bpy-centered oxidations. The 3+ and 4+ states exhibit Nernstian behavior as judged by the usual cyclic voltammetry criteria while the 5+ and 6+ states decompose through reaction with solvent or electrolyte. $[\text{Os}(\text{bpy})_3]^{+2}$ may be oxidized to the stable, metal-centered 3+ and 4+ states. A transient 5+ species $\text{Os}^{\text{IV}}(\text{bpy}^{\cdot+})(\text{bpy})_2$, originates from a bpy oxidation. Standard potentials and the rate constants for the 5+ and 6+ states are presented.¹⁴⁸ Fast-scan cyclic voltammetric measurements have been used to study the reduction of $[\text{Ru}(\text{bpy})]^{+2}$. The heterogeneous rate constant for the +2/+1 and +1/0 redox couples are found to be one order of magnitude larger than previously reported.¹⁴⁹ $[\text{Ru}(\text{bpy})_3]^{+2}$ and $\text{Ru}(\text{acac})_3$ oxidation has been examined at a rotating disk electrode using acetonitrile solvent. The diffusion coefficient and apparent rate of charge-transfer have been determined.¹⁵⁰ pH effects on the redox properties of $[\text{Ru}(\text{bpy})_3]^{+2}$ using a clay-modified electrode have been investigated. The voltammetric waves for the 2+/3+ redox couple are unaffected in the pH range 4-10 and are diminished below pH 4. Electrode passivation results from adsorption on the edges and planar surfaces of clay platelets.¹⁵¹

A photochemical study of $[\text{Ru}(\text{bpy})_3]^{+2}$ in DMF solvent with chloride ions has appeared. The primary photoproducts observed were $\text{cis-Ru}(\text{bpy})_2\text{Cl}_2$ and $\text{cis-}[\text{Ru}(\text{bpy})_2(\text{DMF})\text{Cl}]^{+1}$.¹⁵²

Disproportionation of $({}^3\text{CT})[\text{Ru}(\text{bpy})_3]^{+2}$ in fluid solution to $[\text{Ru}(\text{bpy})_3]^{+1}$ and $[\text{Ru}(\text{bpy})_3]^{+3}$ is shown to compete with unimolecular relaxation at diffusion-controlled rates.¹⁵³ The photochemistry and electrochemistry of $[\text{Ru}(\text{bpy})_3]^{+2}$ and $[\text{Ru}(\text{bpy})_2(\text{MeCN})_2]^{+2}$ in MeCN solvent with chloride ions has been reported. $[\text{Ru}(\text{bpy})_2(\text{MeCN})\text{Cl}]^{-1}$ is ultimately formed from the comproportionation of $[\text{Ru}(\text{bpy})_3]^{+3}$ and $[\text{Ru}(\text{bpy})_3]^{+1}$, persulfate oxidation of $[\text{Ru}(\text{bpy})_3]^{+1}$, and oxalate reduction of $[\text{Ru}(\text{bpy})_3]^{+3}$. Optical excitation of $[\text{Ru}(\text{bpy})_3]^{+2}$ leads to $[\text{Ru}(\text{bpy})_2(\text{MeCN})_2]^{+2}$. For both $[\text{Ru}(\text{bpy})_3]^{+2}$ and $[\text{Ru}(\text{bpy})_2(\text{MeCN})_2]^{+2}$, the lowest excitation state is responsible for ligand substitution.¹⁵⁴ A review article dealing with recent developments in the spectroscopy of $[\text{Ru}(\text{bpy})_3]^{+2}$ and the nature of the charge transfer excited states has been published.¹⁵⁵ IR and resonance Raman spectra of $[\text{Ru}(\text{bpy})_3]^{+2}$ and several of its deuterated analogs have been measured and interpreted by normal-coordinate analysis.¹⁵⁶ The luminescence of $[\text{Ru}(\text{bpy})_3]^{+2}$ using picosecond laser pulses has been shown to function as an optical step signal for detector testing in the nanosecond time domain.¹⁵⁷

The effect of salts on the bimolecular rate constants and cage escape yields in the oxidative quenching of excited $[\text{Ru}(\text{bpy})_3]^{+2}$ in the presence of methylviologen (MV^{+2}) and $[\text{Ru}(\text{NH}_3)_5(\text{py})]^{+3}$ has been examined in aqueous solution. For specific counterions, electron transfer was observed to be faster with added ClO_4^- than Cl^- , suggesting that the rate of the unimolecular electron-transfer step is dependent on an intermediate encounter complex that includes the gegenanion.¹⁵⁸ Cage escape yields from the quenching of excited $[\text{Ru}(\text{bpy})_3]^{+2}$ by MV^{+2} have also been reported in aqueous solution using pulsed-laser flash photolysis. The primary quantum yield for the formation of $[\text{Ru}(\text{bpy})_3]^{+3}$ was examined as a function of MV^{+2} concentration, ionic strength, and pH.¹⁵⁹ Photoelectron transfer

in multilayered Langmuir-Blodgett films has been reported using excited $[\text{Ru}(\text{bpy})_3]^{+2}$ as the reductant to several acceptor molecules has appeared. The dependence of the rate of photoinduced electron transfer on the free energy change supports the possibility of a Marcus inverted region at highly negative ΔG° values.¹⁶⁰

The synthesis and photochemistry of new, covalently-linked ruthenium(II) dimers have been described. The luminescence properties of the complexes $[\text{Ru}(\text{bpy})_2]_2\text{L}$ [where L = 1,2-bis(4'-methyl-2,2'-bipyridin-4-yl)propane] are contrasted to polymer-bound $[\text{Ru}(\text{bpy})_3]^{+2}$ and the component monomer $[\text{Ru}(\text{bpy})_2\text{L}']^{+2}$ (where L' = 4,4'-dimethyl-2,2'-bipyridine). Intramolecular enhanced quenching was not observed in either of the $[\text{Ru}(\text{bpy})_2]_2\text{L}$ analogues and electron-transfer quenching of excited $[\text{Ru}(\text{bpy})_2]_2\text{L}$ with MV^{+2} is compared with the polymer-bound and component monomer complexes. Kinetic evidence is presented that rules out energy migration between the ruthenium centers in $[\text{Ru}(\text{bpy})_2]_2\text{L}$ and the polymer-bound complex.¹⁶¹ A report demonstrating spontaneous organization of a sensitizer-acceptor-secondary acceptor complex at the surface of a zeolite has appeared. A covalently linked $[\text{Ru}(\text{bpy})_3]^{+2}$ -N,N'-dialkyl-2,2'-bipyridinium complex (RuL_3^{+2} -nDQ⁺) functions as the sensitizer-acceptor portion while the secondary benzylviologen acceptor portion, embedded within a zeolite frame, completes the molecular triad. The photochemistry leading to a long-lived charge-separated state is reported.¹⁶² The presence of novel luminescence in an amide-bridged $[\text{Ru}(\text{bpy})_3]^{+2}$ based dimer has been observed and explained by excimer formation. The cyclic voltammogram for the $\text{Ru}^{+3}/\text{Ru}^{+2}$ couple is quasi-reversible, suggesting a sluggish intradimer electron transfer process.¹⁶³

A closed cage ruthenium(II)-polypyridine complex has been prepared and examined photochemically. The noncryptand, spaced tris-bpy ligand renders the ruthenium(II) complex ca. 10^4 times

more stable than $[\text{Ru}(\text{bpy})_3]^{+2}$ towards photodecomposition. The caged complex also promotes an increased excited state lifetime relative to $[\text{Ru}(\text{bpy})_3]^{+2}$. The reasons for the increased stability are presented.¹⁶⁴

Intramolecular electron transfer in linked $[\text{Ru}(\text{bpy})_3]^{+2}/\text{diquat}^{+2}$ complexes has been measured in acetonitrile solution using time-resolved picosecond emission and absorption spectroscopies. The rate of electron transfer from the metal-to-ligand charge transfer (MLCT) states to the diquat acceptor is readily analyzed by a simple kinetic model where MLCT exciton hopping is fast and electron transfer to the diquat is rate limiting. Electrochemical potentials for the ruthenium +2/+1 and +1/0 redox couples are related to the MLCT state energies and a linear correlation between the driving force and rate of electron transfer is demonstrated. Reverse electron transfer (diquat-ruthenium) is observed to be faster than the forward rate of electron transfer.¹⁶⁵

The chromophoric ligand has been varied in a variety of osmium complexes in order to study the properties of the MLCT excited states. The examined compounds include $[\text{Os}(\text{PP})_3]^{+2}$, $[\text{Os}(\text{PP})_2(\text{py})_2]^{+2}$ and $[\text{Os}(\text{PP})_2(\text{LL})]^{+2}$ [where PP = bpy, 1,10-phen, and substituted derivatives; LL = o-phenylenebis(dimethylarsine), 1,2-bis(diphenylphosphino)methane, cis-1,2-bis(diphenylphosphino)-ethylene, or o-phenylenebis(diphenylphosphine)]. Photophysical and electrochemical data reveal that substituent variations in the chromophoric ligand (PP) have little effect on the $d\pi$ osmium levels based on similar $E_{1/2}$ values for the ground-state $\text{Os}^{+3/+2}$ redox couple. The MLCT absorption or emission energies display a linear correlation to the difference in metal-based oxidation and ligand-based reduction potentials $[E_{1/2}(\text{Os}^{+3/+2}) - E_{1/2}(\text{PP}^{0/-1})]$. The energy gap between the ground and excited states is shown to be responsible for all of the observed spectral properties.¹⁶⁶

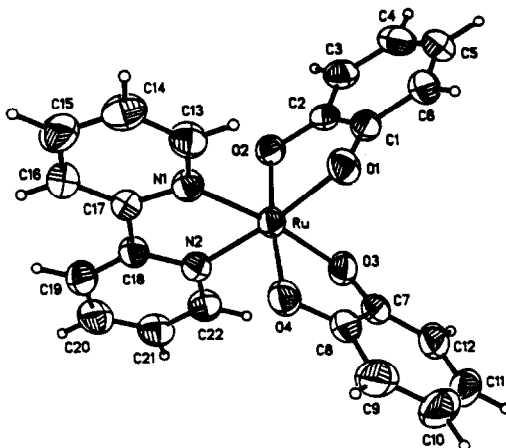
$[\text{RuL}_3]^{+2}$ (where L = bpy or 4,7-dimethyl-1,10-phenanthroline) complexes undergo luminescence quenching by Ag^+ in aqueous solution by the formation of luminescent exciplexes. Both the bimolecular exciplex complex $^*(\text{RuL}_3/\text{Ag})^{+3}$ and the termolecular exciplex complex $^*(\text{RuL}_3/\text{Ag}_2)^{+4}$ have been observed. The spectral properties of the exciplexes, energetics and reaction dynamics are presented.¹⁶⁷

New osmium(II) complexes possessing bpy or 1,10-phen have been prepared using $\text{Os}(\text{bpy})\text{Cl}_4$ or $\text{mer-Os}(\text{PMe}_2\text{Ph})\text{Cl}_3$ as starting materials. Use of the carbonate complex $\text{Os}(\text{bpy})_2\text{CO}_3$ allows for the synthesis of dicationic complexes having the formula $[\text{Os}(\text{bpy})_2(\text{L})_2]^{+2}$ (where L = solvent, phosphine, pyridine, etc.). These complexes have been examined by cyclic voltammetry, UV-visible spectroscopy, emission spectroscopy and NMR spectroscopy.¹⁶⁸

A variable-temperature FTIR study of $\text{Ru}(\text{bpy})_2(\text{NCS})_2$ has been reported and a trans thiocyanate configuration was readily established. Spectral comparison to other analogous thiocyanate complexes is also presented.¹⁶⁹ The ^1H and ^{13}C NMR chemical shifts of $[\text{Ru}(\text{bpy})_3]^{+2}$, $[\text{Ru}\{2-(2\text{-pyridyl})\text{thiazole}\}_3]^{+2}$, $[\text{Ru}\{2-(2\text{-pyrazyl})\text{thiazole}\}_3]^{+2}$, and $[\text{Ru}(2,2'\text{-dithiazole})_3]^{+2}$ have been measured and are compared to the free heterocyclic ligands. Coordination-induced shifts ($\delta_{\text{complexed}} - \delta_{\text{free ligand}}$) have been calculated and are used to assess effects such as electronic σ -donation, $d-\pi^*$ backbonding, van der Waals interactions, and magnetic anisotropy of the chromophoric ligands.¹⁷⁰

$\text{Ru}(\text{bpy})\text{Cl}_3$ has been reacted with various dioxolene ligands to yield new $[\text{Ru}(\text{bpy})(\text{dioxolene})_2]^{+n}$ complexes (where dioxolene = catechol, 3,5-di-tert-butylcatechol, or 3,4,5,6-tetrachlorocatechol; $n = -1, 0, \text{ or } +1$). The oxidation state of these complexes may be controlled to yield catecholate, semiquinone, or quinone based derivatives. A full spectroscopic investigation of the different redox states associated with each

compound is presented along with the ORTEP diagram of $\text{Ru}(\text{bpy})(\text{dioxolene})_2$.¹⁷¹



The redox chemistry, absorption spectra, and luminescence properties of new tris-heteroleptic ruthenium(II) complexes is presented. All of the complexes contain one bipyridine ligand. Three types of ligand-centered and three types of MLCT bands are observed in the absorption spectra with luminescence originating from the lowest lying MLCT triplet state in each complex. The redox chemistry reveals one reversible metal oxidation wave and three reversible reduction waves assigned to separate ligand reduction.¹⁷² The synthesis of these compounds has appeared separately.¹⁷³

The selenocyanate complexes $\text{Ru}(\text{bpy})_2(\text{NCSe})_2$, $[\text{Ru}(\text{bpy})_2(\text{NCSe})\text{Cl}]^{0,+1}$, and $[\text{Cl}(\text{bpy})_2\text{Ru}(\text{NCSe})\text{Ru}(\text{bpy})_2\text{Cl}]^n$ (where $n = +1, +2$, or $+3$) have been prepared and their redox chemistry and vibrational (IR and resonance Raman) spectra reported. The mixed-valence compound $[\text{Cl}(\text{bpy})_2\text{RuNCSeRu}(\text{bpy})_2\text{Cl}]^{+2}$ displays class II charge transfer behavior via pseudosymmetrical π overlap of the $d\pi(\mu) - 3\pi^*(\text{NCSe}) - d\pi(\mu)$ orbitals.¹⁷⁴

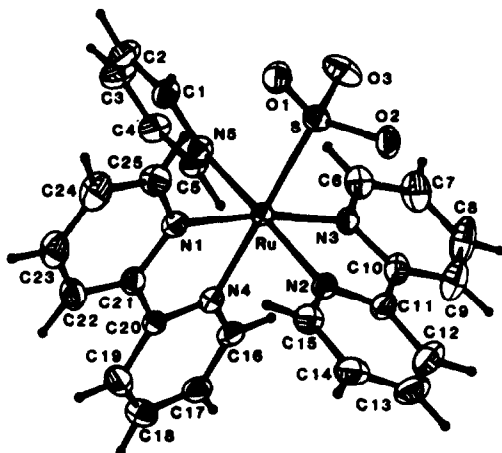
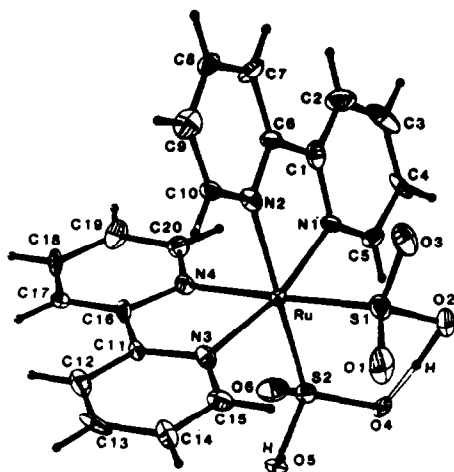
Tri- and tetrametallic ruthenium(II) complexes with ligating 2,2'-bipyrimidine (bpm) and 2,3-bis-(2-pyridyl)quinazoline (bpq) ligands have been synthesized. The homooligonuclear complexes contain a central ruthenium(II) atom as either $[\text{Ru}(\text{bpy})(\text{bpm})_2]^{+2}$, $[\text{Ru}(\text{bpy})(\text{bpq})_2]^{+2}$, or $[\text{Ru}(\text{bpm} \text{ or } \text{bpq})_3]^{+2}$ which may be complexed with two or three $\text{Ru}^{\text{II}}(\text{bpy})_2$ fragments. The resulting complexes, which have the general formula $[\text{Ru}(\text{bpy})(\text{bpmRu}(\text{bpy})_2)_2]^{+6}$, $[\text{Ru}(\text{bpy})(\text{bpqRu}(\text{bpy})_2)_2]^{+6}$, $[\text{Ru}(\text{bpmRu}(\text{bpy})_2)_3]^{+8}$, and $[\text{Ru}(\text{bpqRu}(\text{bpy})_2)_3]^{+8}$, have been studied electrochemically and spectrophotometrically. The energy gap between the $d\pi$ and π^* states may be readily measured using either $\Delta E_{1/2}$ or MLCT energies based on a demonstrated linear free energy relation between the optical and thermodynamic energy gaps.¹⁷⁵

The terpyridyl complexes $[\text{Ru}(\text{trpy})(\text{bpy})(\text{py})]^{+2}$ and $[\text{Ru}(\text{trpy})(4,4'\text{-dph-bpy})(\text{py})]^{+2}$ (where $\text{trpy} = 2,2':6',2''\text{-terpyridine}$ and $4,4'\text{-dph-bpy} = 4,4'\text{-diphenyl-2,2'-bipyridine}$) were examined using spectroelectrochemical techniques. Low-temperature EPR data supports electron localization on the π^* orbital of the trpy ligand during reduction.¹⁷⁶

The complexes $\text{cis-}[\text{Ru}(\text{H}_2\text{O})(\text{bpy})_2(\text{PR}_3)]^{+2}$ (where R = aryl or substituted aryl) have been examined in anation reactions using acetonitrile, 4-acetylpyridine, and chloride ion. The second-order rate constants for ligand substitution are shown to depend on the steric and electronic properties of the coordinated phosphine and the activation parameters support a dissociative-interchange (I_d) mechanism.¹⁷⁷ The anation kinetics for acetonitrile substitution in $\text{trans-}[\text{Ru}(\text{bpy})_2(\text{H}_2\text{O})(\text{OH})]^{+2}$ and $\text{trans-}[\text{Ru}(1,10\text{-phen})_2(\text{H}_2\text{O})(\text{OH})]^{+2}$ have been reported. The reaction is reversible and strongly dependent on the pH. The corresponding ruthenium(III) complexes

catalyze the substitution reaction and the isomerization of the trans diaquo complexes.¹⁷⁸

The acid-base equilibria of coordinated bisulfite have been measured for the complexes $\text{Ru}(\text{bpy})_2(\text{HSO}_3)\text{L}$ (where L = bisulfite, py, or water). The bisulfite ligand reacts with 6 M H_2SO_4 to yield the corresponding SO_2 complex which suggests that the $\text{Ru}(\text{bpy})_2$ moiety is more electrophilic than in $[(\text{NH}_3)_5\text{Ru}]^{+2}$ complexes. The X-ray structures of $\text{Ru}(\text{bpy})_2(\text{HSO}_3)_2$ and $\text{Ru}(\text{bpy})_2(\text{HSO}_3)(\text{py})$ are presented along with the redox chemistry.¹⁷⁹



Mono- and dinuclear bis(bipyridine)ruthenium complexes containing a 3,5-bis(pyridin-2-yl)triazole (bpt) ligand have been prepared and spectroscopically characterized. Both $[\text{Ru}(\text{bpy})_2(\text{bpt})]^{+1}$ and $[\{\text{Ru}(\text{bpy})_2\}_2(\text{bpt})]^{+3}$ are emissive at room temperature and electrochemical measurements reveal that oxidation of the latter complex gives the mixed-valence compound $[\{\text{Ru}(\text{bpy})_2\}_2(\text{bpt})]^{+4}$. A visible intervalence transition at ~750 nm suggests that the mixed-valence dimer should be regarded as a class III charge transfer complex. A proton COSY spectrum of $[\{\text{Ru}(\text{bpy})_2\}_2(\text{bpt})]^{+3}$ is presented, but an unequivocal proton assignment was not possible.¹⁸⁰

Electrocatalytic reduction of CO_2 has been reported using cis- $[\text{Os}(\text{bpy})_2(\text{CO})\text{H}]^{+1}$. CO is the major product under anhydrous conditions with formate being observed under aqueous conditions. Digital simulation of the cyclic voltammograms under electrocatalytic conditions supports an associative mechanism with CO_2 reacting with the reduced complex $[\text{Os}(\text{bpy})_2(\text{CO})\text{H}]^{-1}$ in the rate-limiting step.¹⁸¹ The isocyanide complexes $[\text{Ru}(\text{bpy})_2(\text{CN})(\text{CNMe})]^{+1}$, $[\text{Ru}(\text{bpy})_2(\text{CNMe})_2]^{+2}$, and $[\text{Ru}(\text{bpy})(\text{CNMe})_4]^{+2}$ have been synthesized from the dicyanide complex. The isocyanide ligands cause large hypsochromic shifts in the Ru \rightarrow bpy MLCT transitions and large anodic shifts in the Ru^{+2/+3} redox couple. The excited-state properties (spectral and redox) of all complexes are discussed.¹⁸² Mono- and dinuclear thiocyanato bridged bis(bipyridine)ruthenium complexes have been prepared and examined. The complex $[\text{Ru}(\text{bpy})_2(\text{NCS})\text{Cl}]^{+2}$ is synthesized from the nitrosyl complex while the dimeric complexes are obtained from the reaction of the thiocyanate complex with $[\text{Ru}(\text{bpy})_2(\text{H}_2\text{O})\text{Cl}]^{+1}$. The mixed-valence complex $[\text{Cl}(\text{bpy})_2\text{RuNCSRu}(\text{bpy})_2\text{Cl}]^{+2}$ displays a weak, unsymmetrical intervalence charge transfer band at ~950 nm, suggesting a class II charge transfer complex. The comproportionation constant has

been calculated for production of the latter dimeric (23) complex from the (22) and (33) complexes.¹⁸³

The ^1H NMR chemical shifts of $\text{cis-}[\text{Ru}(\text{bpy})_2(\text{H}_2\text{O})_2]^{+2}$, $\text{cis-}[\text{Ru}(4,4'\text{-Me}_2\text{bpy})_2(\text{H}_2\text{O})_2]^{+2}$, and $\text{cis-}[\text{Ru}(5,5'\text{-Me}_2\text{bpy})_2(\text{H}_2\text{O})_2]^{+2}$ have been reported. The corresponding μ -oxo bridged dimers have been examined using paramagnetic ^1H NMR measurements and the chemical shifts used to follow substitution and oxidation reactions.¹⁸⁴

A report concerning effective, broad band sensitization of TiO_2 to visible light by $[\text{Ru}(2,2'\text{-bipyridyl-4,4'\text{-dicarboxylate})}_2(\text{H}_2\text{O})_2]^{-2}$ has appeared. At pH 4 - 5 the carboxylic acid groups of the bpy ligand are deprotonated, giving rise to the dianion formulation. Photoelectrochemical experiments are described that support electron injection from the ruthenium complex to the conduction band of TiO_2 .¹⁸⁵

The resonance Raman results have been reported for $[\text{Ru}(\text{bpy})_2(\text{DTBSq})]^{+1}$ and $[\text{Ru}(\text{bpy})_2(\text{Q})]^{+2}$ (where DTBSq - 3,5-di-tert-butyl-o-semiquinone and Q = o-quinone) and the identity of the electronic states assigned.¹⁸⁶ Excited-state absorption and resonance Raman spectra of $[\text{Ru}(\text{bpy})_2(1,10\text{-phen})]^{+2}$ and $[\text{Ru}(\text{bpy})_2(\text{DIP})]^{+2}$ (where DIP = 4,7-diphenylphenanthroline) have been reported. The excited-state spectra reveal that the excited-state electron is localized on individual ligands with the bpy^* population being twice that of $1,10\text{-phen}^*$. The DIP complex shows a population reversal with a DIP^* population twice that of bpy^* .¹⁸⁷

New bipyridyl complexes with S-bonded ligands are described. Cis- and trans- $[\text{Ru}(\text{bpy})_2\text{L}_2]^{+2}$, $[\text{Ru}(\text{terpy})\text{L}_2(\text{Cl})]^{+1}$, and cis- $[\text{Ru}(\text{bpy})_2\text{L}(\text{Cl})]^{+1}$ (where L = phenothiazine, 10-methylphenothiazine, Ph_2S , PhSMe , or 1,4-dithiane) have been fully characterized and studied by cyclic voltammetry. Electrochemical oxidation of the phenothiazine complexes in MeCN leads to rapid Ru-S bond scission

and observation of the corresponding acetonitrile complex. The complexes *cis*- and *trans*-[Ru(bpy)₂(phenothiazine-S)₂]⁺² have been examined by X-ray diffraction analysis and their structures compared and the stacking between the bpy and phenothiazine ligands discussed.¹⁸⁸

Coordinated ammonia in [Os(terpy)(bpy)(NH₃)]⁺² has been oxidized in the presence of secondary amines to the corresponding nitrosamine complex [Os(terpy)(bpy)(N(O)NR₂)]⁺². The nitrosamine complexes exhibit a reversible Os^{+2/+3} redox couple and variable-temperature NMR measurements reveal restricted rotation about the N-N bond. The rotational activation barriers for the nitrosamine complexes derived from Et₂NH and morpholine are ~ 8 - 10 kcal/mol lower than for uncomplexed nitrosamines. A plausible oxidation mechanism based on the observed electrochemical stoichiometry (six electrons by coulometry) is presented.¹⁸⁹

The complexes [Ru(tpm)(4,4'-(X)₂-2,2'-bpy)(py)]⁺² [where tpm = tris(1-pyrazolyl)methane; X = C(O)OEt, Ph, Me, NH₂ or H] have been prepared and their MLCT excited states examined. The energy gaps between the (dπ)⁶ ground and (dπ)⁵(π*)¹ excited states increase as the donor ability of the X group increases. A full electrochemical and photophysical evaluation of these complexes is included.¹⁹⁰ The temperature dependent emission lifetimes of the complexes [Ru(bpy)_n(4,4'-dpb-bpy)_{3-n}]⁺² have been examined in propionitrile/ butyronitrile solution from 90-293 K. Photophysical measurements of the ³MLCT emitting level and the photoreactive metal-centered (³MC) level allow calculation of the energy separation between the minimum of the ³MLCT potential curve and the ³MLCT-³MC crossing point.¹⁹¹ Intramolecular energy transfer in the covalently linked dinuclear complex [(bpy)₂Ru(L-L)Ru(biq)₂]⁺⁴ [where L-L = 1,4-bis(2-(4'-methyl-2,2'-bipyridyl-4-yl)ethyl)benzene; biq = 2,2'-biquinoline] has been examined.¹⁹²

The following compounds synthesized for the first time or prepared by a more efficient route include $\text{Ru}(\text{trpy}^*)\text{Cl}_3$, $\text{Ru}(\text{bpy}^*)_2\text{Cl}_2$, $[\text{Ru}(\text{trpy}^*)(\text{bpy})\text{Cl}]^{+1}$, and $[\text{Ru}(\text{trpy}^*(\text{bpy}^*)\text{Cl})]^{+1}$ (where $\text{trpy}^* = 4,4',4''\text{-tri-tert-butylterpyridine}$; $\text{bpy}^* = 4,4'\text{-di-tert-butylpyridine}$), all of which have been examined spectroscopically and electrochemically.¹⁹³

A review on the photophysics, photochemistry, electrochemistry, and chemiluminescence of ruthenium(II) polypyridine complexes has appeared.¹⁹⁴

The nitrile-bridged binuclear complex $[(\text{py})(\text{NH}_3)_4\text{RuNCRu}(\text{bpy})_2(\text{CN})]^{+3}$ and the trinuclear complexes $[(\text{py})(\text{NH}_3)_4\text{RuNCRu}(\text{bpy})_2\text{CNRu}(\text{NH}_3)_4(\text{py})]^{+6}$, and $[(\text{py})(\text{NH}_3)_4\text{RuNCRu}(\text{bpy})_2\text{CNRu}(\text{NH}_3)_5]^{+6}$ have been synthesized and spectroscopically investigated. The binuclear complex is formally a [3,2] localized valence complex while the latter two trinuclear compounds may be considered as [3,2,3] complexes. The redox chemistry, MLCT and intervalence charge-transfer bands are reported and assigned. The intervalence charge-transfer absorption originates from a long-range interaction between the terminal ruthenium centers in the [2,2,3] complexes.¹⁹⁵

The nitrile-bound complex $\text{cis-}[\text{Ru}(\text{bpy})_2(4\text{-cyanopyridine})_2]^{+2}$ has been reacted with $[\text{Fe}(\text{CN})_5(\text{NH}_3)]^{-3}$ and $[\text{Ru}(\text{NH}_3)_5(\text{H}_2\text{O})]^{+2}$ to give binuclear and trinuclear complexes of the form $\text{cis-Ru}(\text{bpy})_2(4\text{-CNpy})_2\text{Fe}(\text{CN})_5$, and $\text{cis-}[\text{Ru}(\text{bpy})_2(4\text{-CNpy})_2\text{Ru}_2(\text{NH}_3)_{10}]^{+6}$, respectively. Spectral and electrochemical data are reported along with chemical oxidation using Br_2 to give valence-trapped mixed-valence complexes where the central $\text{Ru}^{\text{II}}(\text{bpy})_2$ fragment is adjacent to either a $\text{Fe}^{\text{III}}(\text{CN})_5$ or $\text{Ru}^{\text{III}}(\text{NH}_3)_5$ moiety. Visible metal-to-metal charge-transfer adsorption data and the equilibrium constant for the comproportionation reaction involving the [6,8] trinuclear complex are presented.¹⁹⁶

Several new ruthenium complexes derived from di-2-pyridyl ketone have been reported. Spectral and electrochemical studies were carried out and the synthesis of a 1,1-di-2-pyridylethanol complex is described.¹⁹⁷ A study dealing with the acid dependence on photosubstitution quantum yields in $[\text{Ru}(1,10\text{-phen})_3]^{+2}$ has appeared. The results suggest a reactive intermediate with a monodentate phen ligand.¹⁹⁸

The X-ray diffraction structure of trans- $[\text{Ru}(\text{bpy})_2(\text{Ph}_2\text{PNMe})][\text{ClO}_4]_2$ has been published.¹⁹⁹ Reaction of $\text{Ru}(\text{CO})_2\text{Cl}_2$ with 3,6-bis(2-pyridyl)pyridizine (bppi) yields both $[(\text{cis-dicarbonyl})(\text{trans-dichloro})\text{Ru}(\text{bppi})]^{+2}$ and $[(\text{cis-dicarbonyl})(\text{cis-dichloro})\text{Ru}(\text{bppi})]^{+2}$. The bppi complexes were characterized by X-ray diffraction analysis.²⁰⁰

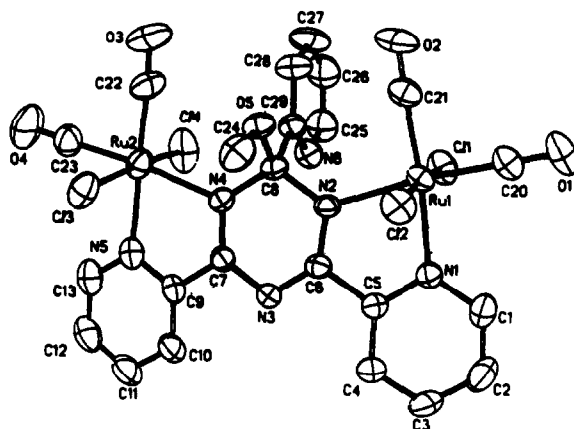
The reaction of $\text{Ru}(\text{DMSO})_4\text{Cl}_2$ and $\text{Ru}(\text{py})_4\text{Cl}_2$ with the heterocyclic ligands bpm, 3,6-di-(2-pyridyl)-1,2,4,5-tetrazine, 2,3-bis(2-pyridyl)-5,6-dihydropyrazine, 2,3-bis(2-pyridyl)-pyrazine (bpp), (bpq)-quinoxaline and 2,3,5,6-tetrakis(2-pyridyl)-pyrazine are described. All new complexes have been spectroscopically characterized.²⁰¹ A report on the reaction between $[\text{Ru}(\text{CO})_2\text{Cl}_2]_n$ and the ligand bpm and bpp has appeared. The product $\text{Ru}(\text{CO})_2\text{Cl}_2\text{L}$ (where L = bpm or bpp) has been further reacted with $[\text{Ru}(\text{CO})_2\text{Cl}_2]_n$ or $\text{M}(\text{DMSO})_2\text{Cl}_2$ (where M = Pd or Pt) to yield the dinuclear complexes $\text{Cl}_2(\text{CO})_2\text{RuLRu}(\text{CO})_2\text{Cl}_2$ or $\text{Cl}_2(\text{CO})_2\text{RuLMCl}_2$, respectively.²⁰²

Solvatochromism in the excited state of cis- $\text{Ru}(1,10\text{-phen})_2(\text{CN})_2$ has been examined. The absorption and emission energies and the temperature dependence of the emission lifetime display a good correlation with Gutmann's solvent acceptor number (AN), supporting an electron donor (complex)-acceptor (solvent) interaction. The linear relationship between the apparent activation energy for emission decay and the solvent AN is

explained by the presence of a solvent-dependent energy level in the lowest emitting MLCT excited state.²⁰³

Ruthenium(II) complexes with the heterocyclic ligand 1,4,5,8-tetraazaphenanthrene (tap) have been prepared. The ground- and excited-state basicities of $[Ru(bpy)_n(tap)_{3-n}]^{+2}$ (for $n = 0, 1, 2$) are reported along with carboxylic acid promoted luminescence quenching studies.²⁰⁴

Reaction of 2,4,6-tris(2-pyridyl)-1,3,5-triazine (tpt) with $[Ru(CO)_2Cl_2]_x$ gives the diruthenium complex $[\mu-tpt]_2[Ru(CO)_2Cl_2]_2$. Each ruthenium is ligated in a bidentate fashion by a pyridine and triazine nitrogen atom. The triazine ring in this complex is activated towards MeOH attack. The methoxide-substituted complex has been characterized in solution and by X-ray diffraction analysis.²⁰⁵



The redox properties of aqua complexes of $Ru^{II}(terpy)$ and $Ru^{II}(tpm)$ are described. *cis*- and *trans*- $[(terpy)(pic)Ru(H_2O)]^{+2}$ (where pic = picolinate anion) exhibit two chemically reversible one-electron oxidations to the $Ru(IV)/Ru(III)$ and $Ru(III)/Ru(II)$ couples. These electrochemical couples are strongly dependent on the pH as demonstrated by Pourbaix plots. The properties and

electrochemistry of the μ -oxo ions cis- and trans- $[(\text{terpy})(\text{pic})\text{Ru}^{\text{III}}]_2\text{O}]^{+2}$ are also reported.²⁰⁶

Intense electrogenerated chemiluminescence has been observed with $[\text{Os}(\text{bpz})_3]^{+2}$ (where bpz = 2,2'-bipyrazine).²⁰⁷

Exciplex formation between Ag^+ ions and the lowest excited state of $[\text{Ru}(\text{bpz})_3]^{+2}$ has been demonstrated in aqueous or acetonitrile solution. Stern-Volmer quenching studies as a function of $[\text{Ag}^+]$ have been carried out and indicate that up to six Ag^+ ions define the exciplex complex. No ground state interaction between $[\text{Ru}(\text{bpz})_3]^{+2}$ and Ag^+ ions is detected.²⁰⁸ The excited state of $[\text{Ru}(\text{bpz})_3]^{+2}$ is readily quenched by persulfate, $[\text{Co}(\text{NH}_3)_5\text{Cl}]^{+2}$, and protons at pH 0. Microsecond flash studies show that $^*[\text{Ru}(\text{bpz})_3]^{+2}$ is quenched oxidatively by persulfate to give the strong and unstable oxidant $[\text{Ru}(\text{bpz})_3]^{+3}$. Photo-oxidation of water from this latter complex is described.²⁰⁹ The one-electron reduction of $[\text{Ru}(\text{bpz})_3]^{+2}$ has been examined using radiolytically generated radicals in aqueous solution. The resulting ligand-radical complex may be regarded as $[\text{Ru}(\text{bpz})_2(\text{bpz}^-)]^{+1}$. HO radicals react with $[\text{Ru}(\text{bpz})_3]^{+2}$ to give an intermediate OH-ring attack adduct that undergoes a bimolecular decay near diffusion limits while reaction with H^\cdot results in hydrogenation at a ring carbon.²¹⁰ A temperature dependence study on the electrogenerated chemiluminescence efficiency (η_{ECL}) of $[\text{Ru}(\text{bpz})_3]^{+2}$ has been reported. A mechanistic interpretation is presented based on the measured luminescence quantum yields and η_{ECL} values.²¹¹ The resonance Raman spectra of $[(\text{Ru}(\text{NH}_3)_5)_n\text{bpz}]^{+2n}$ (where $n = 1, 2$) and $[\text{Ru}(\text{bpz})_3(\text{Ru}(\text{NH}_3)_5)_6]^{+14}$ have been measured as a function of wavelength through the MLCT bands. The latter heptanuclear complex exhibits three types of excitation profiles, consistent with three

MLCT bands involving the peripheral and central ruthenium(II) ions and two π^* levels of the bpz ligand.²¹²

Optical electron transfer in the mixed-valence complex $[(\text{NH}_3)_5\text{Ru}^{\text{II}}-4,4'\text{-bpy-Ru}^{\text{III}}(\text{NH}_3)_5]^+5$ has been studied in mixed solvents in order to investigate molecular aspects of solvent reorganization. The experimental data, corrected for unsymmetrical selective solvation effects, suggests that the majority of solvent reorganization originates from reorientations within the first molecular solvent layer.²¹³ A report dealing with ruthenium and osmium complexes reveals that the activation parameters and separation distances for electron transfer may be used to provide information concerning the relative importance of nuclear and electronic factors in determining the distance dependence of electron-transfer rates.²¹⁴

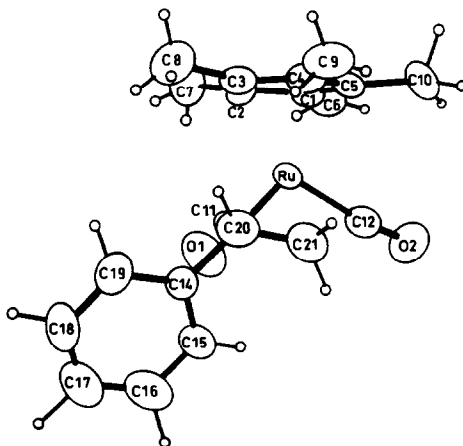
The synthesis, characterization, and oxidation reactivity of the nitro complexes $\text{trans-}[\text{Ru}(\text{terpy})(\text{PMe}_3)_2(\text{NO}_2)]^{+n}$ (where $n = 1, 2$) have appeared. The nitroruthenium(III) complex reacts with benzyl alcohol to give benzaldehyde and the nitroruthenium(II) complex. The second-order rate constants for benzaldehyde and butanol oxidation have been measured at 5 °C. $\text{Trans-}[\text{Ru}(\text{terpy})(\text{PMe}_3)_2(\text{NO}_2)]^{+2}$ is also shown to epoxidize norbornene to produce the exo oxirane and the nitrosyl complex $\text{trans-}[\text{Ru}(\text{terpy})(\text{PMe}_3)_2(\text{NO})]^{+2}$. The nitrosyl complex is shown to react rapidly with unreacted $\text{trans-}[\text{Ru}(\text{terpy})(\text{PMe}_3)_2(\text{NO}_2)]^{+2}$ via fast electron transfer to furnish $\text{trans-}[\text{Ru}(\text{terpy})(\text{PMe}_3)_2(\text{NO}_2)]^{+1}$ and $\text{trans-}[\text{Ru}(\text{terpy})(\text{PMe}_3)_2(\text{NO})]^{+3}$.²¹⁵

(h) Alkenyl and Alkylidene Complexes

CS_2 insertion into the ruthenium-alkenyl bond of $\text{Ru}(\text{CO})\text{Cl}(\text{PPh}_3)_2(\text{HC}=\text{CCHR})$ (where $\text{R} = \text{Ph}$ or $t\text{-Bu}$) does not give the dithioester, but rather the alkenedithiocarboxylate complexes $\text{Ru}(\text{CO})\text{Cl}(\text{PPh}_3)_2(\text{S}_2\text{CCH}=\text{CHR})$. Full spectroscopic characterization

along with the X-ray diffraction results of the phenyl derivative are reported.²¹⁶

The methoxymethyl complex $(\eta^5\text{-C}_5\text{Me}_5)\text{Ru}(\text{CO})_2(\text{CH}_2\text{OMe})$ has been reacted with $[\text{Ph}_3\text{C}][\text{BF}_4]$ to yield the secondary methoxycarbene complex $[(\eta^5\text{-C}_5\text{Me}_5)\text{Ru}(\text{CO})_2(\text{CHOME})]^+1$. Low-temperature NMR measurements (^1H and ^{13}C) reveal that carbene formation is under kinetic control. The initial cis/trans carbene ratio of 95:5 (at -80°C) readily equilibrates to the more thermally stable trans isomer upon warming. Isomerism results from restricted carbene carbon-oxygen bond rotation. Carbene insertion into the Si-H bond of Et_3SiH and Me_2PhSiH yields the corresponding methoxymethyl silanes while the silanes Ph_3SiH , Ph_3SiMe and Ph_3SiOMe react by a hydride/methoxide exchange pathway. The X-ray structure of $[(\eta^5\text{-C}_5\text{H}_5)\text{Ru}(\text{CO})_2(\text{CH}_2=\text{CHPh})]^+1$ is also presented.²¹⁷



A X-ray diffraction study of the methoxymethyl carbene complex $[(\eta^5\text{-C}_5\text{H}_5)\text{Ru}(\text{PPh}_3)_2(\text{CMeOMe})]^+1$ has appeared. The carbene complex was prepared by reacting $[(\eta^5\text{-C}_5\text{H}_5)\text{Ru}(\text{PPh}_3)_2(\text{MeCN})]^+1$ with trimethylsilyl acetylene in MeOH solvent.²¹⁸

(i) π -Complexes

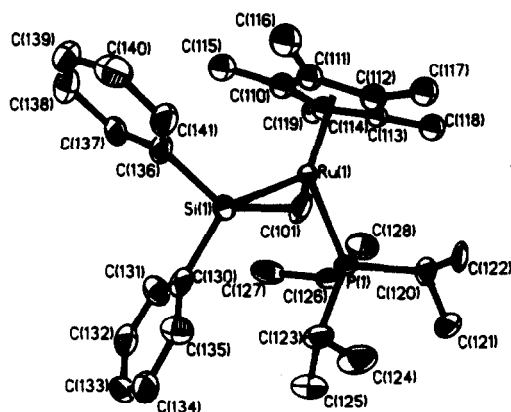
The cyclopentadienyl complexes $(\eta^5\text{-C}_5\text{H}_5)\text{Ru}(\text{Me}_n\text{PPh}_{3-n})_2\text{R}$ and $(\eta^5\text{-C}_5\text{Me}_5)\text{Ru}(\text{Me}_n\text{PPh}_{3-n})_2\text{R}$ (where R = neopentyl or methyl; n = 0-3) have been prepared and their thermolysis reactions studied. The ruthenium-methyl complexes eliminate methane on warming with concomitant intramolecular activation of an ortho H-C (phosphorous phenyl) bond; the neopentyl complexes react intermolecularly with benzene solvent to give neopentane and the corresponding ruthenium-phenyl complexes. Reaction of the phenyl complexes $(\eta^5\text{-C}_5\text{H}_5)\text{Ru}(\text{PPh}_3)_2\text{Ph}$ in toluene leads to an equilibrium mixture of m- and p-tolyl complexes. For comparable reactions, the $(\eta^5\text{-C}_5\text{Me}_5)\text{Ru}$ complex is more reactive than the $(\eta^5\text{-C}_5\text{H}_5)\text{Ru}$ complex in C-H bond activation. An ORTEP diagram of $(\eta^5\text{-C}_5\text{H}_5)\text{Ru}(\text{PMe}_3)(\text{PPh}_3)(\text{CH}_2\text{CMe}=\text{CH}_2)$ is presented.²¹⁹

Two reports dealing with $(\eta^5\text{-C}_5\text{H}_5)\text{Os}(\text{CO})(\text{L})\text{R}$ (where L = CO or phosphine; R = alkyl or aryl) have appeared. Photolysis of $(\eta^5\text{-C}_5\text{Me}_5)\text{Os}(\text{CO})_2(\text{benzyl})$ in the presence of Me_2PPh leads to both $(\eta^4\text{-C}_5\text{Me}_5\text{benzyl})\text{Os}(\text{CO})_2(\text{Me}_2\text{PPh})$ and $(\eta^5\text{-C}_5\text{Me}_5)\text{Os}(\text{CO})(\text{Me}_2\text{PPh})(\text{COCH}_2\text{Ph})$. Homolytic scission of the Os-benzyl bond, followed by radical addition to the $(\eta^5\text{-C}_5\text{Me}_5)$ ring, is postulated in the formation of the former complex.²²⁰ The electrophiles Br_2 , CF_3COOH , and HgBr have been reacted with different $(\eta^5\text{-C}_5\text{Me}_5)\text{Os}(\text{CO})(\text{L})\text{R}$ complexes to ultimately yield normal electrophilic cleavage products. Use of HgBr_2 when L = Me_2PPh and R = Me has allowed isolation of the intermediate osmium(IV) complex $[(\eta^5\text{-C}_5\text{Me}_5)\text{Os}(\text{CO})(\text{Me}_2\text{PPh})(\text{Me})(\text{HgBr})]^+.$ ²²¹

Reaction of $(\eta^5\text{-C}_5\text{H}_5)\text{Ru}(\text{PPh}_3)_2\text{Cl}$ with $(\text{ME}_4)^{-2}$ (where M = Mo or W; E = S or Se) gives the new organoruthenium tetrathio- and tetraselenometalates $[(\eta^5\text{-C}_5\text{H}_5)\text{Ru}(\text{PPh}_3)_2]_2\text{ME}_4$. Both PPh_3 ligands may be replaced with PMe_3 and isocyanides while only one PPh_3 ligand is replaced when treated with CO. The kinetics of the first

substitution step with *t*-BuNC have been examined and are found to be independent of *t*-BuNC. The redox properties of the new complexes and the X-ray structure of $[(\eta^5\text{-C}_5\text{H}_5)\text{Ru}(\text{t-BuNC})_2]_2\text{WS}_4$ are reported.²²² The synthesis, spectral properties, and X-ray diffraction structure of $[(\eta^5\text{-C}_5\text{H}_5)\text{Ru}(\text{PPh}_3)_2(\text{thiirane})]^{+1}$ have been reported. This transition-metal analogue of an episulfonium salt was obtained from the reaction of the ruthenium triflate complex $(\eta^5\text{-C}_5\text{H}_5)\text{Ru}(\text{PPh}_3)_2\text{OTf}$ with thiirane.²²³

The 16-electron ruthenium-silyl complex $(\eta^5\text{-C}_5\text{Me}_5)\text{Ru}(\text{PCy}_3)\text{CH}_2\text{SiMe}_2\text{H}$, prepared from the corresponding ruthenium chloride complex and $\text{ClMgCH}_2\text{SiMe}_2\text{H}$, undergoes a β -elimination to give the thermally unstable η^2 -silene complex $(\eta^5\text{-C}_5\text{Me}_5)\text{Ru}(\text{PCy}_3)(\text{H})(\eta^2\text{-CH=SiMe}_2)$. The stable silene complex $(\eta^5\text{-C}_5\text{Me}_5)\text{Ru}(\text{P}(i\text{-Pr})_3)(\text{H})(\eta^2\text{-CH}_2\text{=SiPh}_2)$ has been prepared similarly and the presence of the η^2 -silene group confirmed by spectroscopic measurements and X-ray diffraction analysis.²²⁴



$\text{Ru}(\text{PPh}_3)_3\text{Cl}_2$ reacts with $\text{C}_5\text{H}_5\text{CH}_2\text{CH}_2\text{PPh}_2$ to give the cyclopentadienyl complexes $(\eta^5\text{-C}_5\text{H}_4\text{CH}_2\text{CH}_2\text{PPh}_2)\text{Ru}(\text{PPh}_3)\text{Cl}$ which has been structurally and spectroscopically characterized. An

anomalous high-field cyclopentadienyl ^1H resonance (δ 2.27 at room temperature; δ 1.91 at -60°C) is ascribed to a shielding effect originating from the PPh_3 ligand. Reaction of this compound with $\text{P}(\text{OMe})_3$ or $\text{AgBF}_4/(\text{+})\text{-PhCH}(\text{Me})\text{NH}_2$ affords the $\text{P}(\text{OMe})_3$ complex and a diastereomeric mixture of $[(\eta^5\text{-C}_5\text{H}_4\text{CH}_2\text{CH}_2\text{PPh}_2)\text{Ru}(\text{PPh}_3)\{(\text{+})\text{-NH}_2\text{CH}(\text{Me})\text{Ph}\}]^+.$ ²²⁵ The X-ray structure of $(\eta^5\text{-C}_5\text{H}_5)\text{Ru}(\text{PPh}_3)$ (dimethyldithiocarbamate), prepared from $[(\eta^5\text{-C}_5\text{H}_5)\text{Ru}(\text{PPh}_3)_2(\text{HSC}_3\text{H}_7)]^+$ and sodium dimethyldithiocarbamate, has been presented.²²⁶

Several new bis(polyene) ruthenium(II) complexes have been prepared and examined. $[(\eta^5\text{-C}_5\text{H}_5)\text{Ru}(\text{MeCN})_3]^+$ has been reacted with indoles to give the mixed-polyene complexes $[(\eta^5\text{-C}_5\text{H}_5)\text{Ru}(\eta^6\text{-indole})]^+.$ ²²⁷ Malonates, alkoxides, amines, and the disodium salt of mercaptoacetic acid all react with the 4- and 5-chloroindole derivatives by a $\text{S}_{\text{N}}\text{Ar}$ mechanism to yield substituted indoles.²²⁷ Unsymmetrical ruthenocenes have been synthesized from polymeric $[(\eta^5\text{-C}_5\text{Me}_5)\text{RuCl}_2]_n$ and alkali metal salts of cyclopentadienyl compounds. Direct reaction of diazotetrachlorocyclopentadienyl with the above oligomer affords $(\eta^5\text{-C}_5\text{Me}_5)\text{Ru}(\eta^5\text{-C}_5\text{Cl}_5).$ The redox properties and XPS data were examined and the electronic effects of the ligands assessed. X-Ray results for $(\eta^5\text{-C}_5\text{Me}_5)\text{Ru}(\eta^5\text{-L})$ (where $\eta^5\text{-L}$ = pentachlorocyclopentadienyl, indenyl, or fluorenyl) are presented.²²⁸ The η^3 -cyclopropenyl complexes $(\eta^5\text{-C}_5\text{R}_5)\text{Ru}(\eta^2\text{-C}_3\text{Ph}_3)\text{X}_2$ (where $\text{R} = \text{H}$ or Me ; $\text{X} = \text{Cl}$ or Br) have been obtained from the oxidative addition of BrC_3Ph_3 to $(\eta^5\text{-C}_5\text{H}_5)\text{Ru}(1,5\text{-COD})\text{X}$ and $[(\eta^5\text{-C}_5\text{Me}_5)\text{RuCl}]_4.$ The dibromo complex $(\eta^5\text{-C}_5\text{H}_5)\text{Ru}(\eta^3\text{-C}_3\text{Ph}_3)\text{Br}_2$ has been examined crystallographically. Metathetical halide displacements and NMR (^1H and ^{13}C) measurements on cyclopropenyl rigidity are reported.²²⁹ Two reports on the synthesis and organ

distribution studies of isotopically labelled (^{103}Ru)ruthenocene derivatives have appeared.^{230, 231}

π -Bound benzo[b]thiophene (BT) complexes of ruthenium have been investigated as models for hydrodesulfurization processes. Reaction of $[(\eta^5\text{-C}_5\text{H}_5)\text{Ru}(\text{MeCN})_3]^+1$ or $(\eta^5\text{-C}_5\text{H}_5)\text{Ru}(\text{PPh}_3)_2\text{Cl}$ and AgBF_4 in the presence of the desired benzo[b]thiophene gives $[(\eta^5\text{-C}_5\text{H}_5)\text{Ru}(\eta^6\text{-BT})]^+1$. The X-ray structure and spectroscopic properties of this complex are reported.²³² Reactions of H^- , MeO^- malonate, ETS^- , and phosphines with the above BT complex proceed by η^6 -ring attack to yield the corresponding neutral cyclohexadienyl complex $(\eta^5\text{-C}_5\text{H}_5)\text{Ru}(\text{BH-nucleophile})$. Of the four isomers observed by nucleophilic attack on a protonated carbon, the major isomer is shown to result from nucleophile addition to the carbon closest to the sulfur atom (C-7). The cyclohexadienyl complex resulting from hydride addition to C-7 has been obtained from the crude isomeric mixture and characterized crystallographically. Hydride abstraction studies using $[\text{Ph}_3\text{C}][\text{BF}_4]$ reveal that the four isomeric cyclohexadienyl complexes react at different rates to regenerate the starting cationic BT complex.²³³

^1H and ^{13}C NMR studies reveal a static arene in the complexes $(\eta^6\text{-1,4-t-BuC}_6\text{H}_4)\text{Ru}(\text{CO})(\text{SiMe}_3)_2$, $(\eta^6\text{-1,4-t-BuC}_6\text{H}_4)\text{Ru}(\text{CO})(\text{GeCl}_3)_2$, and $(\eta^6\text{-1,4-t-BuC}_6\text{H}_4)\text{Os}(\text{CO})(\text{SiCl}_3)_2$. The importance of ring tilting in arene rotation is discussed using other substituted arene complexes as comparative examples.²³⁴ The reaction between $[(\eta^6\text{-C}_6\text{Me}_6)\text{RuCl}_2]_2$ and dimethyl phosphite affords the complex anion $[(\eta^6\text{-C}_6\text{Me}_6)\text{RuCl}(\text{P}(\text{O})(\text{OMe})_2)_2]^{-1}$ which has been further reacted with copper powder under CO to give the O,O,Cl-chelate ligand complex $[(\eta^6\text{-C}_6\text{Me}_6)\text{RuCl}(\text{P}(\text{O})(\text{OMe})_2)_2](\text{CuCO})$.^{235,236} Dimeric $[(\eta^6\text{-C}_6\text{H}_6)\text{RuCl}_2]_2$ has been reacted with PhOTf to give $[(\eta^6\text{-C}_6\text{H}_6)_2\text{Ru}_2(\mu_2\text{-OPh})_3]^+1$.

Treatment of the phenolate cation with H_2O yields the tri(hydroxy) bridged complex $[(\eta^6-C_6H_6)_2Ru_2(\mu_2-OH)_3]^{+1}$ which has been isolated and characterized by 1H NMR and X-ray diffraction analysis.²³⁷ A X-ray structure for $[(\eta^6-C_6Me_6)RuCl_2]_2$ has been reported and no unusual features were observed.²³⁸

Hydride addition to the arene ring in $[(\eta^6-C_6H_6)Os(PMe_3)_2I]^{+1}$ gives the corresponding neutral cyclohexadienyl complex $(\eta^5-C_6H_7)Os(PMe_3)_2I$ in quantitative yield. Sodium amalgam reduction furnishes the highly reactive anion $[(\eta^5-C_6H_7)Os(PMe_3)_2]^{-1}$ which has been reacted with a NH_4PF_6/I_2 mixture to give $(\eta^5-C_6H_7)Os(PMe_3)_2H$ and $(\eta^4-C_6H_8)OsH(I)(PMe_3)_2$. The η^4 -ligand in the latter complex is formulated as a coordinated 1,3-cyclohexadiene moiety based on NMR analysis.²³⁹

The aqua compounds $[(\eta^6-C_6H_6)M(H_2O)_3]^{+2}$ (where $M = Ru$ or Os) have been obtained from the reaction of $[(\eta^6-C_6H_6)MCl_2]_2$ with Ag^+ ions in H_2O or treatment of $[Ru(H_2O)_6]^{+2}$ with cyclohexadiene in EtOH. ^{17}O NMR experiments at variable temperature and pressure have been examined and the water-exchange rates measured. H_2O exchange is observed to be three orders faster in the arene complexes than in $[M(H_2O)_6]^{+2}$. Activation parameters supporting an interchange mechanism (I) with equal bond breaking and making contributions and the X-ray structure of $[(\eta^6-C_6H_6)Ru(H_2O)_3]^{+2}$ are presented.²⁴⁰

III. Dinuclear Complexes

(a) Homonuclear Complexes

Thirteen reports have appeared dealing with the synthesis and properties of ruthenium and osmium bridged carboxylate compounds. $Os_2(O_2CCH_3)_4Cl_2$ has been examined by Raman spectroscopy and the $\nu(OsOs)$, $\nu(OsO)$, and $\nu(OsCl)$ stretching bands assigned. FTIR

studies of the deuterated complex have been conducted and used in the unequivocal assignment for many of the infrared and Raman stretching bands.²⁴¹ The same acetate complex has been reacted with 2-diphenylphosphinopyridine to give $\text{Os}_2(\text{O}_2\text{CCH}_3)(\text{Ph}_2\text{Ppy})_2\text{Cl}_4$. X-Ray diffraction analysis reveals a cisoid orientation of the two Ph_2Ppy ligands which are arranged in a head-to-tail fashion. The observed Os-Os bond distance suggests a formal bond of 2.5.²⁴² Extensive Raman and FTIR studies of the carboxylate complexes $\text{Os}_2(\text{O}_2\text{CR})_4\text{Cl}_2$ (where R = CH_2Cl , Et, or Pr) are reported. The $\nu(\text{OsOs})$ and $\nu(\text{OsCl})$ stretching bands are insensitive to the nature of the R group. The electronic and resonance-Raman spectra support a $\sigma^2\pi^4\delta^2\pi^*\delta^*$ ground state configuration.²⁴³ $\text{Os}_2(\text{O}_2\text{CCH}_3)_2(\text{CO})_6$ reacts with $\text{CF}_3\text{CO}_2\text{H}$ to yield the osmium(II) mononuclear complex $\text{Os}(\text{O}_2\text{CCF}_3)_2(\text{CO})_3$. The same complex is also obtained from $\text{Os}_3(\text{CO})_{12}$ and $\text{CF}_3\text{CO}_2\text{H}$ at elevated temperatures. Reaction of $\text{CF}_3\text{CO}_2\text{H}$ with the more basic, axially substituted carboxylates $\text{Os}_2(\text{O}_2\text{CCH}_3)_2(\text{CO})_4\text{L}_2$ (where L = PMe_2Ph , PMePh_2 , PPh_3 , or pyridine) leads to protonation of the Os-Os bond. The resulting complexes $[\text{Os}_2(\text{O}_2\text{CCH}_3)_2(\mu_2\text{-H})(\text{CO})_4\text{L}_2]^+$ have been spectroscopically characterized and the X-ray structure of the PMe_2Ph complex reported.²⁴⁴

Electronic absorption data has been presented for $[\text{Ru}_2(\text{butyrate})_4\text{X}_n]^{(1-n)+}$ (where X = Cl, Br, or I; n = 0, 1, or 2) in different solvents along with single-crystal visible absorption data for $\text{Ru}_2(\text{propionate})_4\text{Cl}$, $\text{Ru}_2(\text{acetate})_4\text{Cl}$, $\text{Ru}_2(\text{butyrate})_4\text{Br}$, and two crystal forms of $\text{Ru}_2(\text{butyrate})_4\text{Cl}$.²⁴⁵ Near-infrared and Raman spectral data are presented for $\text{Ru}_2(\text{O}_2\text{CH})_4\text{Cl}$ and $[\text{Ru}_2(\text{O}_2\text{CH})_4\text{Cl}_2]^{-1}$. The $\nu(\text{RuRu})$, $\nu(\text{RuCl})$, and $\nu(\text{RuO})$ stretching bands have been assigned and the observed vibronic intensities of the formate complexes compared to similar carboxylate complexes.²⁴⁶ $\text{Ru}_2(\text{propionate})_4\text{Cl}$ has been reacted with AgO_2CCH_3 and propionic acid

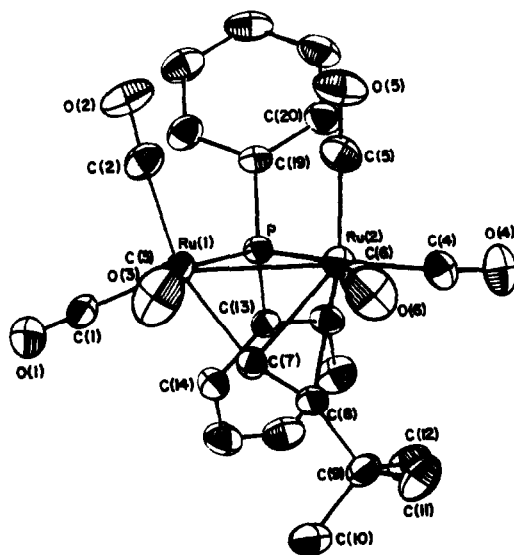
to give $\text{Ru}_2(\text{propionate})_5$ which has been characterized by X-ray diffraction analysis. The structural data for the known acetate complex $\text{Ru}_2(\text{acetate})_6 \cdot 0.7\text{H}_2\text{O}$ suggests that the structure is more accurately represented as $\text{Ru}_2(\text{acetate})_4(\text{acetate})_2 \cdot 0.7\text{H}_2\text{O}$. The spectral and redox properties of these dimers are presented along with the crystallographic structures of the propionate and trifluoroacetate derivatives.²⁴⁷ The reaction of $\text{Ru}_2(\text{O}_2\text{CR})_4\text{Cl}$ (where R = Me or Ph) with AgO_2CCF_3 in MeOH gives the mixed-carboxylate, monotrifluoroacetate complexes $[\text{Ru}_2(\text{O}_2\text{CR})_4(\text{O}_2\text{CCF}_3)_2\text{L}_2]$ (where L = MeOH or H_2O). Use of CF_3COOH furnishes $\text{Ru}_2(\text{O}_2\text{CR})_2(\text{O}_2\text{CCF}_3)_3(\text{H}_2\text{O})_{0.5}$ which upon oxidation gives the paramagnetic Ru_2^{+6} complex $\text{Ru}_2(\text{O}_2\text{CR})_2(\text{O}_2\text{CCF}_3)_4(\text{H}_2\text{O})_2$. Spectral and redox data are reported and structures of the tris- and tetrakis-(trifluoroacetate) complexes presented.²⁴⁸ The synthesis and spectral properties of ruthenium tetraarylcarboxylates have been reported. The complexes $\text{Ru}_2(\text{O}_2\text{CR})_4\text{Cl}$ (where R = Ph or p-MeOC₆H₄) all exhibit a quasi-reversible one-electron reduction at ca. 0.0 V vs. SCE.²⁴⁹ A report of new μ_2 -hydroxo- and μ_2 -oxobis(μ_2 -acetato)diruthenium complexes exhibiting weak intramolecular Ru^{III}-Ru interactions has appeared. Temperature-dependent magnetic moment data and X-ray diffraction structures are presented.²⁵⁰

Reaction of diphosphines and dithioethers with $\text{Ru}_2(\text{O}_2\text{CR})_2(\text{CO})_4(\text{MeCN})_2$ or $[\text{Ru}_2(\text{O}_2\text{CR})_2(\text{CO})_4]_x$ (where R = Me or Et) leads to ruthenium(I) polymers $[\text{Ru}_2(\text{O}_2\text{CR})_2(\text{CO})_4(\mu\text{-L})]_x$ or dinuclear complexes with bridging or chelating ligands. The X-ray structure of $[\text{Ru}_2(\text{O}_2\text{CMe})(\text{CO})_4(\text{L}_2)_2]^{+1}$ (where $\text{L}_2 = \text{dppm}$ or dppe) is reported.²⁵¹

Gas-phase UV photoelectron (both He I and II) spectroscopy and SCF first principle discrete (DV) X α calculations have been used to determine the electronic structure of $\text{Ru}_2(\text{CO})_4(\text{R-DAB})(\mu_2\text{-CO})$ and $\text{Ru}_2(\text{CO})_4(\text{R-DAB})(\mu\text{-acetylene})$ (where R-DAB = 1,4-diaza-1,3-

butadiene). Both theory and experiment confirm the absence of any direct Ru-Ru interaction.²⁵²

The complexes $M_2(CO)_6(\mu_2-\eta^2-C=CR)(\mu_2-PPh)_2$ (where $M = Ru$ or Os ; $R = Ph, t-Bu, \text{ or } i-Pr$) are obtained by pyrolysis of $M_3(CO)_{11}(Ph_2PC=CR)$. The crystallographic structures of $Ru_2(CO)_6(\mu_2-\eta^2-C=C-t-Bu)(\mu_2-PPh)_2$ and the analogous osmium complex are reported. Variable-temperature NMR measurements (1H , ^{13}C , and ^{31}P) reveal two fluxional processes that involve acetylide $\sigma-\pi$ interchange and $M(CO)_3$ trigonal rotation.²⁵³ The alkyne complexes $M_2(CO)_6[\mu_2-CHC(Ph)NEt_2](\mu_2-PPh)_2$ have been prepared by addition of Et_2NH to the above phenylacetylide complexes. The spectral properties and X-ray structures of both zwitterionic μ_2 -alkylidene complexes are presented.²⁵⁴



An electrochemical investigation of the ruthenium flyover bridge complexes $Ru_2(CO)_6[C(R)=C(R')COC(R'')=C(R''')]$ (where $R', R'', \text{ and } R''' = \text{either Me or Ph}$) has appeared. All derivatives exhibit a one-electron reduction process that is reversible only at high

scan rates ($> 20 \text{ V s}^{-1}$) along with an irreversible oxidation wave. Cyclic voltammetric studies suggest that the oxidation process represents a one-electron totally irreversible charge transfer.²⁵⁵

Lithium di-*p*-tolyltriazene has been reacted with $\text{Ru}_2(\text{OAc})_4$ to yield the diamagnetic ruthenium(II) complex $\text{Ru}_2[(p\text{-CH}_3\text{C}_6\text{H}_4)\text{NNN}(p\text{-CH}_3\text{C}_6\text{H}_4)]_4$. Characterization by X-ray diffraction analysis, cyclic voltammetry, and NMR and absorption spectroscopy is included. The solid-state structure possesses idealized D_{4h} symmetry as required for an eclipsed conformation. A ground state electron configuration of $\sigma^2\pi^4\delta^2\pi^*4$ is proposed based on the eclipsed conformation and short Ru-Ru bond (2.417 Å).²⁵⁶

Dithiobis(β -diketones) have been reacted with $\text{RuH}(\text{Cl})(\text{CO})(\text{PPh}_3)_2$ and $[\text{RuCl}(\text{CO})(\text{PPh}_3)_2(\text{acrylonitrile})]_2$ to give $[\text{RuCl}(\text{CO})(\text{PPh}_3)_2]_2\text{L}$, $[\text{RuH}(\text{CO})(\text{PPh}_3)_2]_2\text{L}$, and $[\text{Ru}(\text{CO})(\text{PPh}_3)_2(\text{acrylonitrile})]_2\text{L}$ [where $\text{L} = \{\text{RC}(\text{O})\text{CHC}(\text{O})\text{R}\}_2\text{S}_2$ and $\text{R} = \text{Me}$ or Ph]. Treatment of the product disulfides with MeLi leads only to decomposition with no evidence for mercaptan complexes.²⁵⁷

The X-ray structure of $\text{Os}_2(\text{CO})_6(\mu_2\text{-Br})(\text{Br})_2[\mu\text{-OCNHCH}(\text{Me})_2]$, prepared from the reaction of Br_2 with $\text{Os}_3(\text{CO})_{10}(\mu_2\text{-H})[\mu\text{-OCNHCH}(\text{Me})_2]$ has been reported. The molecule consists of two $\text{Os}(\text{CO})_3$ groups and one terminal bromine group that are trans to each other.²⁵⁸

The diaosmacyclopropane complex $\text{Os}_2(\text{CO})_8(\mu_2\text{-CHMe})$ has been prepared from $\text{Os}_2(\text{CO})_8^{-2}$ and the bistriflate $\text{CH}_3\text{CH}(\text{OTf})_2$. Unlike the parent diaosmacyclopropane $\text{Os}_2(\text{CO})_8(\mu_2\text{-CH}_2)$, $\text{Os}_2(\text{CO})_8(\mu_2\text{-CHMe})$ undergoes facile CO insertion at elevated temperature in the presence of CO to give the diaosmacycloalkanone compound $\text{Os}_2(\text{CO})_8(\eta^2\text{-CH}(\text{Me})=\text{CO})$.²⁵⁹ A new, improved synthesis of $[\text{Os}_2(\text{CO})_6\text{Cl}_2]_2$ is described using OsCl_3 . The chlorocarbonyl dimer may be used as a starting material in the preparation of

cyclopentadienylruthenium complexes. The X-ray structure of the β -form of $[\text{Os}(\text{CO})_3\text{Cl}_2]_2$ is presented.²⁶⁰

Several ruthenium(II) dimers containing CO and t-BuNC ligands have been synthesized starting with RuCl_2 . Isolation of cis- or trans- $[\text{RuCl}_2(\text{CO})(\text{t-BuNC})_2]_2$ is dependent on the reaction temperature. Product characterization by IR spectroscopy and the synthetic route leading to the cis and trans complexes are presented.²⁶¹

$(\eta^5\text{-C}_5\text{Me}_4\text{Et})_2\text{Ru}_2\text{S}_4$ reacts with CO to give $(\eta^5\text{-C}_5\text{Me}_4\text{Et})_2\text{Ru}_2\text{S}_{4-x}(\text{CO})_x$ (where $x = 1, 2$) in the first reported example of a metal-centered ligand addition to a cyclopentadienyliulfide complex. The carbonylation is facile using PBu_3 as a sulfur abstraction agent.²⁶²

Two reports dealing with the diruthenium tetrahydride complex $(\eta^5\text{-C}_5\text{Me}_5)_2\text{Ru}(\mu_2\text{-H})_4\text{Ru}(\eta^5\text{-C}_5\text{Me}_5)$ have appeared. Reaction of $[(\eta^5\text{-C}_5\text{Me}_5)_2\text{RuCl}_2]_2$ with LiAlH_4 gives the tetrahydride in moderate yield. The identity of the four bridging hydrides has been confirmed using NMR (^1H and ^{13}C), FD-MS, and X-ray diffraction analysis. ^1H NMR spin-lattice relaxation studies (T_1) and J_{HD} values from the d_2 -isotopomer support the presence of hydride ligands and not a η^2 -coordinated hydrogen(s).²⁶³ The tetrahydride reacts with ethylene (1 atm) at room temperature to give $(\eta^5\text{-C}_5\text{Me}_5)_2\text{Ru}(\eta^1\text{-}\mu_2\text{-CHCH}_2)_2(\mu_2\text{-CH}_2\text{CH}_2)\text{Ru}(\eta^5\text{-C}_5\text{Me}_5)$. NMR spectral data and X-ray diffraction analysis for the above complex and the products of carbonylation and PMe_3 addition are given.²⁶⁴

The diruthenium complex $[\text{Ru}(\text{H})_2\text{Cl}(\text{Ptol}_3)_2]_2$ has been reformulated as $(\text{Ptol}_3)_2\text{RuH}(\mu_2\text{-H})(\mu_2\text{-Cl})_2\text{Ru}(\eta^2\text{-H}_2)(\text{Ptol}_3)_2$ based on ^1H NMR spin relaxation studies. This complex represents the first example of a dimeric complex possessing a η^2 -coordinated H_2 ligand.²⁶⁵ Reaction of $(\text{P-N})\text{Ru}(\text{PPh}_3)\text{Cl}_2$ [where $\text{P-N} = \text{Fe}(\eta^5\text{-$

$C_5H_3(CHMeNMe_2)P(i-Pr)_{2-1,2}(\eta^5-C_5H_5)]$ with H_2 affords the dinuclear η^2-H_2 complex $(P-N)(\eta^2-H_2)Ru(\mu_2-Cl)_2(\mu_2-H)RuH(PPh_3)_2$. A X-ray structure, with successfully refined hydrogen positions, reveals the presence of the η^2-H_2 moiety. T_1 studies confirm the existence of the coordinated H_2 group while variable-temperature 1H NMR analysis indicates that intramolecular exchange between the η^2-H_2 and the μ_2-H ligands is facile.²⁶⁶

(b) Heteronuclear Complexes

The complexes $M(CO)_4(\eta^2-HFB)$ (where $M = Ru$ or Os ; $HFB =$ hexafluorobutyne) react with $Ru(CO)_5$ or $Os(CO)_5$ to give the homo- and heteronuclear complexes $M_2(CO)_8(\mu_2-\eta^1, \eta^1-HFB)$. These complexes adopt a dimetallacyclobutene structure and have been examined by ^{13}C NMR spectroscopy. Variable-temperature ^{13}C NMR measurements on $RuOs(CO)_8(\mu_2-\eta^1, \eta^1-HFB)$ reveal a "merry-go-round" exchange process which allows equilibration of six carbonyl groups. The carbonyls trans to the parallel HFB ligand are static under these conditions. Reaction of $(\eta^5-C_5Me_5)M'(CO)_2$ (where $M' = Co, Rh,$ or Ir) with the $M(CO)_4(\eta^2-HFB)$ gives $M(CO)_4M'(CO)(\eta^5-C_5Me_5)(\mu-\eta^1, \eta^1-HFB)$ in good yield for $M' = Rh$ and Ir . The heterodimetallacyclobutene complex ($M = Ru$; $M' = Co$) readily loses CO to give the tetrahedral complex $(CO)_3Ru(\mu_2-CO)Co(\eta^5-C_5Me_5)(\mu_2-\eta^2, \eta^2-HFB)$.²⁶⁷

IV. Polynuclear Complexes

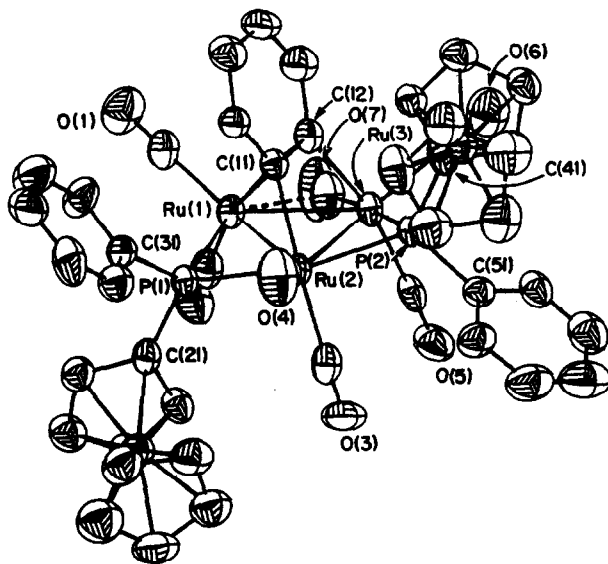
(a) Trinuclear Clusters

1. Simple and Hydrocarbon Ligands

^{13}C and ^{17}O NMR spin-lattice relaxation times for the carbonyl ligands in $M_3(CO)_{12}$ (where $M = Ru$ or Os) have been measured. The T_1 data was next used to calculate the ^{17}O quadrupole coupling constants (QCC) and the correlation times (τ_c) at different temperatures.²⁶⁸ The solid-state structure of the same two clusters was also examined by ^{13}C NMR spectroscopy employing magic angle

spinning (MAS). T_1 measurements of $\text{Ru}_3(\text{CO})_{12}$ in the solid state indicate that the equatorial carbonyls relax faster than the axial carbonyls.²⁶⁹

The reaction between $\text{Os}_3(\text{CO})_{10}(\text{MeCN})_2$ and formylferrocene leads to acyl oxidative addition and isolation of $\text{Os}_3(\text{CO})_{10}(\text{H})(\mu_2\text{-OCFc})$ (where Fc = ferrocene). NMR and X-ray characterization is presented. The redox properties were investigated by CV which indicates the existence of a reversible, Fe-based one-electron oxidation and an irreversible, cluster-based two-electron reduction. IR spectroelectrochemistry measurements are presented.²⁷⁰ Thermolysis of $\text{Ru}_3(\text{CO})_{10}(\text{Ph}_2\text{PFC})_2$ gives the μ_3 -benzynes complex $\text{Ru}_3(\text{CO})_7(\mu_3\text{-}\eta^2\text{-C}_6\text{H}_4)(\mu_2\text{-Ph}_2\text{PFC})_2$. X-Ray diffraction analysis reveals that the Fc groups are oriented trans with respect to the triangular Ru_3 plane and the benzyne ligand is planar. The fluxional nature of the benzyne ligand has been examined by ^1H NMR spin-saturation studies.²⁷¹



Cationic allyl complexes of ruthenium and osmium are reported from thermal and photochemical reactions of $M_3(CO)_{12}$ and allyl alcohol. $Me_3NO \cdot 2H_2O$ induced decarbonylation of $Os_3(CO)_{12}$ in the presence of allyl alcohol, followed by acidification, affords $[Os_3(CO)_{11}(C_3H_5)]^{+1}$.²⁷²

The equilibria reactions between $Ru_3(CO)_{12}$ and halides have been investigated as a function of temperature, CO partial pressure, and halide. Treatment of $Ru_3(CO)_{12}$ with Cl^- or Br^- (as the PPN⁺ salt) gives $[Ru_3(\mu_2-Cl \text{ or } Br)(CO)_{10}]^{-1}$ via the intermediate cluster $[Ru_3(Cl \text{ or } Br)(CO)_{11}]^{-1}$. Use of I^- gives the analogous decacarbonyl cluster, but without spectroscopic evidence of $[Ru_3(I)(CO)_{11}]^{-1}$. Upon heating, CO is lost and the tetranuclear butterfly clusters $[Ru_4(\mu_2-Cl \text{ or } Br)(CO)_{13}]^{-1}$ or $[Ru_3(\mu_3-I)(CO)_9]^{-1}$ are obtained. The tetranuclear butterfly clusters revert back to the decacarbonyl clusters upon exposure to CO and halide. The X-ray structure of $[Ru_3(\mu_3-I)(CO)_9]^{-1}$ is presented along with reactions under H_2 and H_2/CO mixtures.²⁷³ The transient formyl complex $[Ru_3(CO)_{11}(CHO)]^{-1}$, prepared from $Ru_3(CO)_{12}$ and Et_3BH^- , has been characterized at $-78^\circ C$ by NMR (1H and ^{13}C) and FT-IR spectroscopies. Facile decarbonylation is observed at $-50^\circ C$ to give the known hydride cluster $[Ru_3(CO)_{11}(\mu_2-H)]^{-1}$. Formyl decomposition by a radical-chain process was ruled out using Bu_3SnH .²⁷⁴

The products from vacuum pyrolysis of $Os_3(CO)_{12}$ have been analyzed using high-performance liquid chromatography (HPLC). Many of the pyrolysis products were isolated in pure form in a matter of minutes by HPLC compared to conventional chromatographic separation.²⁷⁵ The reaction of $Os_3(CO)_{11}(MeCN)$ and primary arsines $RAsH_2$ (where $R = Ph, Me, \text{ or } H$) initially yields the transient arsine complex $Os_3(CO)_{11}(RAsH_2)$, followed by transformation to the

opened arsinidene cluster $\text{Os}_3(\text{CO})_{11}(\text{H})_2(\mu_3\text{-AsR})$. This cluster consists of $\text{HOs}(\text{CO})_4$ and $\text{HOs}_2(\text{CO})_7$ units tethered by a $\mu_3\text{-AsR}$ group. The reactivity of these triosmium clusters with Os sources and their thermolysis reactions are described.²⁷⁶ Lithium phenylacetylide reacts with $\text{Os}_3\text{K}(\text{Cl})_2(\text{CO})_9\text{L}$ (where $\text{L} = \text{Cl}$ or PMe_2Ph) to give the bridging acetylene cluster $\text{Os}_3\text{H}(\text{CO})_9(\text{L})(\mu\text{-}\eta^2\text{-C}\equiv\text{CPh})$. When $\text{L} = \text{Cl}$, rapid $\pi \rightarrow \sigma$, $\sigma \rightarrow \pi$ acetylene scrambling between the bridged osmium atoms is observed, whereas the PMe_2Ph derivative is stereochemically rigid. Two isomeric forms of the latter cluster are shown to exist by ^1H and ^{31}P NMR spectroscopy. A crystal structure of the major isomer is reported.²⁷⁷ A Fourier transform ion cyclotron resonance (FT-ICR) mass spectrometry study of $\text{H}_2\text{Os}_3(\text{CO})_{10}$ has appeared. The ion-molecule pathways and measured rate constants for individual ionic species are reported.²⁷⁸ The X-ray structure of $\text{Os}_3(\mu_3\text{-O}_2\text{CMe})(\mu_2\text{-R})(\text{CO})_{10}$ has been redetermined and the results of normal probability plot analysis reported.²⁷⁹

The synthesis of the fluoromethylidyne cluster $\text{Os}_3(\mu_2\text{-H})_3(\text{CO})_9(\mu_3\text{-CF})$ is described. The ^{13}C NMR chemical shift of the apical carbon in this and other apically substituted osmium clusters is compared with analogous tricobalt alkylidyne clusters.²⁸⁰ The alkylidyne radical $\text{Os}_3(\mu_2\text{-H})_3(\text{CO})_9(\mu_3\text{-C}\cdot)$ has been generated from $\text{Os}_3(\mu_2\text{-H})_2(\text{CO})_9(\mu_3\text{-CBr})$ and $\text{Re}_2(\text{CO})_{10}$ upon photolysis. The alkylidyne radical abstracts hydrogen from cyclohexane and toluene while benzene gives the phenyl complex $\text{Os}_3(\mu_2\text{-H})_3(\text{CO})_9(\mu_3\text{-CPh})$. Use of deuterated solvents confirms the D(H) atom abstraction reactions and in the case of d_{12} -cyclohexane affords the diketone cluster $[\text{Os}_3(\mu_2\text{-H})_3(\text{CO})_9(\mu_3\text{-CCO})]_2$ which has been structurally characterized.²⁸¹ Reaction of $[\text{Os}_3(\mu_2\text{-H})_3(\text{CO})_9(\mu_3\text{-C})]_3(\text{O}_3\text{B}_3\text{O}_3)$ with B_5H_9 or $1,2\text{-C}_2\text{B}_{10}\text{H}_{12}$ in the presence of BF_3 gives the boron-osmium clusters $\text{Os}_3(\mu_2\text{-H})_3(\text{CO})_9(\mu_3\text{-C})(\text{B}_5\text{H}_9)$ and

$\text{Os}_3(\mu_2\text{-H})_3(\text{CO})_9(\mu_3\text{-C})(\text{C}_2\text{B}_{10}\text{H}_{11})$, respectively. Hydrolysis of the apical C-B bond furnishes the methylidyne cluster $\text{Os}_3(\mu_2\text{-H})_3(\text{CO})_9(\mu_3\text{-CH})$. ^{11}B NMR and FT-ICR mass spectra were employed in cluster characterization.²⁸²

A theoretical study concerning the effect of μ_2 -bridging ligands on the cluster frame of $\text{M}_3(\text{CO})_{10}(\mu_2\text{-H})(\mu_2\text{-X})$ (where $\text{M} = \text{Ru}$ or Os ; $\text{X} = \text{Cl}$, SH , or PH_2) has appeared. Fenske-Hall calculations indicate that metal to main-group μ_2 -bridging interactions outweigh direct M-M overlap in determining the bridged M-M bond length. Periodic trends as a function of the $\mu_2\text{-X}$ ligand are presented and discussed.²⁸³

Reaction of the pyridine-2-carbaldimine ligand 6-MeC₅H₃N-2-CH=N(i-Pr) with $\text{Os}_3(\text{CO})_{10}(\text{MeCN})_2$ at room temperature affords $\text{Os}_3(\text{CO})_9(\mu_2\text{-H})[6\text{-CH}_2\text{C}_5\text{H}_3\text{N-2-CH=N(i-Pr)}]$ as a result of methyl C-H bond activation. The pyridine ligand coordinates in a tridentate fashion with both nitrogen atoms chelating a single osmium atom while the alkyl group is coordinated to an adjacent osmium center. Thermolysis at 130 °C leads to CO loss and formation of the μ_2 -alkylidene cluster $\text{Os}_3(\text{CO})_8(\mu_2\text{-H})_2[6\text{-CHC}_5\text{H}_3\text{N-2-CH=N(i-Pr)}]$ as a result of a second C-H bond activation.²⁸⁴

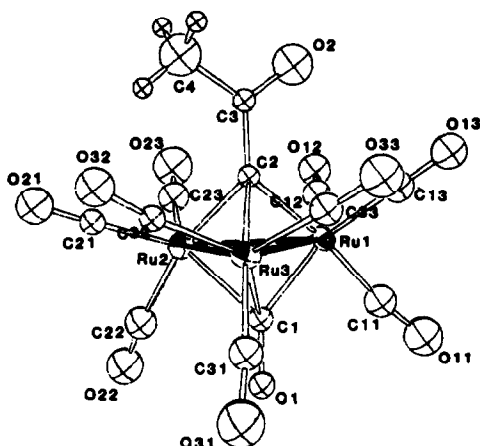
Protonation rates in the ruthenium and osmium clusters $[\text{M}_3(\text{CO})_{11}(\mu_2\text{-H})]^{-1}$ have been investigated at low temperature using ^1H and ^{13}C NMR spectroscopy. A pre-equilibrium exchange between the initial anion and protonated cluster indicates that protonation is not instantaneous. The initial site of protonation is shown to involve the oxygen atom of the $\mu_2\text{-CO}$ group, followed by slow rearrangement to the dihydride cluster $\text{M}_3(\text{CO})_{11}(\mu_2\text{-H})_2$. While no kinetic isotope effect is observed with the formation of $\text{M}_3(\text{CO})_{10}[\mu_2\text{-COH(D)}](\mu_2\text{-H})$, the ruthenium cluster exhibits a large isotope effect ($k_{\text{H}}/k_{\text{D}} \approx 47$ at -40 °C) for rearrangement to the

dihydride cluster. The magnitude of the isotope effect observed in the ligand-to-metal hydrogen transfer is discussed with respect to other cluster protonations.²⁸⁵

The allenic cluster $\text{Os}_3(\text{CO})_9(\mu_2\text{-H})(\mu_3\text{-}\eta^3\text{-CH}_3\text{CH}_2\text{C}=\text{C}=\text{C}(\text{H})\text{CH}_3)$, 80% enriched in deuterium at the μ_2 -hydride position, has been examined for carbon-hydrogen interchange reactivity. At 110 °C the deuterium is incorporated into the allenic hydrogen position and the methylene hydrogens only. The alkyne complex $\text{Os}_3(\text{CO})_9(\mu_3\text{-}\eta^2\text{-CH}_3\text{CH}_2\text{C}=\text{CCH}_2\text{CH}_3)$ is postulated as a key intermediate. The analogous ruthenium cluster was also examined, yielding similar results. Plausible mechanisms for hydride scrambling are presented.²⁸⁶

Reversible C-C and C-H bond forming reactions are described when the acylmethylidyne cluster $[\text{Ru}_3(\text{CO})_9(\mu_3\text{-CO})(\mu_3\text{-CC}(\text{O})\text{CH}_3)]^{-1}$ is treated with CO or H_2 . CO addition furnishes the $\mu_2\text{-}\eta^2$ -acyl cluster $[\text{Ru}_3(\text{CO})_7(\mu_3\text{-CO})_3(\mu_2\text{-}\eta^2\text{-CH}_3\text{C}(\text{O})\text{CCO})]^{-1}$ while H_2 addition gives the $\mu_3\text{-}\eta^2$ -acyl cluster $[\text{HRu}_3(\text{CO})_9(\mu_3\text{-}\eta^2\text{-CHC}(\text{O})\text{CH}_3)]^{-1}$. The former reaction is reversible and the equilibrium constant at room temperature is reported. Isotopic tracer studies reveal that ketenyl carbon in the $\mu_2\text{-}\eta^2$ -acyl cluster is derived from a CO group initially present in the starting cluster. Protonation and alkylation studies of these new anionic clusters are described. The X-ray structure of the acylmethylidyne cluster is included.²⁸⁷

An infrared and Raman study of the ketenylidene clusters $[\text{Ru}_3(\text{CO})_9(\mu_2\text{-CO})_3(\mu_3\text{-CCO})]^{-2}$ and $\text{H}_2\text{Ru}_3(\text{CO})_9(\mu_3\text{-CCO})$ has appeared. The stretching vibrations of the ketenylidene ligand have been identified and subjected to approximate normal-coordinate analysis. Metal framework vibrations are also reported in addition to Raman depolarization ratios.²⁸⁸ A brief review dealing, in part, with ruthenium and osmium ketenylidene clusters and the transformations available to the ancillary CO groups has been published.²⁸⁹

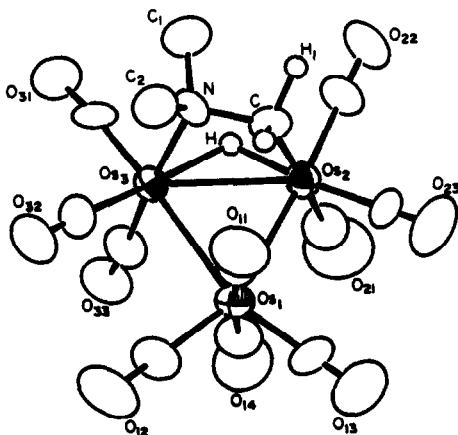


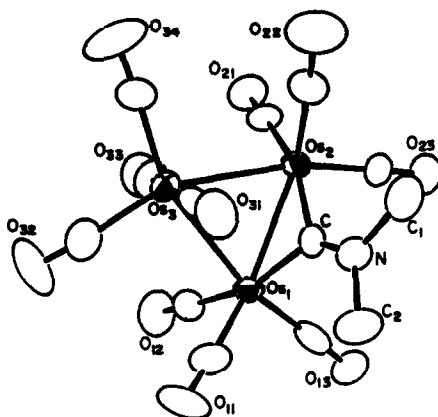
Pyrolysis of the (dimethylamino)carbene cluster $\text{Ru}_3(\text{CO})_{10}(\mu_2\text{-CNMe}_2)(\mu_2\text{-H})$ at 185 °C yields the higher nuclearity clusters $\text{Ru}_4(\text{CO})_{12}(\mu_4\text{-}\eta^2\text{-CNMe}_2)(\mu_2\text{-H})$, $\text{Ru}_5(\text{CO})_{13}(\mu_4\text{-}\eta^2\text{-CNMe}_2)(\mu_4\text{-CNMe}_2)$, and $\text{Ru}_6(\mu_6\text{-C})(\text{CO})_{14}(\mu_2\text{-CNMe}_2)_2$ in low yields. Full spectral characterization and X-ray structures of the new carbene clusters are reported. Direct synthesis of the former tetranuclear cluster may also be achieved in moderate yield from the reaction of $\text{Ru}(\text{CO})_5$ with $\text{Ru}_3(\text{CO})_{10}(\mu_2\text{-CNMe}_2)(\mu_2\text{-H})$. The tetra- and pentanuclear carbene clusters are postulated to arise from a combination of $\text{Ru}(\text{CO})_4$ and $\text{Ru}_2(\text{CO})_6(\text{CNMe}_2)(\text{H})$ units while the hexanuclear cluster derives from the formal fusion of two starting Ru_3 clusters.²⁹⁰

Bis(dimethylamino)methane reacts with $\text{Os}_3(\text{CO})_{10}(\mu_2\text{-H})_2$ to yield $\text{Os}_3(\text{CO})_{10}(\mu\text{-}\eta^2\text{-CH}_2\text{NMe}_2)(\mu_2\text{-H})$. X-Ray diffraction analysis reveals a triangular osmium cluster with a bridging (dimethylamino)methyl ligand. Heating the new cluster at 98 °C furnishes $\text{Os}_3(\text{CO})_9(\mu_3\text{-}\eta^2\text{-C(H)NMe}_2)(\mu_2\text{-H})_2$ and $\text{Os}_3(\text{CO})_{10}(\mu_2\text{-CNMe}_2)(\mu_2\text{-H})$. The X-ray structures of both clusters are presented. Plausible mechanistic pathways involving multicenter osmium C-H bond activations are proposed.²⁹¹ Photoinduced decarbonylation of $\text{Os}_2(\text{CO})_{10}(\mu_2\text{-CHCHNET}_2)(\mu_2\text{-H})$ gives

latter cluster is also the exclusive product obtained when the starting cluster is refluxed in hexane. Both products have been characterized spectroscopically in addition to X-ray diffraction analysis. Reaction of HN-n-Pr_2 with the latter cluster gives the corresponding (dipropylamino)alkenylidene cluster via replacement of the Et_2N group.²⁹² $\text{Os}_3(\text{CO})_{10}(\mu_2\text{-Ome})(\mu_2\text{-H})$ reacts with $\text{CH}_2(\text{NMe}_2)_2$ at 98 °C to give isomeric (dimethylamino)carbene clusters $\text{Os}_3(\text{CO})_9(\mu_3\text{-}\eta^2\text{-CHNMe}_2)(\mu_2\text{-Ome})(\mu_2\text{-H})$ and $\text{Os}_3(\text{CO})_9(\text{CHNMe}_2)(\mu_2\text{-Ome})(\mu_2\text{-H})$. The carbene ligand in the former open triangular cluster is bound to two osmiums by a μ_2 -carbon bridge while the dimethylamine group is coordinated to the remaining osmium atom. The latter cluster contains a terminal (dimethylamino)carbene ligand. Coupling of methyl propiolate with the carbene ligand of the former cluster is described. X-Ray structures of all new products and mechanistic schemes are presented.²⁹³

Reaction of I_2 with $\text{Os}_3(\text{CO})_{10}(\mu\text{-OCNHCHMe}_2)(\mu_2\text{-H})$ leads to cluster fragmentation and production of several di- and mononuclear osmium complexes. The complexes $\text{Os}_2(\text{CO})_6(\mu\text{-OCNHCHMe}_2)(\mu_2\text{-I})\text{I}_2$ and $\text{trans-HIOs}(\text{CO})_4$ have been observed using 2 equivalents of I_2 . The latter complex isomerizes in solution to the cis isomer and reacts





with excess I_2 to yield $cis-I_2Os(CO)_4$. The former dimer has been characterized crystallographically. Formation of the mononuclear amine complex $Os(C)_3(NH_2CRMe_2)$ (where $R = H$ or Me) is observed when 3 equivalents of I_2 are used.²⁹⁴

2. Phosphine Ligands

Ligand substitution in the ruthenium and osmium clusters $M_3(CO)_{12}$ and $M_3(CO)_{11}L$ (where $L =$ phosphine or arsine) has been examined using Me_3NO as a decarbonylation reagent. These reactions obey second-order kinetics, being first order in initial cluster concentration and first order in Me_3NO concentration. No incoming ligand dependence was observed. The rate-determining step involves nucleophilic attack of the oxygen atom of Me_3NO on a carbonyl carbon atom followed by CO_2 loss and ligand capture. Differences in the rates of reaction between similar ruthenium and osmium complexes are discussed.^{295,296}

Three extensive reports concerning the X-ray crystal structures of ruthenium and osmium clusters of the form $M_3(CO)_{11}L$, $M_3(CO)_{10}L_2$, and $M_3(CO)_9L_3$ (where $L =$ phosphine or phosphite) have appeared. The factors leading to the observed ligand disposition and metal framework distortion are presented.^{297,298,299} The X-ray structure of $Ru_3(CO)_{10}(PPh_3)_2$ has been the subject of a separate

paper. The two PPh_3 groups are bound to adjacent ruthenium atoms and are equatorially disposed. Several carbonyl groups are semibridging and the unique ruthenium atom and four carbonyl groups are noticeably twisted relative to $Ru_3(CO)_{12}$.³⁰⁰

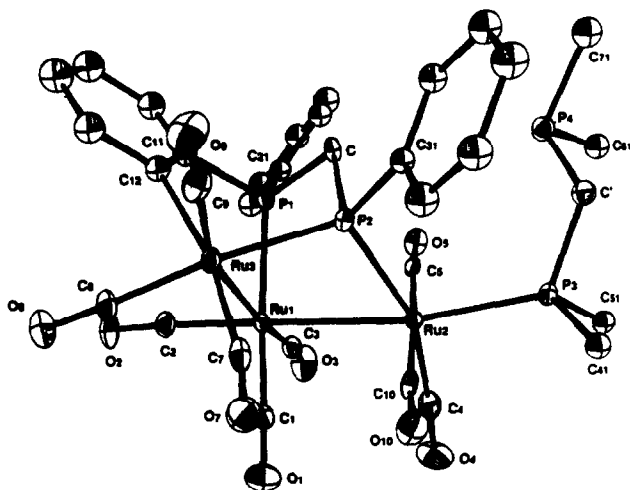
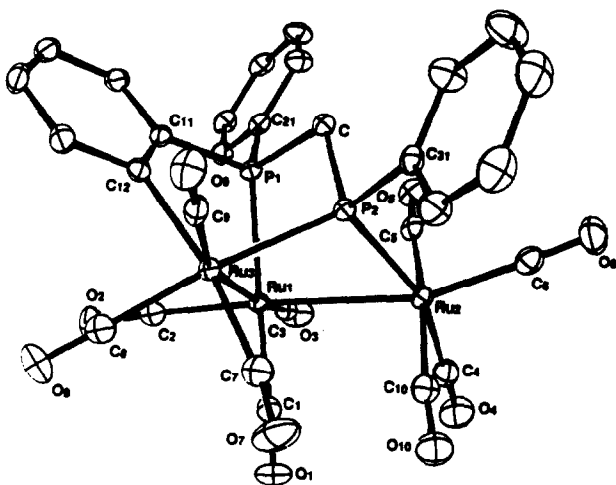
$Ru_3(CO)_{10}(dppee)$ [where $dppee = \text{vinylidenebis(diphenylphosphine)}$] has been examined crystallographically. The $dppee$ ligand bridges adjacent ruthenium atoms via equatorial coordination. The bond length of the vinyl group is not affected by phosphine coordination.³⁰¹ The reaction between $\text{tris(isopropylphosphine) methane}$ and $Ru_3(CO)_{12}$ has been studied in the presence of a PPN-CN catalyst. The first observable product is the bridged cluster $Ru_3(CO)_{10}(\mu_2-P)(\mu_2-P)(\mu_2-P)$ which is shown to exist in two isomeric forms (syn and anti isopropyl groups) by NMR spectroscopy. Also isolated is the cluster $Ru_3(CO)_9(\mu_2-H)(\mu_3-\eta^2-1-PPHCH_2P-1-PP)$ which is derived by CO loss and subsequent intramolecular P-H oxidative addition to the above cluster.³⁰² Photolysis of $Ru_3(CO)_{12}$ in the presence of the bidentate phosphines $Me_2PCH_2PMe_2$ ($dpmm$), $Ph_2PCH_2PPh_2$ ($dpbm$), and $Ph_2PN(Et)PPh_2$ ($dppea$) furnishes tri-, di- or mononuclear complexes depending upon the reaction conditions. The crystal structure of $Ru_3(CO)_{10}(dppea)$ reveals equatorial coordination of the aminophosphine ligand and a 0.06 Å shortening of the bridged Ru-Ru bond relative to the other two unbridged Ru-Ru bonds.³⁰³ In a related reaction, the arsine ligand $t-Bu_2As(NSN)As-t-Bu_2$ reacts with $Ru_3(CO)_{12}$ to give $Ru_3(CO)_8(\mu_2-H)(\mu_3-As-t-Bu)(\mu_2-NSNAs(t-Bu)_2)$. Use of the eight-membered heterocyclic arsine $t-BuAs(NSN)_2As-t-Bu$ yields the arsine coordinated cluster $Ru_3(CO)_{10}(t-BuAs(NSN)_2As-t-Bu)$.³⁰⁴

The substitution and fragmentation reactions of $Ru_3(CO)_{12-n}(PBU_3)_n$ (where $n = 0 - 2$) in the presence of PBU_3 have

been examined. A phosphine-independent path always leads to ligand substitution while the phosphine-dependent path leads to substitution and/or cluster fragmentation. Estimates of $k_{\text{fragmentation}}/k_{\text{substitution}}$ are reported as a function of temperature.³⁰⁵

The reaction between $\text{Ru}_3(\text{CO})_9(\mu_3\text{-}\eta^3\text{-P(Ph)CH}_2\text{P(Ph)(C}_6\text{H}_4))$ and CO has been reinvestigated. Facile CO addition is observed upon Ru-Ru bond scission to give $\text{Ru}_3(\text{CO})_{10}(\mu_3\text{-}\eta^3\text{-P(Ph)CH}_2\text{P(Ph)(C}_6\text{H}_4))$ which has been isolated and subjected to X-ray diffraction analysis. Phosphines trap the same intermediate at low temperature to give $\text{Ru}_3(\text{CO})_9\text{L}(\mu_3\text{-}\eta^3\text{-P(Ph)CH}_2\text{P(Ph)(C}_6\text{H}_4))$. In the case of $\text{L} = \text{PPh}_3$, warming leads to several compounds from which the dinuclear complex $\text{Ru}_2(\text{CO})_6(\mu\text{-}\eta^3\text{-P(Ph)CH}_2\text{P(Ph)(C}_6\text{H}_4))$ has been isolated and characterized.³⁰⁶ The acyl cluster $\text{Ru}_3(\eta\text{-C(O)Ph})(\mu_3\text{-P(Ph)(C}_5\text{H}_4\text{N)})(\text{CO})_8\text{L}$ (where $\text{L} = \text{CO, Ph}_2\text{PH, or Cy}_2\text{PH}$) has been the subject of thermolysis and hydrogenation reactions. Thermolysis of the R_2PH -substituted clusters gives benzaldehyde and $\text{Ru}_3(\mu_3\text{-P(Ph)(C}_5\text{H}_4\text{N)})(\mu_2\text{-PR}_2)(\mu_2\text{-CO})_2(\text{CO})_6$ while reaction of the nonacarbonyl cluster with H_2 yields benzene and $\text{Ru}_3(\mu_2\text{-H})(\mu_3\text{-P(Ph)(C}_5\text{H}_4\text{N)})(\text{CO})_9$. The role of metal-metal bond cleavage in substitution and hydrogenation reactions is discussed.³⁰⁷

Reaction of $\text{Ru}_3(\text{CO})_{12}$ with $t\text{-Bu}_2\text{PH}$ affords the phosphido-bridged cluster $\text{Ru}_3(\text{CO})_8(\mu_2\text{-H})_2(\mu_2\text{-P-}t\text{-Bu}_2)_2$, characterized by spectroscopic and X-ray diffraction analysis. Facile hydrogen addition is observed under mild conditions to give the 50-electron cluster $\text{Ru}_3(\text{CO})_8(\mu_2\text{-H})(\text{H})_2(\mu_2\text{-P-}t\text{-Bu}_2)_2$. The unbridged Ru-Ru bond in the starting material is cleaved during hydrogen addition to yield the terminal Ru-hydrides that point away from each other. ^1H NMR measurements indicate bridge \leftrightarrow terminal hydride exchange and T_1 values rule out a molecular hydrogen complex.³⁰⁸ The products



obtained from the thermolysis of $\text{Ru}_3(\text{CO})_{12}$ with PhPH_2 have been isolated and fully characterized. The nature and yields of the observed tri-, tetra-, penta-, and hexanuclear clusters are dependent on the reaction time and molar ratios with the majority of the products possessing a nuclearity greater than three.³⁰⁹

Cluster racemization in $\text{Ru}_3(\text{CO})_7(\mu_2\text{-H})(\text{C}\equiv\text{C-t-Bu})(\text{dppe})$ has been demonstrated by NMR spectroscopy (^1H , ^{13}C , and ^{31}P). X-Ray diffraction analysis reveals an ordered racemic array of

enantiomers which racemize in solution by a concerted acetylide rotation/hydride migration mechanism.³¹⁰

Controlled oxidative insertion into the phosphinoalkyne bond in $\text{Ru}_3(\text{CO})_{11}(\text{Ph}_2\text{PC}=\text{CR})$ (where R = i-Pr or t-Bu) furnishes the 50-electron cluster $\text{Ru}_3(\text{CO})_9(\mu_3-\eta^2-\text{C}=\text{CR})(\mu_2-\text{PPh}_2)$. Both clusters lose CO on heating to give $\text{Ru}_3(\text{CO})_6(\mu_2-\text{CO})_2(\mu_3-\eta^2-\text{C}=\text{CR})(\mu_2-\text{PPh}_2)$. The latter cluster (R = i-Pr) reacts with diazomethane to yield the μ_3 -allenyl cluster $\text{Ru}_3(\text{CO})_8(\mu_3-\eta^3-\text{CH}_2=\text{C}=\text{C}-\text{i-Pr})(\mu_2-\text{PPh}_2)$ through the formal coupling of a methylene fragment with the acetylide. Further reaction with diazomethane gives the methylene-bridged cluster $\text{Ru}_3(\text{CO})_7(\mu_2-\text{CH}_2)(\mu_3-\eta^2-\text{CH}_2=\text{C}=\text{C}-\text{i-Pr})(\mu_2-\text{PPh}_2)$. The X-ray structures of many of these clusters are presented in addition to the role the μ_2 -phosphido group plays in promoting C-C bond forming processes.³¹¹ The chemistry associated with the above methylene-bridged cluster has been the subject of a separate report. A slow isomerization to the corresponding 2-isopropyl-1,3-butadienediyl cluster $\text{Ru}_3(\text{CO})_7(\mu_2-\text{H})(\mu_3-\eta^4-\text{CH}=\text{C}(\text{i-Pr})\text{C}=\text{CH}_2)(\mu_2-\text{PPh}_2)$ is observed. Crystallographic analysis reveals a triangular Ru_3 core with bridging phosphido and hydride groups on the same edge. Exposure of methylene-bridged cluster to CO in methanol gives the open allenyl cluster $\text{Ru}_3(\text{CO})_9(\mu_3-\eta^3-\text{CH}_2=\text{C}=\text{C}(\text{i-Pr}))(\mu_2-\text{PPh}_2)$ and methyl acetate via CO insertion into the Ru- $(\mu_2-\text{CH}_2)$ bond to give a transient C,C-ligated bridging ketylenyl cluster. Isotopic labelling studies reveal that a CO group originally associated with the methylene-bridged cluster undergoes insertion into the Ru- $(\mu_2-\text{CH}_2)$ bond. Mechanistic schemes for hydrocarbon chain growth on a cluster surface are discussed.³¹² The reactivity of the allenyl cluster $\text{Ru}_3(\text{CO})_8(\mu_3-\eta^3-\text{CH}_2=\text{C}=\text{C}(\text{i-Pr}))(\mu_2-\text{PPh}_2)$ towards CO, $\text{P}(\text{OMe})_3$, H_2 , and alkynes is reported. The Ru-Ru bond bridged by the phosphido group is cleaved upon CO addition to give the 50-electron cluster $\text{Ru}_3(\text{CO})_9(\mu_3-\eta^3-\text{CH}_2=\text{C}=\text{C}(\text{i-Pr}))(\mu_2-\text{PPh}_2)$. Isotopic labelling

studies with ^{13}C reveal a regiospecific ^{13}C incorporation trans to one arm of the phosphido bridge. Alkynes react to give clusters of the form $\text{Ru}_3(\text{CO})_7(\mu_3-\eta^5-\text{CH}_2=\text{C}=\text{C}(\text{i-Pr})\text{C}(\text{R})\text{C}(\text{R}'))(\mu_2-\text{PPh}_2)$ which all contain a "wrap-around" five carbon hydrocarbon fragment. Variable-temperature NMR measurements of these latter clusters support the presence of a "hidden partner" exchange process involving axial-equatorial $\mu_2\text{-PPh}_2$ isomerism. Full spectral characterization and crystallographic structures for many of these novel clusters are included.³¹³

A communication describing the photoinduced dimetallation of face-capping benzene ligands in the osmium clusters $\text{Os}_3(\text{CO})_8(\text{PR}_3)_2(\mu_3-\eta^2:\eta^2:\eta^2-\text{C}_6\text{H}_6)$ (where $\text{R} = \text{Ph}$ or MeO) gives the hydride clusters $\text{Os}_3(\text{CO})_8(\text{PR}_3)_2(\mu_2-\text{H})_2(\mu_3-\eta^1:\eta^2:\eta^1-\text{C}_6\text{H}_4)$. The cluster analogue for benzene activation is discussed with respect to adsorbate overlayers on metal surfaces.³¹⁴ The use of platinum(σ) complexes as catalysts in the synthesis of $\text{Os}_3(\text{CO})_{11}(\text{PPh}_2)$ starting from $\text{Os}_3(\text{CO})_{12}$ is reported. The described procedure offers a convenient, high-yield route to the monosubstituted cluster in essentially quantitative yield. An electron-transfer catalysis scheme is proposed.³¹⁵

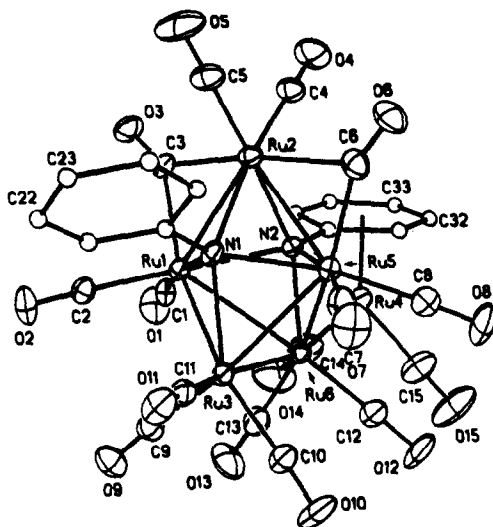
The bidentate phosphine ligand dppe reacts with $\text{Os}_3(\text{CO})_{10}(\text{MeCN})_2$ to give the bridged complex $\text{Os}_3(\text{CO})_{10}(\text{dppe})$ as the major product. Treatment of this dppe-substituted cluster with $\text{CF}_3\text{CO}_2\text{H}$ gives $[\text{Os}_3(\mu_2\text{-H})(\text{CO})_{10}(\text{dppe})]^{+1}$ as a result of Os-Os bond protonation. Low-temperature ^1H NMR studies indicate that protonation occurs at both the unsubstituted and substituted Os-Os bonds. The thermodynamically favored and isolated isomer is shown to originate from protolysis of the phosphine-substituted bond. Variable-temperature NMR measurements indicate that the $\overline{\text{OsPCCPOs}}$ ring in the neutral cluster is fluxional via an inversion process whereas it is frozen out in the cationic cluster. Both clusters

have been structurally characterized.³¹⁶ Os-Os bond protonation reactions have been examined for chelating phosphine complexes $\text{Os}_3(\text{CO})_{10}(\text{L-L})$ (where L-L = dppe or dppp). Protonation occurs at a Os-Os bond bearing the diphosphine ligand based on spectral analysis. The reactivity of the parent clusters towards H_2 and the X-ray structure of $\text{Os}_3(\text{CO})_8(\mu_2\text{-H})_2(\text{Ph}_2\text{P}(\text{CH}_2)_3\text{PC}_6\text{H}_4)$ is described.³¹⁷ Protonation and hydrogenation reactions are described for the bridging phosphine complexes $\text{Os}_3(\text{CO})_{10}(\text{dppm})$ and $\text{Os}_3(\text{CO})_{10}(\text{dppb})$. The geometric and electronic factors involved in the protonation reactions of those and other bidentate phosphines are discussed and compared.³¹⁸

A report dealing with reversed ortho-hydrogen abstraction has appeared. Reaction of $\text{Sn}(\text{CH}(\text{SiMe}_3)_2)_2$ with the known osmium cluster $\text{Os}_3(\text{CO})_8(\mu_2\text{-H})(\text{Ph}_2\text{PCH}_2\text{P}(\text{Ph})\text{C}_6\text{H}_4)$ leads to the dppm-substituted cluster $\text{Os}_3(\text{CO})_8[\mu_2\text{-Sn}(\text{CH}(\text{SiMe}_3)_2)]_2(\mu\text{-dppm})$. This triangular osmium cluster is paramagnetic as determined by NMR and EPR measurements.³¹⁹

3. Nitrogen Ligands

Thermolysis of $\text{Ru}_3(\text{CO})_{10}(\mu_3\text{-NPh})$ gives the hexaruthenium cluster $\text{Ru}_6(\text{CO})_{15}(\mu_4\text{-NPh})_2$ in high yield. X-Ray diffraction analysis reveals the presence of a distorted pentagonal-bipyramidal core. Three ruthenium atoms and the two $\mu_4\text{-NPh}$ groups define the pentagonal plane with two capping ruthenium atoms completing the polyhedron. The remaining ruthenium atom is bonded to one of the polyhedral ruthenium atoms and π -coordinated to the phenyl group of a capping $\mu_4\text{-NPh}$ ligand. Reaction of the starting μ_3 -imido cluster with $\text{Ru}_3(\text{CO})_{12}$ also yields the same hexaruthenium cluster. The heptaruthenium cluster $\text{Ru}_7(\text{CO})_{16}(\mu_4\text{-NPh})_2$ has been isolated and spectroscopically characterized.³²⁰



Nitrogen heterocycles have been reacted with $\text{Ru}_3(\text{CO})_{12}$ to afford new heterocyclic ruthenium clusters. 1*H*-Pyrrolo[2,3-*b*]pyridine (Hppy) and benzimidazole (Hbzim) react to give $\text{Ru}_3(\text{CO})_9(\mu_2\text{-H})(\mu_3\text{-ppy})$ and $\text{Ru}_3(\text{CO})_{10}(\mu_2\text{-H})(\mu\text{-bzim})$, respectively. Reaction with benzotriazole (Hbztz) leads to cluster fragmentation and $\text{Ru}_2(\text{CO})_6(\mu\text{-bztz})_2$ while 1,8-naphthyridine (napy) furnishes the carbonyl-bridged cluster $\text{Ru}_3(\text{CO})_7(\mu_2\text{-CO})_3(\mu\text{-napy})$. The ppy and napy clusters have been structurally characterized. The napy cluster undergoes facile Ru-Ru bond protonation and deprotonation.³²¹

Reaction of $\text{Os}_3(\text{CO})_{10}(\text{MeCN})_2$ with $(\eta^5\text{-C}_5\text{H}_5)\text{Fe}(\eta^5\text{-C}_4\text{H}_4\text{N})$ (azaferrocene) leads to $\text{Os}_3(\text{CO})_{10}(\mu_2\text{-H})\{(\eta^5\text{-C}_5\text{H}_5)\text{Fe}(\eta^5\text{-C}_4\text{H}_3\text{N})\}$, via a C-H bond activation sequence involving the pyrrolyl ring. The ortho-metallated pyrrolyl ring functions as a three-electron donor.³²²

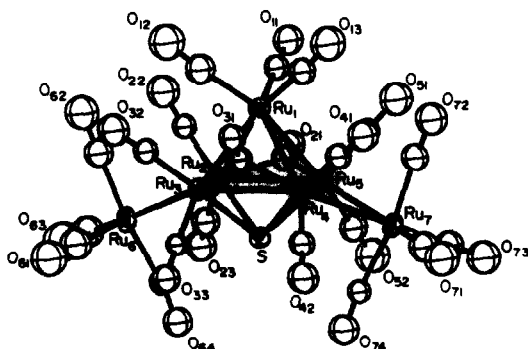
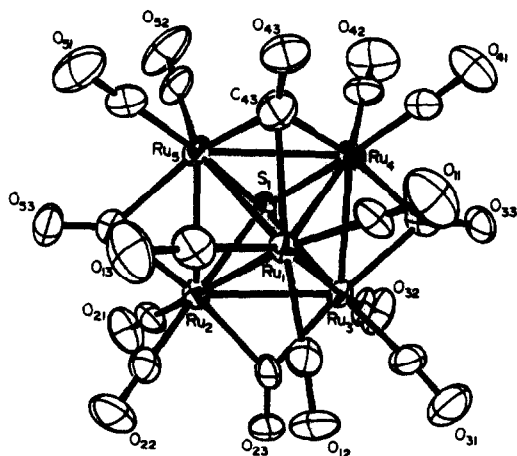
1,4-Disubstituted-1,4-diaza-1,3-butadienes (R-DAB) react with $\text{Os}_3(\text{CO})_{10}(\text{MeCN})_2$ to yield two isomers of $\text{Os}_3(\text{CO})_{10}(\text{R-DAB})$; the isomer product ratio is dependent on the R-substituent. One isomer exhibits a 4-electron R-DAB ligand which coordinates to the

triangular osmium core via axial and equatorial sites. The other isomer is a 50-electron cluster that possesses an opened osmium polyhedron with a 6-electron R-DAB ligand, coordinated in a σ -N, μ_2 -N', η^2 -C=N' fashion. Clusters with the 4-electron R-DAB ligand reveal a low-temperature rocking process about one axial and two equatorial sites on the substituted osmium atom as determined by ^1H and ^{13}C NMR studies. At higher temperature, pairwise bridge-terminal carbonyl exchange perpendicular to the triangular osmium core is observed. Crystallographic structures of many of these clusters are presented.³²³ In an accompanying paper the 48-electron cluster $\text{Os}_3(\text{CO})_{10}(\text{i-Pr-DAB})$ with a chelating i-Pr-DAB ligand transforms into the 50-electron cluster $\text{Os}_3(\text{CO})_{10}(\text{i-Pr-DAB})$ in refluxing hexane. Prolonged heating leads to CO loss and the new cluster $\text{Os}_3(\text{CO})_9(\text{i-Pr-DAB})$. The diimine ligand functions as an 8-electron donor and the cluster polyhedron may be viewed in terms of a dodecahedron geometry. Full spectral and crystallographic analyses are reported along with IR kinetics which support the stepwise nature of these cluster transformations.³²⁴

4. Sulfur Ligands

Two reports dealing with trinuclear sulfur clusters have appeared. Reaction of the chalcogen-bridged cluster $\text{Ru}_3(\text{CO})_9(\mu_3\text{-CO})(\mu_3\text{-S})$ with $\text{Ru}(\text{CO})_5$ in refluxing hexane yields the clusters $\text{Ru}_5(\text{CO})_{15}(\mu_4\text{-S})$, $\text{Ru}_6(\text{CO})_{15}(\mu_2\text{-CO})_3(\mu_4\text{-S})$, and $\text{Ru}_7(\text{CO})_{19}(\mu_3\text{-CO})_2(\mu_4\text{-S})$. All three clusters have been fully characterized by spectroscopic and structural techniques. The stepwise formation of hexa- and heptaruthenium clusters is demonstrated by thermolysis of $\text{Ru}(\text{CO})_5$ with the corresponding lower nuclearity cluster. Cluster degradation with CO also proceeds in a stepwise fashion.³²⁵

The trinuclear osmium clusters $\text{Os}_3(\text{CO})_9(\mu_3\text{-X})_2$ (where X = S or Se) have been examined by photoelectron spectroscopy (He I only) and Fenske-Hall MO calculations. The HOMO is composed primarily



of e_g -like orbitals associated with the $Os(CO)_3$ fragments which account for the majority of in-phase Os-Os bonding. A comparison of these clusters with the analogous triiron sulfide cluster is presented.³²⁶

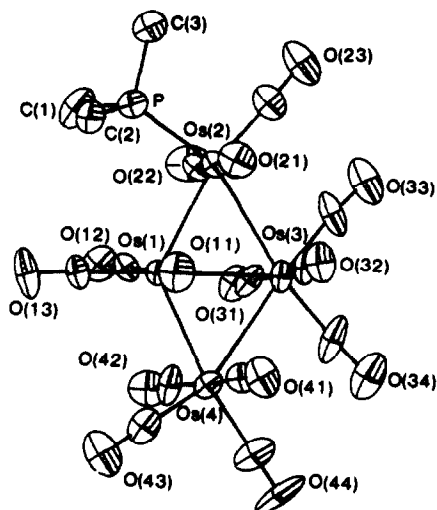
(b) Tetranuclear Clusters

The pK_a values of $H_4Ru_4(CO)_{11}P(OMe)_3$ and $H_4Ru_4(CO)_{10}[(P(OMe)_3)_2]$ have been measured in acetonitrile solution. Values of 12.4 and 15.4, respectively, were calculated.³²⁷ ~~Mononuclear~~ (E) - $(CH_3C(H)=C(H)C(H)=NR)$ (R-MAD) have been reacted with $Ru_2(CO)_{12}$ to give the linear tetraruthenium cluster $Ru_4(CO)_{10}[CH_3C=C(H)C(H)=NR]_2$. The R-MAD ligands in this 66-electron cluster are coordinated in a σ -

N , σ -C, η^2 -N=C, η^2 -C=C fashion as demonstrated by X-ray diffraction analysis. The use of CVMO theory to describe the cluster's polyhedral shape and its isolobal relationship to $\{(\eta^5\text{-C}_5\text{H}_5)\text{Ru}(\text{CO})_2\}_2$ are discussed.³²⁸

The μ_4 -phosphinidene capped clusters $\text{Fe}_3\text{Ru}(\text{CO})_{11}(\mu_4\text{-PPh})_2$, $\text{Fe}_2\text{Ru}_2(\text{CO})_{11}(\mu_4\text{-PPh})_2$, and $\text{Ru}_4(\text{CO})_{11}(\mu_4\text{-PPh})_2$ have been examined using electrochemical techniques. EPR spectra of the radical anions become increasingly broad as the number of ruthenium atoms increases.³²⁹ Two new 64-electron phosphido-bridged clusters with elongated Ru-Ru bonds have been synthesized and characterized. Reaction of $[\text{Ru}_4(\text{CO})_{13}]^{-2}$ with Ph_2PCl and $\text{Ru}_3(\text{CO})_{12}$ with Ph_2PPPh_2 gives the quasiplanar butterfly clusters $\text{Ru}_4(\text{CO})_{13}(\mu_2\text{-PPh}_2)_2$ and $\text{Ru}_4(\text{CO})_{10}(\mu_2\text{-PPh}_2)_4$, respectively. The cluster's electron count and its relationship to the observed polyhedron and Extended Hückel MO calculations are presented.³³⁰

The tetraosmium cluster $\text{Os}_4(\text{CO})_{15}(\text{PMe}_3)$ has been obtained from the reaction of $\text{Os}(\text{CO})_4(\text{PMe}_3)$ with either $\text{Os}_3(\text{CO})_{11}(\text{MeCN})$ or $\text{Os}_3(\text{CO})_{10}(\mu_2\text{-H})_2$. Me_3NO induced decarbonylation affords $\text{Os}_4(\text{CO})_{14}(\text{PMe}_3)$ which may be transformed into $\text{Os}_4(\text{CO})_{13}(\text{PMe}_3)$ upon thermolysis or photolysis. All three clusters have been structurally characterized and the fluxional behavior of the ancillary CO groups have been evaluated by ^{13}C NMR spectroscopy. The stepwise decarbonylation provides the first documented paradigm of a 64- \rightarrow 62- \rightarrow 60-electron transformation.³³¹ Photolysis of $\text{Os}_4(\text{CO})_{15}$ gives the new binary cluster $\text{Os}_4(\text{CO})_{14}$ which exhibits an irregular tetrahedral Os_4 core with weakly semibridging CO groups. A limiting ^{13}C NMR spectrum could not be obtained due to rapid CO exchange (-130°C). From the estimated CO exchange rate constant at -130°C and the observed broadness in the room temperature IR spectrum, the ancillary CO groups are predicted to be fluxional on



the IR time scale.³³² $\text{Os}_4(\text{CO})_{13}(\mu_2\text{-H})_2(\text{PMe}_3)$ has been isolated from the reaction of $\text{Os}_3(\text{CO})_{10}(\mu_2\text{-H})_2$ and $\text{Os}(\text{CO})_4(\text{PMe}_3)$ in the presence of Me_3NO . The butterfly polyhedron adopted by the cluster is confirmed by x-ray diffraction analysis. The PMe_3 ligand is shown to occupy a wing-tip site with one hydride ligand bridging an adjacent Os-Os bond and the other bridging the hinge Os-Os bond. A comparison with other planar 62-electron complexes that have no bridging ligands is presented.³³³

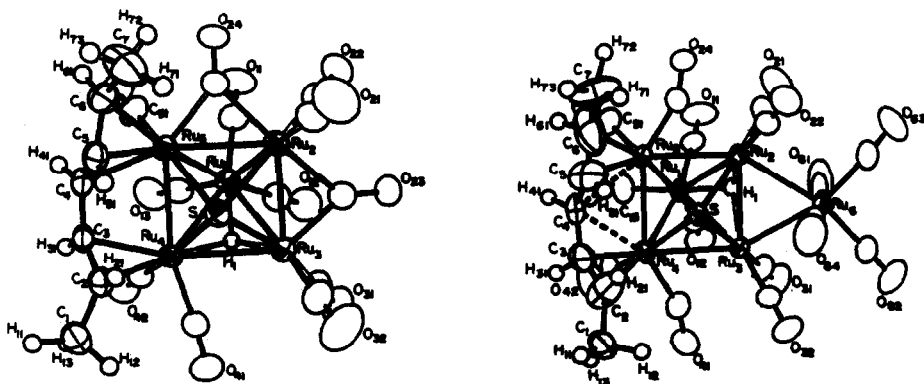
Treatment of $[\text{Os}_3(\text{CO})_{12}(\mu_2\text{-H})_3(\text{MeCN})]^{-1}$ with $[(\text{PPh}_3)_2\text{N}][\text{X}]$ (where X = NO_2 , Cl, Br, or I) gives $[\text{Os}_4(\text{CO})_{12}(\mu_2\text{-H})(\mu_3\text{-NC}(\text{O})\text{Me})]^{-1}$ when X = NO_2 , and $\text{Os}_4(\text{CO})_{12}(\mu_2\text{-H})_3(\mu_2\text{-X})$ and $[\text{Os}_4(\text{CO})_{12}(\mu_2\text{-H})_2\text{X}]^{-1}$ for the halides. All products were characterized spectroscopically in solution. The amido cluster derives from an oxygen transfer from the nitrite anion to the coordinated MeCN ligand. Reaction of iodo cluster $[\text{Os}_4(\text{CO})_{12}(\mu_2\text{-H})\text{I}]^{-1}$ with methyl or ethyl triflate affords the unstable alkyl iodide clusters $\text{Os}_4(\text{CO})_{12}(\mu_2\text{-H})_2(\text{IR}')$ (where $\text{R}' = \text{CH}_3$ or Et). Isolation of these coordinated alkyl iodide clusters was unsuccessful due to disproportionation to

$\text{Os}_4(\text{CO})_{12}(\mu_2\text{-H})_3\text{I}$ and $\text{Os}_4(\text{CO})_{12}(\mu_2\text{-H})_4$. Functionalization of the anionic clusters with $\text{Cu}(\text{PPh}_3)\text{Cl}$ and $\text{Au}(\text{PPh}_3)\text{Cl}$ and X-ray diffraction analysis of the resulting mixed-metal clusters are included.³³⁴

Reaction of the phosphinidene-capped cluster $\text{Os}_3(\text{CO})_9(\mu_2\text{-H})_2(\mu_3\text{-PR})$ (where $\text{R} = \text{Ph}$ or Cy (cyclohexyl)) with $\text{M}_3(\text{CO})_{12}$ (where $\text{M} = \text{Ru}$ or Os) gives the tetranuclear clusters $\text{Os}_3\text{M}(\text{CO})_{12}(\mu_2\text{-H})_2(\mu_3\text{-PR})$ in addition to the known penta- and hexanuclear clusters $\text{Os}_3\text{M}_2(\text{CO})_{15}(\mu_4\text{-PR})$ and $\text{Os}_3\text{M}_3(\text{CO})_{17}(\mu\text{-PR})$, respectively. The X-ray crystal structure of $\text{Os}_4(\text{CO})_{12}(\mu_2\text{-H})_2(\mu_3\text{-PPh})$ is reported along with complete solution NMR and IR characterization of all new clusters. The tetranuclear clusters adopt a butterfly conformation consistent with the 62-electron count.³³⁵

(c) Pentanuclear Cluster

The pentaruthenium cluster $\text{Ru}_5(\text{CO})_{15}(\mu_4\text{-S})$ has been reacted with *trans*-2-heptene to give the pentadienyl cluster $\text{Ru}_5(\text{CO})_{12}(\mu_4\text{-S})(\mu_3\text{-H})(\eta^5\text{-1,5-Me}_2\text{C}_5\text{H}_5)$ in low yield. Use of 2,4-heptadiene instead of *trans*-2-heptene gives a higher yield of the product cluster. X-Ray diffraction analysis reveals a square-pyramidal core of five rutheniums capped by a μ_4 -sulfido ligand. The



synthesis and structural characterization of the related hexaruthenium cluster $\text{Ru}_6(\text{CO})_{15}(\mu_4\text{-S})(\mu_3\text{-H})(\eta^5\text{-1,5-Me}_2\text{C}_5\text{H}_5)$ is also described. The conditions necessary for interconversion of the penta- and hexaruthenium pentadienyl clusters are presented.³³⁶

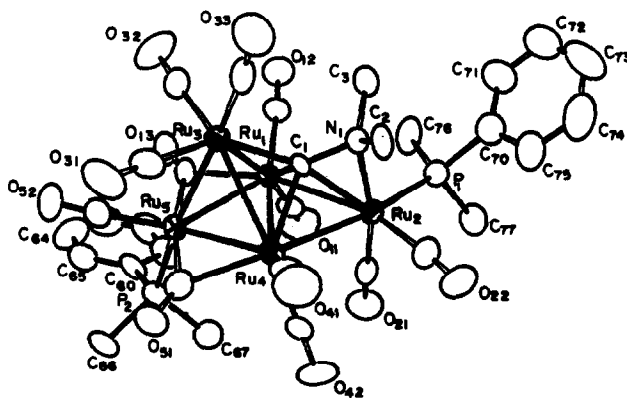
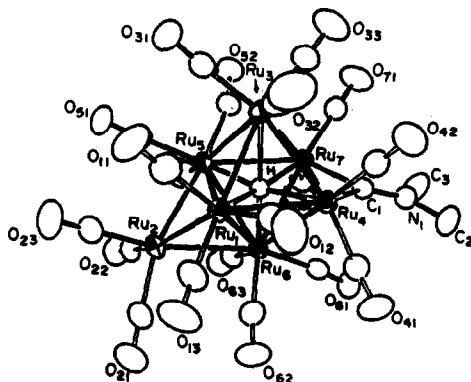
(d) Hexanuclear Clusters

The hexaosmium cluster $\text{Os}_6(\text{CO})_{21}(\mu_2\text{-H})(\mu_3\text{-PH})$ has been obtained from the reaction of $\text{Os}_3(\text{CO})_{11}(\text{MeCN})$ with $\text{Os}_3(\text{CO})_{10}(\mu_2\text{-H})(\mu_2\text{-PH}_2)$. Use of $\text{Os}_3(\text{CO})_{10}(\text{MeCN})_2$ instead of the mono-acetonitrile cluster gives $\text{Os}_6(\text{CO})_{20}(\text{MeCN})(\mu_2\text{-H})_2(\mu_3\text{-PH})$. Crystallographic analysis of the latter cluster reveals that the $\mu_3\text{-PH}$ group serves to ligate two Os_3 triangles; one Os_3 triangle is symmetrically bridged via an Os-Os edge while the other triangle bonds to the $\mu_3\text{-PH}$ ligand in a terminal fashion. Facile deprotonation of one of the $\mu_2\text{-H}$ ligands in the former cluster gives the anionic cluster $[\text{Os}_6(\text{CO})_{21}(\mu_2\text{-H})(\mu_3\text{-PH})]^{-1}$, while thermolysis leads to $\text{Os}_6(\text{CO})_{18}(\mu_2\text{-H})(\mu_6\text{-P})$. Deprotonation of the $\mu_6\text{-P}$ cluster gives $[\text{Os}_6(\text{CO})_{18}(\mu_6\text{-P})]^{-1}$ which has been structurally characterized.³³⁷ $\text{P}(\text{OMe})_3$ reacts with $\text{Os}_6(\text{CO})_{16}(\text{MeCN})_2$ to yield two isomers of $\text{Os}_6(\text{CO})_{16}(\text{P}(\text{OMe})_3)_2$ as the major products. ^1H NMR analysis reveals that one of the isomers has equivalent $\text{P}(\text{OMe})_3$ groups while the other has inequivalent $\text{P}(\text{OMe})_3$ groups. X-Ray structural examination of both isomers establishes the phosphite regiochemistry about the cluster polyhedron. The symmetrical isomer is shown to have $\text{P}(\text{OMe})_3$ ligands on the capping osmium atoms while the other isomer is substituted at a capping and internal osmium atom of the bicapped-tetrahedral frame. The observed solution isomerism and possible interconversion mechanism are discussed.³³⁸

The crystal structure of the hexaruthenium carbide cluster $\text{Ru}_6(\text{CO})_{13}(\mu_2\text{-CO})(\eta^6\text{-toluene})$ has been reported.³³⁹

(e) Higher Nuclearity Clusters

The heptaruthenium cluster $\text{Ru}_7(\text{CO})_{19}(\mu\text{-CNMe}_2)(\mu_6\text{-H})$ has been obtained from the reaction of $\text{Ru}(\text{CO})_5$ with $\text{Ru}_4(\text{CO})_{12}(\mu_4\text{-}\eta^2\text{-CNMe}_2)(\mu_2\text{-H})$ or $\text{Ru}_5(\text{CO})_{14}(\mu_4\text{-}\eta^2\text{-CNMe}_2)(\mu_2\text{-H})$. X-Ray diffraction analysis reveals a capped octahedral cluster with an interstitial hydride. The μ_6 -hydride is observed to be slightly displaced toward the capping ruthenium atom.³⁴⁰



Electrochemical oxidation of $[\text{Os}_{10}(\text{CO})_{24}(\mu_6\text{-C})]^{-2}$ at a hanging drop mercury electrode initially affords $[\text{Os}_{20}(\text{CO})_{48}(\mu_6\text{-C})_2\text{Hg}_2]^{-2}$. The latter cluster transforms to $[\text{Os}_{20}\text{Hg}(\text{CO})_{48}(\mu_6\text{-C})_2]^{-2}$. Cyclic voltammetric studies of the parent dianion support the presence of

a two-electron reduction process to give the tetraanion $[\text{Os}_{10}(\text{CO})_{24}(\mu_6\text{-C})]^{-4}$. Independent synthesis and electrochemical study of the trianion $[\text{Os}_{10}(\text{CO})_{24}(\mu_6\text{-C})]^{-3}$ has established the stepwise nature of reduction in these clusters. The IR spectra of the di-, tri-, and tetraanion are presented and the structural changes associated with cluster polyhedron are briefly discussed.³⁴¹ A separate report dealing with the design of a thin layer, IR-transparent electrochemical cell along with its application in the redox study of $[\text{Os}_6(\text{CO})_{18}(\mu_6\text{-P})]^{-1}$ and $[\text{Os}_{10}(\text{CO})_{24}(\mu_6\text{-C})]^{-1}$ is presented.³⁴²

The spin-lattice relaxation times for several decanuclear osmium clusters possessing interstitial hydrides have been reported. The inversion recovery technique was employed and interstitial hydrides in a tetrahedral core appear to relax more rapidly than hydrides located in an octahedral site.³⁴³ Hydride fluxionality in several hydrido decaosmium clusters has been examined using the observed $^1\text{J}({}^{187}\text{Os}-^1\text{H})$ values. Polynuclear structures and hydride exchange pathways are postulated based on the NMR data.³⁴⁴

The ruthenium cluster $\text{Ru}_{55}(\text{P-t-Bu}_3)_{12}\text{Cl}_{20}$ has been studied using high-resolution electron microscopy (HREM). The cluster's morphology and atomic structure has been observed by dynamic in situ HREM measurements at TV rate using low-light-level, silicon-intensified target cameras.³⁴⁵

(f) Mixed-Metal Clusters

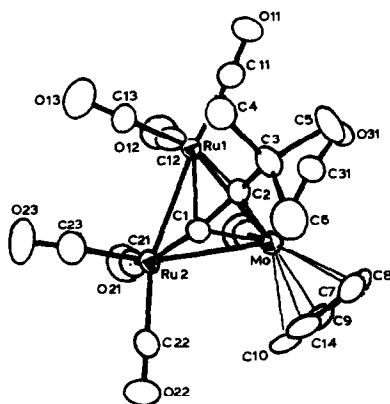
1. Clusters Containing Main Group Atoms

One or two bismuth atoms have been incorporated into ruthenium clusters. Reaction of $\text{Bi}(\text{NO}_3)_3$ with $[\text{Ru}_4(\text{CO})_{12}(\mu_2\text{-H})_3]^{-1}$ leads to $\text{Ru}_3(\text{CO})_9(\mu_2\text{-H})_3(\mu_3\text{-Bi})$ which is shown by X-ray diffraction analysis to possess a distorted tetrahedral core. Each Ru-Ru edge is bridged by a hydride ligand. Other bismuth clusters synthesized

and structurally studied include $\text{Ru}_3(\text{CO})_9(\mu_3\text{-Bi})_2$ and $\text{Ru}_4(\text{CO})_{12}(\mu_4\text{-Bi})_2$.³⁴⁶ $\text{Bi}(\text{NO}_3)_3$ has been reacted with $[\text{Ru}(\text{CO})_{11}(\mu_2\text{-H})]^{-1}$ in methanol to yield the pentaruthenium cluster $\text{Ru}_5(\text{CO})_{18}(\mu_2\text{-H})(\mu_4\text{-Bi})$. X-Ray diffraction analysis indicates a spiro-cluster where the μ_4 -bismuth atom ligates a $\text{Ru}_2(\text{CO})_8$ and a $\text{Ru}_3(\text{CO})_{10}(\mu_2\text{-H})$ fragment. The coordination geometry about the bismuth atom is observed to be pseudo-tetrahedral.³⁴⁷

2. Clusters Containing Other Metals

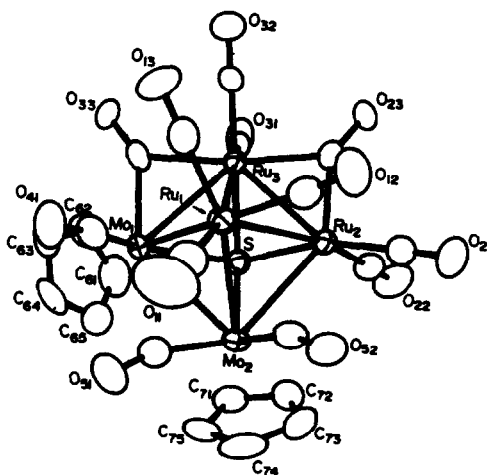
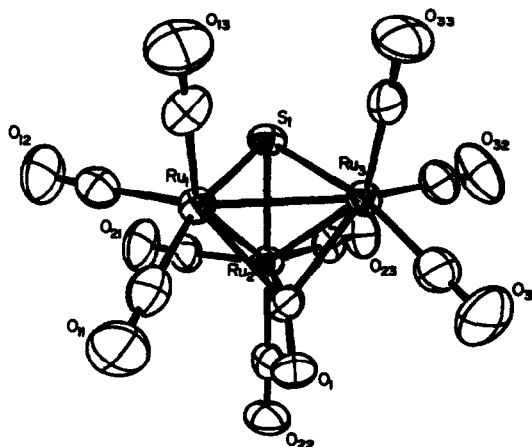
The mercury-bridged cluster $[\text{Ru}_3(\text{CO})_9(\mu_3\text{-}\eta^2\text{-C=C-t-Bu})](\mu_3\text{-Hg})[(\eta^5\text{-C}_5\text{H}_5)\text{Mo}(\text{CO})_3]$ has been examined in thermolysis, photolysis, and ligand substitution reactions. The $\mu_2\text{-Hg-Ru}_2$ bond is shown to be less labile than the Hg-Mo bond. Photolysis leads to elimination of Hg^0 and formation of the new triangular cluster $(\mu_2\text{-}\eta^2\text{-C=C-t-Bu})\text{Ru}_2\text{Mo}(\eta^5\text{-C}_5\text{H}_5)(\text{CO})_8$. X-Ray diffraction analysis and variable-temperature ^{13}C NMR results are presented. The acetylide ligand exhibits fluxional behavior interpreted by an edge-hopping motion between the two Ru-Mo edges.³⁴⁸ Reaction of $\text{Ru}_3(\text{CO})_{12}$ with



$[(\eta^5\text{-C}_5\text{H}_5)\text{M}(\text{CO})_3]^{-1}$ (where M = Mo or W) gives $[\text{Ru}_3\text{M}(\eta^5\text{-C}_5\text{H}_5)(\text{CO})_{12}]^{-1}$ in good yield. The X-ray structure of the molybdenum cluster and its reactions with H^+ , H_2 , and alkynes are presented. The cluster

$[\text{Ru}_3\text{W}(\eta^5\text{-C}_5\text{H}_5)(\text{CO})_{10}(\mu_4\text{-}\eta^2\text{-MeC=CMe})]^{-1}$ has been isolated and characterized structurally. The polyhedral core exhibits a butterfly arrangement of metal atoms.³⁴⁹

The tetrahedrane cluster $\text{RuMo}_2(\text{CO})_7(\eta^5\text{-C}_5\text{H}_5)_2(\mu_3\text{-S})$ has been prepared from $\text{Ru}_3(\text{CO})_9(\mu_3\text{-CO})(\mu_3\text{-S})$ and $\{\{\eta^5\text{-C}_5\text{H}_5\}\text{Mo}(\text{CO})_2\}_2$ at 83 °C. The pentanuclear cluster $\text{Ru}_3\text{Mo}_2(\text{CO})_{10}(\mu_2\text{-CO})_2(\eta^5\text{-C}_5\text{H}_5)_2(\mu_4\text{-S})$ was also isolated in 2 % yield. All the ruthenium clusters have been structurally characterized. The pentanuclear cluster transforms into the RuMo_2 cluster under similar reaction conditions and is suggested to be an intermediate in the formation of the tetrahedrane cluster. A plausible sequence for the construction of the pentanuclear and tetrahedrane clusters is presented.³⁵⁰ In a separate paper, the above tetrahedrane cluster has been examined in phenyl acetylene oligomerization reactions. The clusters $\text{Mo}_2\text{Ru}(\text{CO})_2(\eta^5\text{-C}_5\text{H}_5)_2[\mu_3\text{-}\eta^6\text{-HCC(Ph)C(H)C(Ph)C(H)C(Ph)}](\mu_3\text{-S})$ and $\text{Mo}_2\text{Ru}(\text{CO})_2(\eta^5\text{-C}_5\text{H}_5)_2[\mu\text{-}\eta^3\text{-PhCC(H)CPh}][\mu_3\text{-}\eta^3\text{-HCC(Ph)CH}](\mu_3\text{-S})$ have been isolated and fully characterized. The former cluster exhibits a 1,3,5-triphenyldimetallaheptatrienyl face bridging ligand, formed from the head-to-tail coupling of three phenyl acetylene molecules. The latter cluster possesses a triply bridging 2-phenyldimetalallyl ligand and an edge bridging 1,3-diphenyldimetalallyl ligand. The reactivity of these new clusters and their interconversion chemistry are fully described.³⁵¹ $\text{Ru}(\text{CO})_5$ has been reacted with $\text{RuMo}_2(\text{CO})_7(\eta^5\text{-C}_5\text{H}_5)_2(\mu_3\text{-S})$ to give the new clusters $\text{Mo}_2\text{Ru}_4(\text{CO})_{13}(\mu_4\text{-}\eta^2\text{-CO})(\eta^5\text{-C}_5\text{H}_5)_2(\mu_4\text{-S})$ and $\text{Mo}_2\text{Ru}_5(\text{CO})_{14}(\mu_4\text{-}\eta^2\text{-CO})_2(\eta^5\text{-C}_5\text{H}_5)_2(\mu_4\text{-S})$. IR spectral analysis indicates that the $\mu_4\text{-CO}$ groups in the Mo_2Ru_5 cluster are vibrationally coupled, giving rise to a symmetric and antisymmetric C-O stretch. Cluster growth sequences are presented and discussed.³⁵²



The mixed-metal clusters $(\mu_3\text{-X})\text{RuCo}_2(\text{CO})_9$ (where X = alkyne, vinylidene, S, or PPh) have been examined for site selectivity in phosphine substitution reactions. Both metal sites react with incoming P-ligands. Cobalt substitution is kinetically controlled while ruthenium substitution is thermodynamically favored. The migratory aptitude of P-Co \rightarrow Ru-P rearrangement decreases in the order $\text{PMe}_3 > \text{PMe}_2\text{Ph} > \text{PMePh}_2 > \text{PPh}_3$. The X-ray structures of many of these new substituted clusters along with a reactivity comparison to the analogous FeCo_2 clusters are presented.³⁵³

Selective substitution by amines or phosphines at ruthenium is observed in the mixed-metal cluster $\text{HRuCo}_3(\text{CO})_{12}$. Solution characterization by IR and ^1H and ^{59}Co NMR support the preferential substitution at ruthenium. The X-ray crystal structure of $\text{HRuCo}_2(\text{CO})_{11}(\text{PPh}_3)$ is included.³⁵⁴ The structure of $\text{CoRu}_3(\text{CO})_{10}(\mu_2\text{-CO})_3(\mu_2\text{-H})$ has been solved and comparison to the $\mu_2\text{-AuPPh}_3$ derivative is discussed. It was concluded that use of the phosphineaurio ligand positions should be used cautiously in defining hydride ligand positions, despite the H and AuPPh_3 isolobal relationship.³⁵⁵

The tetranuclear cluster $(\eta^5\text{-C}_5\text{Me}_5)_2\text{Ru}_2\text{Rh}_2(\text{CO})_6(\mu_3\text{-CO})_2$ has been prepared from $\text{Ru}_3(\text{CO})_{12}$ and $(\eta^5\text{-C}_5\text{Me}_5)\text{Rh}(\text{CO})_2$ in the presence of H_2 . The tetrahedral metal core and $\mu_3\text{-CO}$ ligands are confirmed by X-ray diffraction analysis. Cluster cleavage to $\text{Ru}(\text{CO})_5$ and $(\eta^5\text{-C}_5\text{Me}_5)\text{Rh}(\text{CO})_2$ by CO occurs readily with a half-life of ca. 4.5 hrs at ambient temperature and pressure. Reaction with H_2 gives $(\eta^5\text{-C}_5\text{Me}_5)\text{Rh}(\text{CO})_2$ as the only identifiable product.³⁵⁶ The related cluster $\text{Ru}_3\text{Rh}(\text{CO})_9(\mu_2\text{-CO})(\eta^5\text{-C}_5\text{H}_5)(\mu_2\text{-H})_2$ was obtained from $\text{Rh}_2(\text{CO})_4\text{Cl}_2$ and $\text{Ru}_4(\text{CO})_{13}(\mu_2\text{-H})_2$ in the presence of $\text{Tl}(\eta^5\text{-C}_5\text{H}_5)$. X-Ray crystallography reveals a distorted Ru_3Rh tetrahedron and hydride bridging of the Ru-Ru edges. The $\mu_2\text{-CO}$ ligand bridges a Ru-Rh edge. The hydride ligands are inequivalent at low temperature in the ^1H NMR spectrum and the activation energy for hydride coalescence is reported.³⁵⁷ In a separate paper, the stereochemical non-rigidity of the above Ru_3Rh cluster and the clusters $\text{Ru}_3\text{Rh}(\text{CO})_9(\mu_2\text{-CO})(\mu_2\text{-H})_2(\eta^5\text{-C}_5\text{Me}_5)$ and $\text{Ru}_3\text{Rh}(\text{CO})_9(\eta^5\text{-C}_5\text{Me}_5)(\mu_2\text{-H})_2$ have been studied by NMR spectroscopy.³⁵⁸

The heterometallic clusters $\text{M}_2\text{Ru}_4(\text{CO})_{12}(\mu\text{-Ph}_2\text{P}(\text{CH}_2)_n\text{PPh}_2)(\mu_3\text{-H})_2$ (where $\text{M} = \text{Cu}$ or Ag ; $n = 1\text{-}6$) have been prepared from $[\text{Ru}_4(\text{CO})_{12}(\mu\text{-H})_2]^{-1}$ and $[\text{M}(\text{MeCN})_4]^{-1}$. For $\text{M} = \text{Cu}$ and $n = 2, 3$, or

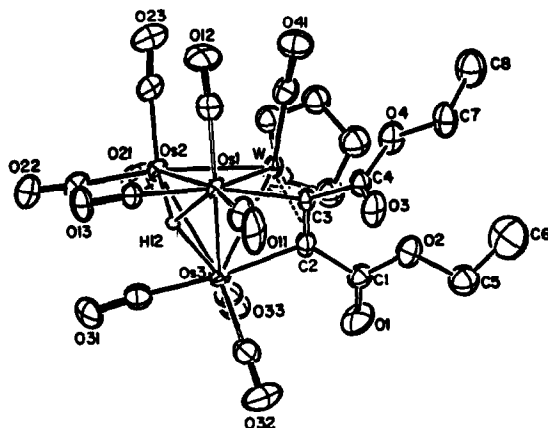
5, X-ray diffraction analysis reveals a tetrahedral ruthenium core which is capped by a copper metal atom. The remaining copper fragment caps a CuRu_2 face to complete the observed trigonal-bipyramidal geometry common for these derivatives. The bidentate phosphine bridges the two coinage metals. Facile site-exchange of the two coinage metals has been demonstrated by ^1H and ^{31}P NMR measurements.³⁵⁹ Solution fluxionality and the X-ray structures of $\text{Cu}_2\text{Ru}_4(\text{CO})_{12}(\text{PR}_3)_2(\mu_3\text{-H})_2$ (where R = cyclohexyl or CHMe_2) have been communicated. The ligand's cone angle is shown to influence the polyhedral structure adopted by the cluster.³⁶⁰ An in-depth study of the metal framework fluxionality in $\text{Cu}_2\text{Ru}_4(\text{CO})_{12}\text{L}_2(\mu_3\text{-H})_2$ (where L = various phosphines and phosphites) has appeared. The activation parameters for coinage metal site-exchange have been calculated by band-shape analysis (^{31}P NMR).³⁶¹ The synthesis of the gold/ruthenium clusters $\text{Au}_2\text{Ru}_4(\text{CO})_{12}(\mu\text{-Ph}_2\text{E}(\text{CH}_2)_n\text{E}'\text{Ph}_2)(\mu_3\text{-H})(\mu_2\text{-H})$ (where E = E' = P, n = 2; E = E' = As, n = 1 or 2; E = As, E' = P, n = 1 or 2) has appeared. X-Ray diffraction analysis of $\text{Au}_2\text{Ru}_4(\text{CO})_{12}(\mu\text{-Ph}_2\text{AsCH}_2\text{PPh}_2)(\mu_3\text{-H})(\mu_2\text{-H})$ reveals the presence of a square-pyramidal core with a face-capping $\text{Ru}(\text{CO})_3$ fragment. ^{197}Au Mossbauer spectra are reported and the results used to determine the polyhedral structures of the other gold-containing clusters.³⁶²

The related Ag/Ru cluster $\text{Ag}_2\text{Ru}_4(\text{CO})_{12}(\mu\text{-Ph}_2\text{PCH}_2\text{PPh}_2)(\mu_3\text{-H})_2$ has been synthesized and crystallographically analyzed. ^{109}Ag (^1H) INEPT NMR spectra for the dppm, dppe, dppb, and the bis(triphenylphosphine) clusters are reported. Values of $^1J(^{107}, ^{109}\text{Ag}-^{107}, ^{109}\text{Ag})$ have been measured and reported.³⁶³ The X-ray structure of $\text{Au}_3\text{Ru}_4(\text{CO})_{12}(\mu\text{-Ph}_2\text{PCH}_2\text{PPh}_2)(\text{PPh}_3)(\mu_2\text{-H})$ has been reported. The polyhedral structure is based on a Au_2Ru_3 square pyramid with adjacent face-capping $\text{Ru}(\text{CO})_3$ and $\text{Au}(\text{PPh}_3)$ fragments.³⁶⁴

New heterobimetallic Au/Ru and Au/Os hydrido complexes have been prepared. Reaction of $\text{AuPPh}_3\text{NO}_3$ with $\text{M}(\text{H})_4(\text{PPh}_3)_3$ (where M = Ru or Os) leads to $[\text{Au}_2\text{M}(\text{H})_3(\text{PPh}_3)_5]^{+1}$. The carbonyl complexes $[\text{AuM}(\text{H})_2(\text{CO})(\text{PPh}_3)_4]^{+1}$ and $[\text{AuM}(\text{H})_2(\text{CO})_2(\text{PPh}_3)_3]^{+1}$ were synthesized similarly from $\text{M}(\text{H})_2(\text{CO})(\text{PPh}_3)_3$ and $\text{M}(\text{H})_2(\text{CO})_2(\text{PPh}_3)_2$, respectively. X-Ray diffraction analysis of $[\text{Au}_2\text{Os}(\text{H})_3(\text{PPh}_3)_5]^{+1}$ and $[\text{AuRu}(\text{H})_2(\text{CO})(\text{PPh}_3)_4]^{+1}$ is included. Isomerization of 1-hexene to cis- and trans-2-hexene using $[\text{AuRu}(\text{H})_2(\text{CO})(\text{PPh}_3)_4]^{+1}$ is higher than with the parent ruthenium complex.³⁶⁵

The mixed-metal clusters $\text{HRu}_2\text{Os}(\mu\text{-COMe})(\text{CO})_{10}$, $\text{H}_3\text{Ru}_2\text{Os}(\mu_3\text{-COMe})(\text{CO})_9$, $\text{HRuOs}_2(\mu\text{-COMe})(\text{CO})_{10}$, and $\text{H}_3\text{RuOs}_2(\mu_3\text{-COMe})(\text{CO})_9$ have been synthesized and examined in ligand substitution reactions and for reductive elimination of hydrogen. Equilibrium constants for hydrogenation and polyhedral isomerization have provided estimates of the Ru-H-Ru and Os-H-Os bond energies. Reductive elimination of H_2 occurs at a single metal atom.³⁶⁶

Free rotation of the $\text{Cr}(\text{CO})_5$ fragment in $(\text{OC})_5\text{Cr}[\text{Os}(\text{CO})_3\text{PMe}_3]_2$ suggests the presence of a centrally directed, three-center two-electron bond between the three metal atoms. The crystal structure and variable-temperature ^{13}C NMR measurements are presented.³⁶⁷ Alkynes react with $(\eta^5\text{-C}_5\text{H}_5)\text{WOS}_3(\text{CO})_{12}\text{H}$ to give clusters of the form $(\eta^5\text{-C}_5\text{H}_5)\text{WOS}_3(\text{CO})_{10}(\mu_3\text{-}\eta^2\text{-RC=CR}')$. Symmetrical and/or unsymmetrical isomers are formed depending on the nature of the R and R' groups. Facile intramolecular C=C bond scission is observed (R = R' = Ph, tol; R = Ph, R' = tol) upon Me_3NO -induced decarbonylation to give the corresponding dialkylidyne clusters $(\eta^5\text{-C}_5\text{H}_5)\text{WOS}_3(\text{CO})_9(\mu_3\text{-CR})(\mu_3\text{-CR}')\text{H}$ and alkyne-oxo clusters $(\eta^5\text{-C}_5\text{H}_5)\text{WOS}_3(\text{CO})_8(\mu\text{-O})(\mu_3\text{-}\eta^2\text{-RC=CR}')\text{H}$ and full spectroscopic characterization of all new clusters is included.³⁶⁸



The crystal structure of $\text{ReOs}_3(\text{CO})_{12}(\mu\text{-H})_5$ has been solved and is shown to exhibit a tetrahedral ReOs_3 core.³⁶⁹ Ligand substitution reactions in $\text{Fe}_2\text{Os}(\text{CO})_{12}$ are reported. The kinetics reveal a first-order dependence in cluster and zero-order dependence in ligand. A dissociative CO loss is suggested to be rate-limiting based on the observed kinetics and the activation parameters. CO loss is believed to occur from an iron atom, followed by rearrangement of an osmium carbonyl to the iron center. Ligand capture at the unsaturated osmium atom leads to the observed product.³⁷⁰

Hydride and carbonyl fluxionality in $\text{Os}_3\text{Pt}(\text{CO})_{10}(\text{PCy}_3)(\mu_2\text{-H})_2$ has been examined by NMR spectroscopy. Protonation of the Os_3Pt cluster with HBF_4 leads to $[\text{Os}_3\text{Pt}(\text{CO})_{10}(\text{PCy}_3)(\mu_2\text{-H})_3]^+$ which has been crystallographically characterized. The fluxional behavior of the two $\text{Os}(\mu_2\text{-H})\text{Os}$ hydrides is demonstrated by NOE studies while carbonyl exchange was studied using the DANTE pulse sequence. The fluxional behavior of the butterfly clusters $\text{Os}_3\text{Pt}(\text{CO})_{10}(\text{PCy}_3)\text{L}(\mu_2\text{-H})_2$ (where $\text{L} = \text{CO}$ or PCy_3) is different and has been examined by ^{13}C 2D exchange correlation NOESY studies. The hydrides in these butterfly clusters are nonfluxional. Values of $^1J(^{187}\text{Os}-^{13}\text{C})$

coupling constants are included.³⁷¹ Reaction of $\text{Os}_3\text{Pt}(\text{CO})_{10}(\text{PCy}_3)(\mu_2\text{-H})_2$ with isocyanides gives the corresponding 60-electron butterfly clusters $\text{Os}_3\text{Pt}(\text{CO})_9(\text{PCy}_3)(\text{RNC})(\mu_2\text{-H})_2$. NMR studies indicate that the RNC ligand is coordinated to an osmium atom. Thermolysis leads to CO loss and $\text{Os}_3\text{Pt}(\text{CO})_9(\text{PCy}_3)(\text{RNC})(\mu_2\text{-H})_2$. X-Ray diffraction analysis reveals a Os_3Pt tetrahedral core with the RNC group coordinated to platinum. This 58-electron cluster reacts with diazomethane to give $\text{Os}_3\text{Pt}(\text{CO})_9(\text{PCy}_3)(\text{RNC})(\mu_2\text{-H})_2(\mu_2\text{-CH}_2)$. The methylene is shown to bridge an Os-Os edge. Facile protonation of the remaining Os-Os edge is observed with $\text{CF}_3\text{CO}_2\text{H}$ or HBF_4 .³⁷² The crystal structures of $\text{Os}_2\text{Pt}_2(\text{CO})_8(\text{PCy}_3)_2(\mu_2\text{-H})_2$ and $\text{Os}_3\text{Pt}(\text{CO})_{10}(\text{PCy})_2(\mu_2\text{-H})_2$ in toluene are reported.^{373,374}

The heteronuclear clusters $\{\text{Os}_{10}(\text{CO})_{24}(\mu_6\text{-C})(\text{NPR}_3)_n\}^{\text{M}+}$ (where $n = 1, m = 1, M = \text{Au, Ag, or Cu}; n = 2, m = 0, M = \text{Au or Ag}$) have been synthesized and NMR analysis indicates the presence of two isomeric forms. The proposed isomeric forms and a general interconversion pathway involving cap/edge bridge/cap exchange are presented.³⁷⁵

V. Miscellaneous Chemistry

(a) Heterogeneous and Supported Complexes

Siloxy-bridged diruthenium(II) complexes have been prepared and examined as model systems for cluster-derived, silica supported catalysts.³⁷⁶ ESCA results of Ru(III) and Ru(IV) oxides deposited on Al_2O_3 and MoO_3 -covered Al_2O_3 before and after reduction with hydrogen are reported. MoO_3 covering increases the stability of the ruthenium to reduction.³⁷⁷ EXAFS and XANES analyses of electropolymerized films of $[\text{M}(\text{v-bpy})_3]^{+2}$ (where v-bpy = 4-vinyl-4'-methyl-2,2'-bipyridine; $M = \text{Ru or Os}$) and $[\text{Os}(\text{phen}(\text{v-bpy})_2)]^{+2}$ have been published. These results are discussed with respect to in situ investigation of electrocatalytic systems.³⁷⁸ A paper

dealing with the role of preparative variables on the surface composition of supported Pt-Ru bimetallic clusters has appeared.³⁷⁹

The morphology changes of Al₂O₃-supported Ru₃(CO)₁₂ have been analyzed by EXAFS measurements. Addition of CO disrupts the cluster and gives Ru(CO)_n species while CO removal leads to the formation of new ruthenium clusters.³⁸⁰ XANES, AES, and LEED studies of Ru₃(CO)₁₂ adsorbed on Cu(III) are reported. Conditions leading to the formation of bimetallic Ru/Cu clusters are discussed.³⁸¹ Hydrogenation of CO by Ru-Al₂O₃ catalysts is dependent on the initial treatment of the supported catalyst. The effect of oxidation/reduction on the microstructure of the Ru particles and the resulting catalytic activity are discussed.³⁸² Fischer-Tropsch activity and methanation of CO₂ is reported for Ru₃(CO)₁₂ supported on pyrolyzed polyacrylonitrile. A comparison with ruthenium on Al₂O₃ is made.³⁸³

Ru₃(CO)₁₂ reacts with magnesia to give the anionic cluster [Ru₃(CO)₁₁(H)]⁻¹(Mg⁺²)₁. Zinc and lanthanum oxide supports also give the same cluster. Programmed thermal decomposition studies of the anionic cluster lead to mononuclear Ru^{II}(CO)_n(OMgC)₂ and metallic ruthenium depending on the atmosphere, temperature, and amount of support hydroxylation. Water gas shift, methanation, and CO oxidation chemistry is described.³⁸⁴ An isotope-labeling study has been conducted in order to study the effect of subcarbonyl surface intermediates from Ru₃(CO)₁₂ supported on Al₂O₃. Temperature-programmed decomposition (TPD) results are presented along with surface mechanisms for CO and H₂ utilization.³⁸⁵

Al₂O₃ supported Fe_xRu_{3-x}(CO)₁₂ (where x = 0, 1, 2, or 3) have been examined by EXAFS, IR and UV-visible-diffuse reflectance spectroscopies, and by TPD studies. The cluster's integrity was maintained in all cases and support attachment was through the

oxygen atom of a carbonyl group.³⁸⁶ The thermal behavior of $\text{Fe}_2\text{Ru}(\text{CO})_{12}$ supported on SiO_2 has been investigated by IR spectroscopy. Facile decomposition to $\text{Ru}^0(\text{CO})_2$, $\text{Ru}^{\text{II}}(\text{CO})_2$, and $\text{Ru}^{\text{III}}(\text{CO})_2$ surface-supported fragments are observed. Treatment with hydrogen followed by vacuum leads to the surface-bound clusters $\text{H}_2\text{FeRu}_3(\text{CO})_{13}$, $\text{H}_4\text{FeRu}_3(\text{CO})_{12}$, $\text{H}_4\text{Ru}_4(\text{CO})_{12}$, and $\text{HRu}_3(\text{CO})_{10}(\text{OSi-surface})$.³⁸⁷

$\text{Ru}(\text{CO})_3\text{Cl}_2(\text{THF})$ has been reacted with hydroxylated aluminum to yield supported $[\text{Ru}_3(\text{CO})_{11}(\text{H})]^{-1}$. Evidence is presented that supports the intermediacy of mononuclear $\text{Ru}^{\text{II}}(\text{CO})_3(\text{ads})$ as a precursor to the trinuclear cluster.³⁸⁸ $\text{H}_4\text{Ru}_4(\text{CO})_{12}$ has been physisorbed on SiO_2 , TiO_2 , $\gamma\text{-Al}_2\text{O}_3$, and MgO . Aggregates of metal particles are observed using SiO_2 while oxidation by the surface hydroxyls on TiO_2 and $\gamma\text{-Al}_2\text{O}_3$ yields mononuclear ruthenium complexes. Use of MgO allows for the stabilization of the initially formed anionic ruthenium clusters relative to the other supports.³⁸⁹

The polynuclear carbide cluster $[\text{Os}_5(\text{CO})_{14}(\text{C})]^{-2}$ was obtained from MgO -supported $\text{Os}_3(\text{CO})_{12}$. The surface-mediated reaction affords the carbide cluster in much higher yield (~65 %) than the previously reported pyrolytic route.³⁹⁰ Deposition of $\text{Os}_3(\text{CO})_{12}$ on SiO_2 has been examined by IR, XPS, and TPD analyses. Oxidized osmium(II) surface species are observed in both an argon and oxygen atmosphere. The original trinuclear framework was restored at elevated temperature under CO .³⁹¹ Diffuse Reflectance IR (DRIFTS) measurements are reported for the thermal decomposition of $\text{Os}_3(\text{CO})_{12}$. Rapid transformation to $\text{H}_4\text{Os}_4(\text{CO})_{12}$ is observed under H_2 .³⁹² Potassium-modified Os /alumina catalysts are described using $\text{Os}_3(\text{CO})_{12}$ and $\text{K}_2[\text{OsO}_2(\text{OH})_4]$. The role potassium plays in blocking CO adsorption and the relationship of the observed

carbonate/bicarbonate species to the water-gas shift reaction are discussed.³⁹³

The bonding of $\text{H}_2\text{Os}(\text{CO})_4$ and $\text{H}_4\text{Os}_4(\text{CO})_{12}$ to basic MgO has been examined using CP/MAS ^{13}C NMR and IR spectroscopies. A strong, localized adsorbate-support interaction of $[\text{Hos}(\text{CO})_4]^{-1}$ to a surface Mg^{+2} ion is indicated. The interaction is through the oxygen atom of a CO group. In contrast, only a weak surface association is observed with $[\text{H}_3\text{Os}_4(\text{CO})_{12}]^{-1}$.³⁹⁴

MAS ^{13}C NMR spectroscopy has been employed to identify the nature of the surface-bound cluster that results from $\text{Os}_3(\text{CO})_{12}$ impregnation of silica or alumina. Based on solid-state NMR measurements and spectral comparison to $\text{Os}_3(\text{CO})_{10}(\mu_2\text{-H})(\mu_2\text{-OX})$ (where X = SiEt_3 or O_2CH) and $\text{Os}_3(\text{CO})_{10}(\mu_2\text{-OMe})_2$ the supported osmium cluster is suggested to resemble the above open polyhedral clusters.³⁹⁵

Evidence for cluster catalysis using the silica-supported osmium cluster $\text{Os}_3(\text{CO})_{10}(\mu_2\text{-H})(\mu_2\text{-OSi-surface})$ is presented. The supported cluster catalyzes the hydrogenation of ethylene under mild conditions. A mechanism involving facile $3e^- = 1e^-$ interconversion of the surface-oxygen ligands allows for the generation of a vacant coordination site and entry into productive catalysis. A comparison of the catalytic activity of the supported cluster to the homogeneous cluster $\text{Os}_3(\text{CO})_{10}(\mu_2\text{-H})(\mu_2\text{-OPh})$ is made. The latter cluster is transformed into $\text{H}_2\text{Os}_3(\text{CO})_{10}$ and $\text{H}_2\text{Os}_4(\text{CO})_{12}$ under catalytic conditions. Support stabilization of the triosmium framework is clearly indicated and is discussed in the context of cluster catalysis.³⁹⁶

(b) CO and CO_2 Reduction

Reductive polymerization of CO in the Fischer-Tropsch reaction has been theoretically examined using the model complex

$\text{ClRuH}(\text{CH}_2)$.³⁹⁷ An electrochemical study has shown that ruthenium cathodes will reduce both CO and MeOH to methane. The rates and faradaic efficiencies are reported.³⁹⁸

Hydrocarbonylation of $\text{C}_2 - \text{C}_4$ alcohols using Co-Ru catalysts and synthesis gas has been reported. Iodine and iodides promote hydrocarbonylation. The cocatalytic effect displayed by the ruthenium and a plausible mechanism involving an intermediate olefin complex are discussed.³⁹⁹

Photochemical reduction of CO_2 to CO and HCO_2^- has been observed using the electron donor compound 1-benzyl-1,4-dihydronicotinamide and the ruthenium complexes $[\text{Ru}(\text{bpy})_3]^{+2}$ and $[\text{Ru}(\text{bpy})_2(\text{CO})_2]^{+2}$.⁴⁰⁰ Electrochemical reduction of CO_2 to methane using electroplated ruthenium electrodes has been reported. The effect of electrolyte impurities as promoters in methane formation is discussed.⁴⁰¹

(c) Oxidation Reactions

The dioxoruthenium(VI) complexes $[\text{Ru}(\text{O})_2\text{Cl}_4]^{-2}$ and $[\text{Ru}(\text{O})_2\text{Cl}_3]^{-1}$ have been prepared and structurally characterized. Halide loss in the former complex gives the five-coordinate dioxo complex. The dissociation constant for this equilibrium reaction has been spectrophotometrically determined and is reported. $[\text{Ru}(\text{O})_2\text{Cl}_3]^{-1}$ oxidized phosphines to phosphine oxides and reacts with cyclohexene to afford cyclohexene oxide, 2-cyclohexenone, 2-chlorocyclohexanone and cyclohexene chlorohydrin. 2,6-Di-tert-butylphenol was oxidized to corresponding benzoquinone in addition to yielding some 3,5,3',5'-tetra-tert-butylidiphenoquinone.⁴⁰² The crystal structure of $\text{trans-}[\text{Ru}(\text{O})_2(\text{HIO}_6)_2]^{-6}$ (as the NaK_5 salt) has been solved. IR and Raman spectral data are reported along with electrochemical results. The periodate complex and the analogous tellurate complex $[\text{Ru}(\text{O})_2(\text{H}_2\text{TeO}_6)_2]^{-6}$ have been examined in oxidation reactions. The periodate complex oxidizes primary and

secondary alcohols to carboxylic acids and ketones, respectively. The reactions become catalytic with the addition of periodate as a co-catalyst.⁴⁰³ The synthesis and oxidation chemistry of $\text{Ru}(\text{Saloph})(\text{L})\text{Cl}$ and $[\text{Ru}(\text{Saloph})\text{Cl}_2]^{-1}$ [where $\text{SolphH}_2 = \text{bis}(\text{salicylaldehyde})\text{-o-phenylenediamine}$; $\text{L} = \text{imidazole, 2-methylimidazole, or pyridine}$] have been presented. Both ruthenium complexes react with O_2 to form 1:1 complexes. Cyclohexene oxidation to cyclohexene oxide is observed and a mechanism based on rate and equilibrium constants is reported.⁴⁰⁴

A report describing the oxidation of H_2O to O_2 by mononuclear $\text{Ru}(\text{amine})$ complexes and a $\text{Ce}(\text{IV})$ oxidant has appeared.⁴⁰⁵

The complexes $[\text{Ru}(\text{bpy})_2(\text{H}_2\text{O})_2]^{+2}$ and $[\text{Ru}(1,10\text{-phen})_2(\text{H}_2\text{O})_2]^{+2}$ catalytically oxidize alkanes to alcohols and ketones in the presence of $t\text{-BuOOH}$. Based on kinetic isotope effect measurements ($K_{\text{H}}/k_{\text{D}} = 3.5$ for cyclohexane) and C-H bond relative reactivities ($k_3/k_2 \approx 6.5$ for adamantane) a hydrogen abstraction mechanism is proposed.⁴⁰⁶ The electrocatalytic oxidation of alkenes and ketones has been described using $[\text{Ru}(\text{trpy})(\text{bpy})(\text{O})]^{+2}$. Substrates examined include cyclohexene, safrole, isosafrole, isophorone, deoxybenzoin, and acetophenone.⁴⁰⁷

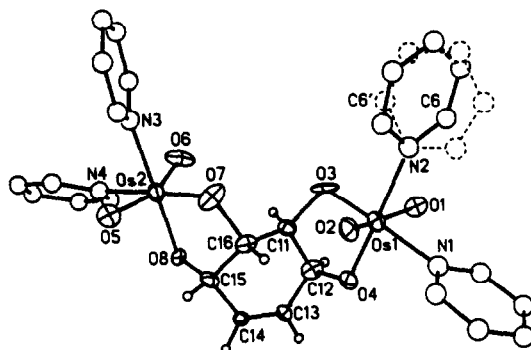
The pH-dependent redox properties of *cis*- and *trans*- $[\text{Ru}(\text{bpy})_2(\text{H}_2\text{O})_2]^{+2}$ are reported. The electrochemical data establish the relative stabilities of each isomer and the oxidation states associated with them. Aspects of catalytic H_2O oxidation to O_2 are presented within a 4-electron scheme involving aqua/hydroxo/oxo redox couples.⁴⁰⁸ Electrochemical oxidation of $[(\text{bpy})_2(\text{HO})\text{Ru}^{\text{III}}\text{ORu}^{\text{IV}}(\text{OH})(\text{bpy})_2]^{+3}$ gives $[(\text{bpy})_2(\text{O})\text{Ru}^{\text{IV}}\text{ORu}^{\text{V}}(\text{O})(\text{bpy})_2]^{+3}$ which is shown to be a powerful oxidant. Isopropanol, propanic, propenoic, and crotonic acid oxidation results are presented.⁴⁰⁹

The ruthenium oxo complex $[\text{Ru}(\text{bpy})(\text{L})(\text{O})]^{+2}$ (where L = phosphine or arsine) has been prepared from the corresponding aquo complex. Oxidation of alcohols to aldehydes and ketones, aldehydes to acids, and alkenes to epoxides and/or allylic oxidation products is reported.⁴¹⁰ Oxidation of $[\text{Ru}(\text{bpy})(\text{biq})(\text{L})(\text{H}_2\text{O})]^{+2}$ (where L = phosphine) yields the ruthenium oxo complex $[\text{Ru}(\text{bpy})(\text{biq})(\text{L})(\text{O})]^{+2}$. The kinetics for benzyl and allyl alcohol oxidation are reported along with the results of cyclobutanol oxidation which display reactivity consistent with two-electron oxidations. The reactivity of the mixed bpy/biq oxo complex is greater than the above bis(bpy) oxo complex as a result of increased hydrophobicity.⁴¹¹

The triruthenium oxo cluster $[\text{Ru}_3(\mu_3\text{-O})(\text{pfb})_6(\text{Et}_2\text{O})_3]^{+1}$ (where pfb = perfluorobutyrate) has been prepared and examined as a catalyst in alkene oxidations using molecular O_2 as the oxidant. Substrates studied include cyclohexene, trans- β -methylstyrene, and norbornene. From the effects of inhibitors, observed induction periods, and solvent effects, a free-radical chain process is suggested.⁴¹²

A communication reporting the catalytic epoxidation activity of the ruthenium and osmium phosphine complexes $[\text{MCl}(\text{L-L})_2]^{+1}$ [where M = Ru or Os; L-L = dppp or 1-diphenylphosphino-2-(2'-pyridyl)ethane] has appeared. A wide variety of alkenes are oxidized in the presence of PhIO, hypochlorites, and H_2O_2 .⁴¹³

Two papers have appeared dealing with arene osmylation reactions. Arenes and OsO_4 react to form 1:2 adducts which have been shown to be electron-donor-acceptor (EDA) complexes. The EDA complexes have been spectrally characterized and the association constants are reported. Photochemical excitation within the charge-transfer manifold of the EDA complex leads initially to the ion pair $[\text{ArH}^+\text{OsO}_4^-]$ and ultimately to complexes of the form $(\text{ArH})(\text{OsO}_4)_2(\text{py})_4$.^{414, 415}



(d) Carbon-Carbon Bond Forming Reactions

The hydroformylation of 1-pentene, styrene, and ethyl acrylate has been achieved using $[\text{HRu}(\text{CO})_4]^{-1}$. A comparison with $[\text{Ru}_3(\text{CO})_{11}(\mu_2\text{-H})]^{-1}$ and $\text{Ru}_3(\text{CO})_{12}$ reveals that mononuclear complex is the most active catalyst.⁴¹⁶

Fischer-Tropsch catalysis has been observed using metal cluster catalysts encapsulated in alumina pillared montmorillonite (APM) galleries. $\text{Ru}_3(\text{CO})_{12}$, $\text{Os}_3(\text{CO})_{12}$, $\text{H}_2\text{Os}_3(\text{CO})_{12}$, and $\text{H}_4\text{Ru}_4(\text{CO})_{12}$ were immobilized within the clay support. Crystalline ruthenium aggregates, obtained from the reduction of $[\text{Ru}_3(\text{CO})_{12}(\text{H})]^{+1}$ -APM, displayed unusual selectivity to branched products in the Fischer-Tropsch reaction. Carbonium ions arising from protonated Fischer-Tropsch olefins are suggested as participants in these reactions.⁴¹⁷

(e) Hydrogen Production

The formation of H_2 at a RuO_2 film electrode has been explored in order to better understand the chemistry observed with the colloidal RuO_2 system. Voltammetric results are presented.⁴¹⁸

Water photolysis using ruthenium/bpy complexes leads to H_2 formation. The complexes $[\text{Ru}(\text{bpy})_2(4\text{-R-4'-R'-bpy})]^{+2}$ (where R and R' = a wide variety and combination of substituents) function as sensitizers in a four component system ($\text{Ru}^{+2}/\text{MV}^{+2}/\text{EDTA}/\text{colloidal Pt}$)

used for H_2 production. Complexes with electron withdrawing substituents are the most active.⁴¹⁹ H_2 production from another four component system ($Ru^{+2}/MV^{+2}/EDTA/colloidal RuO_2$) has also been reported. The reaction has been examined as a function of light intensity, pH, temperature, and component concentration.⁴²⁰

$RuH_2(N_2)(PPh_3)_3$ reacts catalytically with alcohols to give H_2 via alcohol dehydrogenation. High turnover rates are reported and a plausible mechanism is presented and discussed.⁴²¹

VI. Acknowledgment

Ms. Claudia L. Williams and Ms. Carol N. Richmond are thanked for their library and typing assistance, respectively. The author thanks the Dean's Office of UNT and the Robert A. Welch Foundation for partial financial support during the writing of this review.

VII. References

1. K. S. J. Brewer, Diss. Abstr. B, 49 (1988) 104; DA No. 8803912.
2. B. G. R. T. Treco, Diss. Abstr. B., 49 (1988) 110; DA No. 8803416.
3. M. E. Marmion, Diss. Abstr. B, 49 (1988) 1692; DA No. 8812363.
4. R. S. Lumpkin, Diss. Abstr. B, 48 (1988) 2644; DA No. 8728462.
5. P. E. Neveux, Jr., Diss. Abstr. B, 48 (1988) 1976; DA No. 8722330.
6. W. F. Wacholtz, Diss. Abstr. B, 49 (1988) 2187; DA No. 8811325.
7. E. B. G. Megehee, Diss. Abstr. B, 48 (1988) 2187; DA No. 8722322.
8. J. P. Fitzgerald, Diss. Abstr. B, 48 (1988) 3280; DA No. 8800932.
9. P. M. Jackman, Diss. Abstr. B, 49 (1988) 1690; DA No. BRDX 81319.
10. W. D. Harman, Diss. Abstr. B, 48 (1988) 1975; DA No. 8723011.
11. M. R. Cordone, Diss. Abstr. B, 49 (1988) 2183; DA No. 8814990.
12. W. B. Tolman, Diss. Abstr. B, 49 (1988) 1697; DA No. 8814095.
13. R. T. Hembre, Diss. Abstr. B, 49 (1988) 1165; DA No. 8808945.
14. M. J. Sailor, Diss. Abstr. B, 49 (1988) 1694; DA No. 8811507.
15. S. Wang, Diss. Abstr. B, 48 (1988) 2980; DA No. 8729156.
16. J. L. Zuffa, Diss. Abstr. B, 48 (1988) 1168; DA No. 8808516.
17. H. S. Kim, Diss. Abstr. B, 48 (1988) 2967; DA No. 8728356.
18. R. Shojaie, Diss. Abstr. B, 48 (1988) 2969; DA No. 8727747.
19. M. W. Payne, Diss. Abstr. B, 48 (1988) 2645; DA No. 8726708.

20. T. P. Duggan, *Diss. Abstr. B*, 48 (1988) 2966; DA No. 8727693.
21. L. C. Hasselbring, *Diss. Abstr. B*, 49 (1988) 1287; DA No. 8808039.
22. G. D. VanderVelde, *Diss. Abstr. B*, 49 (1988) 110; DA No. 8803226.
23. J. D. Mangold, *Diss. Abstr. B*, 49 (1988) 108; DA No. 8802112.
24. T. J. Hass, *Diss. Abstr. B*, 48 (1988) 2966; DA No. 8728873.
25. J. C. Wang, *Diss. Abstr. B*, 49 (1988) 1697, DA No. 8811442.
26. D. W. Krassowski, *Diss. Abstr. B*, 48 (1988) 3281; DA No. 8724236.
27. S. C. Hockett, *Diss. Abstr. B*, 49 (1988) 405; DA No. 8805084.
28. J. P. Collman, J. I. Brauman, J. P. Fitzgerald, P. D. Hampton, Y. Naruta, J. W. Sparapany, J. A. Ibers, *J. Am. Chem. Soc.* 110 (1988) 3477-3486.
29. J. P. Collman, J. I. Brauman, J. P. Fitzgerald, J. W. Sparapany, J. A. Ibers, *J. Am. Chem. Soc.* 110(1988) 3486-3494.
30. A. L. Balch, Y. W. Chan, M. M. Olmstead, M. W. Renner, F. E. Wood, *J. Am. Chem. Soc.* 110 (1988) 3897-3902.
31. C. M. Che, W. C. Chung, T. F. Lai, *Inorg. Chem.* 27 (1988) 2801-2804.
32. M. J. Camenzind, B. R. James, D. Dolphin, J. W. Sparapany, J. A. Ibers, *Inorg. Chem.* 27 (1988) 3054-3057.
33. B. R. James, A. Pacheco, S. J. Rettig, J. A. Ibers, *Inorg. Chem.* 27 (1988) 2414-2421.
34. C. Crotti, C. Sishta, A. Pacheco, B. R. James, *Inorg. Chim. Acta* 141 (1988) 13-15.
35. N. J. Boldt, K. E. Goodwill, D. F. Bocian, *Inorg. Chem.* 27 (1988) 1188-1191.
36. D. R. Paulson, S. B. Bhakta, R. Y. Hyun, M. Yuen, C. E. Beard, S. C. Lee, I. Kim, J. Ybarra, Jr., *Inorg. Chim. Acta* 144 (1988) 213-216.
37. K. Rachlewicz, L. Latos-Grazynski, *Inorg. Chim. Acta* 144 (1988) 213-216.
38. A. Bettelheim, D. Ozer, R. Harth, R. W. Murray, *J. Electroanal. Chem., Interfacial Electrochem.* 246 (1988) 139-154.
39. L. M. A. Levine, D. Holten, *J. Phys. Chem.* 92 (1988) 714-720.
40. J. Rodriguez, L. McDowell, D. Holten, *Chem. Phys. Lett.* 147 (1988) 235-240.
41. J. H. Holloway, G. Stranger, E. G. Hope, W. Levason, J. S. Ogden, *J. Chem. Soc., Dalton Trans.* (1988) 1341-1345.
42. E. Alessio, G. Mestroni, G. Nardin, W. M. Attia, M. Calligaris, G. Sava, S. Zorzet, *Inorg. Chem.* 27 (1988) 4099-4106.
43. C. C. Hinckley, M. Matusz, P. D. Robinson, *Acta Cryst.* C44 (1988) 371-372.
44. P. D. Robinson, C. C. Hinckley, M. Matusz, P. A. Kibala, *Acta Cryst.* C44 (1988) 619-621.
45. G. R. Clark, K. Marsden, C. E. F. Rickard, W. R. Roper, L. J. Wright, *J. Organomet. Chem.* 338 (1988) 393-410.
46. P. A. Harding, S. D. Robinson, K. Henrick, *J. Chem. Soc., Dalton Trans.* (1988) 415-420.
47. A. Romero, A. Santos, A. Vegas, *Organometallics* 7 (1988) 1988-1993.
48. M. I. Bruce, A. Catlow, M. G. Humphrey, G. A. Koutsantonis, M. R. Snow, E. R. Tiekink, *J. Organomet. Chem.* 338 (1988) 59-80.
49. K. A. Kubat-Martin, G. J. Kubas, R. R. Ryan, *Organometallics* 7 (1988) 1657-1659.
50. A. R. Siedle, R. A. Newmark, G. A. Korba, L. H. Pignolet, P. D. Boyle, *Inorg. Chem.* 27 (1988) 1593-1598.
51. C. Ammann, F. Isaia, P. S. Pregosin, *Magn. Reson. Chem.* 26 (1988) 236-238.

52. T. Arliguie, B. Chaudret, R. H. Morris, A. Sella, Inorg. Chem. 27 (1988) 598-599..
53. M. T. Bautista, K. A. Earl, R. H. Morris, Inorg. Chem. 27 (1988) 1126-1128.
54. M. T. Bautista, K. A. Earl, P. A. Maltby, R. H. Morris, C. T. Schweitzer, A. Sella, J. Am. Chem. Soc. 110 (1988) 7031-7036.
55. M. T. Bautista, K. A. Earl, P. A. Maltby, R. H. Morris, J. Am. Chem. Soc. 110 (1988) 4056-4057.
56. R. J. Kulawiec, R. H. Crabtree, Organometallics 7 (1988) 1891-1893.
57. T. Ohta, H. Takaya, R. Noyori, Inorg. Chem. 27 (1988) 566-569.
58. J. R. Bleeke, D. J. Rauscher, Organometallics 7 (1988) 2328-2339.
59. L. Weber, E. Lucke, R. Boese, Organometallics 7 (1988) 978-983.
60. D. W. Krassowski, J. H. Nelson, K. R. Brower, D. Havenstein, R. A. Jacobson, Inorg. Chem. 27 (1988) 4294-4307.
61. D. W. Krassowski, K. Reimer, H. E. LeMay, Jr., J. H. Nelson, Inorg. Chem. 27 (1988) 4307-4309.
62. A. L. Balch, M. M. Olmstead, P. E. Reed, Jr., S. P. Rowley, Inorg. Chem. 27 (1988) 4289-4294.
63. L. F. Rhodes, C. Sorato, L. M. Venanzi, F. Bachechi, Inorg. Chem. 27 (1988) 604-610.
64. R. A. Leising, J. J. Grzybowski, K. J. Takeuchi, Inorg. Chem. 27 (1988) 1020-1025.
65. M. Antberg, L. Dahlenburg, K. M. Frosin, N. Hock, Chem. Ber. 121 (1988) 859-863.
66. L. Dahlenburg, K. M. Frosin, Chem. Ber. 121 (1988) 865-869.
67. M. M. Taqui-Khan, M. K. Nazeeruddin, Inorg. Chim. Acta 147 (1988) 33-43.
68. M. M. Taqui-Khan, E. R. Rao, Polyhedron 7 (1988) 29-36.
69. H. E. Toma, P. S. Santos, A. Bolanos, J. Chem. Res., Synop. (1988) 124-125.
70. Y. M. Wu, C. Zou, M. S. Wrighton, Inorg. Chem. 27 (1988) 3039-3044.
71. G. Cardaci, G. Reichenbach, G. Bellachioma, B. Wassink, M. S. Baird, Organometallics 7 (1988) 2475-2479.
72. M. Abed, I. Goldberg, Z. Stein, Y. Shvo, Organometallics 7 (1988) 2054-2057.
73. J. Huang, K. Hedberg, R. K. Pomeroy, Organometallics 7 (1988) 2049-2053.
74. A. O. Baghlaif, M. Ishaq, S. A. Rahman, A. B. Al-Tahir, A. Zaidan, R. A. Kabli, Polyhedron 7 (1988) 219-221.
75. P. D. Robinson, C. C. Hinckley, A. Ikuo, Acta Cryst. C44 (1988) 1491-1492.
76. T. J. Collins, J. T. Keech, J. Am. Chem. Soc. 110 (1988) 1162-1167.
77. D. S. Bohle, C. E. F. Rickard, W. R. Roper, Angew. Chem. Int. Ed. Eng. 27 (1988) 302-304.
78. S. L. Soong, J. H. Hain, Jr., M. Millar, S. A. Koch, Organometallics 7 (1988) 556-557.
79. I. Rapaport, L. Helm, A. E. Merbach, P. Bernhard, A. Ludi, Inorg. Chem. 27 (1988) 873-879.
80. M. M. Taqui-Khan, G. Ramachandraiah, R. S. Shukla, Inorg. Chem. 27 (1988) 3274-3278.
81. D. Cruz-Garritz, S. Gelover, H. Torrens, J. Leal, R. L. Richards, J. Chem. Soc., Dalton Trans. (1988) 2393-2396.
82. M. Herberhold, A. F. Hill, J. Chem. Soc., Dalton Trans. (1988) 2027-2031.
83. T. Kobayashi, Y. Nishina, K. Shimizu, G. P. Sato, Chem. Lett. (1988) 1137-1140.
84. H. Doine, T. W. Swaddle, Inorg. Chem. 27 (1988) 665-670.

85. H. Matsuzawa, Y. Ohashi, Y. Kaizu, H. Kobayashi, Inorg. Chem. 27 (1988) 2981-2985.
86. N. Bag, G. K. Lahiri, S. Bhattacharya, L. R. Falvello, A. Chakravorty, Inorg. Chem. 27 (1988) 4396-4402.
87. L. Heerman, H. van Nijen, M. D'Olieslager, Inorg. Chem. 27 (1988) 4320-4323.
88. D. Sellmann, O. Kappler, Angew. Chem. Int. Ed. Engl. 27 (1988) 689-691.
89. D. Sellmann, F. Knoch, C. Wronna, Angew. Chem. Int. Ed. Engl. 27 (1988) 691-692.
90. A. E. D. McQueen, A. J. Blake, T. A. Stephenson, M. Schroder, L. J. Yellowlees, J. Chem. Soc., Chem. Commun. (1988) 1533-1535.
91. K. Buetje, W. Preetz, Z. Naturforsch. 43B (1988) 371-381.
92. K. Buetje, W. Preetz, Z. Naturforsch. 43B (1988) 382-388.
93. H. E. Bryndza, W. Tam, Chem. Rev. 88 (1988) 1163-1188.
94. B. Banas, Acta Chim. Hung. 125 (1988) 17-22.
95. C. Sartori, W. Preetz, Z. Naturforsch., Phys. Sci. 43A (1988) 239-247.
96. M. O. Elout, W. G. Haije, W. J. A. Maaskant, Inorg. Chem. 27 (1988) 610-614.
97. C. M. Che, W. K. Cheng, T. C. W. Mak, Inorg. Chem. 27 (1988) 250-253.
98. Y. Sasaki, M. Suzuki, A. Tokiwa, M. Ebihara, T. Yamaguchi, C. Kabuto, T. Ito, J. Am. Chem. Soc. 110 (1988) 6251-6252.
99. M. M. Taqui-Khan, A. Hussain, K. Venkatasubramanian, G. Ramachandriah, V. Oomen, J. Mol. Catal. 44 (1988) 117-127.
100. M. M. Taqui-Khan, H. C. Bajaj, M. R. H. Siddiqui, J. Mol. Catal. 44 (1988) 279-283.
101. W. D. Harman, M. Sekine, H. Taube, J. Am. Chem. Soc. 110 (1988) 2439-2445.
102. W. D. Harman, H. Taube, J. Am. Chem. Soc. 110 (1988) 5403-5407.
103. W. D. Harman, M. Sekine, H. Taube, J. Am. Chem. Soc. 110 (1988) 5725-5731.
104. W. D. Harman, H. Taube, J. Am. Chem. Soc. 110 (1988) 7906-7907.
105. W. D. Harman, H. Taube, J. Am. Chem. Soc. 110 (1988) 7555-7557.
106. P. A. Lay, R. H. Magnuson, H. Taube, Inorg. Chem. 27 (1988) 2364-2371.
107. P. A. Lay, R. H. Magnuson, H. Taube, Inorg. Chem. 27 (1988) 2848-2853.
108. W. D. Harman, H. Taube, Inorg. Chem. 27 (1988) 3261-3262.
109. M. Sekine, W. D. Harman, H. Taube, Inorg. Chem. 27 (1988) 3604-3608.
110. D. M. Bryan, S. D. Pell, R. Kumar, M. J. Clarke, V. Rodriguez, M. Sherban, J. Charkoudian, J. Am. Chem. Soc. 110 (1988) 1498-1506.
111. M. J. Akhtar, A. Haim, Inorg. Chem. 27 (1988) 1608-1610.
112. K. Lu, J. F. Ojo, J. E. Earley, Inorg. Chem. 27 (1988) 2325-2330.
113. A. Burewicz, A. Haim, Inorg. Chem. 27 (1988) 1611-1614.
114. M. G. Elliot, R. E. Shephard, Inorg. Chem. 27 (1988) 3332-3337.
115. W. Preetz, K. Buetje, Z. Anorg. Allg. Chem. 557 (1988) 112-122.
116. J. K. Beattie, P. Del Favero, T. W. Hambley, N. S. Hush, Inorg. Chem. 27 (1988) 2000-2002.
117. M. L. Bento, E. Tfouni, Inorg. Chem. 27 (1988) 3410-3413.
118. J. C. do Nascimento Filho, J. M. De Rezende, B. D. S. Lime Neto, D. W. Franco, Inorg. Chim. Acta 145 (1988) 111-115.
119. A. Vogler, H. Kunkely, Inorg. Chim. Acta 144 (1988) 149-150.

120. C. K. Che, T. F. Lai, K. Lau, T. C. W. Mak, J. Chem. Soc., Dalton Trans. (1988) 239-241.
121. M. R. Rhodes, T. J. Meyer, Inorg. Chem. 27 (1988) 4772-4774.
122. S. Zhang, R. E. Shepherd, Inorg. Chem. 27 (1988) 4712-4719.
123. M. C. Berjef, R. van Eldik, Inorg. Chem. 27 (1988) 4052-4055.
124. F. Bernhardt, A. M. Sargason, F. C. Anson, Inorg. Chem. 27 (1988) 2754-2760.
125. F. Bernhardt, A. M. Sargason, Inorg. Chem. 27 (1988) 2582-2587.
126. R. Schmidt, J. Straube, Z. Naturforsch. 54b (1988) 533-539.
127. S. F. Olsson, S. S. Robinson, Polyhedron 7 (1988) 455-456.
128. S. F. Olsson, S. S. Robinson, Inorg. Chim. Acta 149 (1988) 15-14.
129. A. Vogler, H. Kunkely, Inorg. Chim. Acta 150 (1988) 3-4.
130. G. Pneumatikakis, A. Pannopoulos, J. Markopoulos, Inorg. Chim. Acta 151 (1988) 243-248.
131. R. E. Stevens, D. E. Fjare, W. L. Gladfelter, J. Organomet. Chem. 347 (1988) 373-381.
132. A. R. Butler, A. M. Calsy-Harrison, C. Glidewell, I. L. Johnson, Inorg. Chim. Acta 146 (1988) 187-191.
133. P. A. Shapley, N. Zhang, Inorg. Chem. 27 (1988) 976-977.
134. P. A. Shapley, H. S. Kim, S. R. Wilson, Organometallics 7 (1988) 928-933.
135. N. Zhang, S. R. Wilson, P. A. Shapley, Organometallics 7 (1988) 1126-1131.
136. Y. Kamata, E. Miki, R. Hirota, K. Mizumachi, T. Ishimori, Bull. Chem. Soc. Jpn. 61 (1988) 594-596.
137. H. Kamata, Y. Konishi, Y. Kamata, E. Miki, K. Mizumachi, T. Ishimori, T. Nagai, M. Tanaka, Chem. Lett. (1988) 159-162.
138. H. Nishimura, H. Nagao, P. S. Howell, M. Mukaida, H. Kakihana, Chem. Lett. (1988) 491-494.
139. R. Figge, U. Patt-Siebel, E. Conradi, U. Mueller, K. Dehnicke, Z. Anorg. Allg. Chem. 558 (1988) 107-113.
140. A. K. Deb, P. C. Paul, S. Goswami, J. Chem. Soc., Dalton Trans. (1988) 2051-2054.
141. T. Bao, K. Krause, R. A. Krause, Inorg. Chem. 27 (1988) 759-761.
142. R. Hage, R. Prins, R. A. G. de Graaf, J. G. Haasnoot, J. Reedijk, J. G. Vos, Acta Cryst. C44 (1988) 56-58.
143. P. K. L. Chan, P. K. H. Chan, D. C. Frost, B. R. James, K. A. Skov, Can. J. Chem. 66 (1988) 117-122.
144. T. M. M. Khan, S. Srivastava, Polyhedron 7 (1988) 1063-1065.
145. A. G. Albertin, S. Antoniutti, G. Pelizzi, F. Vitali, E. Bordignon, Inorg. Chem. 27 (1988) 829-835.
146. N. V. Vugman, V. K. Jain, Rev. Roum. Phys. 33 (1988) 981-993.
147. F. R. Saana, K. R. Snow, P. J. Stephenson, E. R. T. Tiekink, Inorg. Chem. 27 (1988) 2040-2045.
148. E. Garcia, J. Cook, A. J. Bari, Inorg. Chem. 27 (1988) 4377-4382.
149. U. G. Wige, E. W. Kristiansen, K. R. Osaki, E. K. Wightman, Anal. Chem. 60 (1988) 306-310.
150. M. Morita, Y. Tanaka, K. Tanaka, F. Matsuda, T. Matsumura-Inoue, Bull. Chem. Soc. Jpn. 61 (1988) 2711-2714.
151. K. Inoue, S. Hagi, C. Iwakura, K. Yonayama, J. Electroanal. Chem., Interfacial Electrochem. 249 (1988) 133-141.
152. S. G. Farina, W. Yuey, C. Ambrose, P. E. Hoggard, Inorg. Chim. Acta 148 (1988) 97-100.
153. G. Ferraudi, G. A. Arguello, Inorg. Chim. Acta 144 (1988) 53-55.
154. F. Bolletta, L. DeCola, M. Ciano, V. Balzani, Gazz. Chim. Ital. 118 (1988) 327-331.
155. E. Krausz, Comm. Inorg. Chem. 7 (1988) 139-158.
156. P. K. Mallick, G. D. Danzer, D. P. Strommen, J. R. Kincaid, J. Phys. Chem. 92 (1988) 5628-5634.

157. K. Brettel, E. Schlodder, Rev. Sci. Instrum. 59 (1988) 670-671.
158. C. Chiorboli, M. T. Indelli, M. A. Rampi-Scandola, F. Scandola, J. Phys. Chem. 92 (1988) 156-163.
159. M. Z. Hoffman, J. Phys. Chem. 92 (1988) 3458-3464.
160. M. Fujihira, K. Aoki, Proc. Electrochem. Soc. 88 (1988) 280-286.
161. M. Furue, N. Kuroda, S. Sano, J. Macromol. Sci., Chem. A25 (1988) 1263-1274.
162. J. S. Krueger, J. E. Mayer, T. E. Mallouk, J. Am. Chem. Soc. 110 (1988) 8232-8234.
163. M. Inoue, R. Cedeno, Inorg. Chim. Acta 145 (1988) 117-120.
164. L. DeCola, F. Barigelletti, V. Balzani, P. Belser, A. von Zelewsky, F. Vogtle, F. Ebmeyer, S. Grammenudi, J. Am. Chem. Soc. 110 (1988) 7210-7212.
165. L. F. Cooley, C. E. L. Headford, C. M. Elliott, D. F. Kelley, J. Am. Chem. Soc. 110 (1988) 6673-6682.
166. S. R. Johnson, T. D. Westmoreland, J. V. Caspar, K. R. Barqawi, T. J. Meyer, Inorg. Chem. 27 (1988) 3195-3200.
167. N. P. Ayala, J. N. Demas, B. A. DeGraff, J. Am. Chem. Soc. 110 (1988) 1523-1529.
168. E. M. Kober, J. V. Caspar, B. P. Sullivan, T. J. Meyer, Inorg. Chem. 27 (1988) 4587-4598.
169. R. H. Herber, G. Nan, Inorg. Chem. 27 (1988) 2644-2647.
170. G. Orellana, G. A. Iberra, J. Santoro, Inorg. Chem. 27 (1988) 1025-1030.
171. A. B. P. Lever, P. R. Auburn, E. S. Dodsworth, M. A. Haga, W. Liu, M. Melnik, W. A. Nevin, J. Am. Chem. Soc. 110 (1988) 8076-8084.
172. A. Juris, S. Campagna, V. Balzani, G. Gremaud, A. von Zelewsky, Inorg. Chem. 27 (1988) 3652-3655.
173. A. von Zelewsky, G. Gremaud, Helv. Chim. Acta 71 (1988) 1108-1115.
174. V. Palaniappan, U. C. Agarwala, Inorg. Chem. 27 (1988) 3568-3574.
175. R. Sahai, L. Morgan, D. P. Rillema, Inorg. Chem. 27 (1988) 3495-3500.
176. R. M. Berger, D. R. McMillin, Inorg. Chem. 27 (1988) 4245-4249.
177. R. A. Leising, J. S. Ohman, K. J. Takeuchi, Inorg. Chem. 27 (1988) 3804-3809.
178. J. Chang, S. Meyerhoffer, L. R. Allen, B. Durham, J. L. Walsh, Inorg. Chem. 27 (1988) 1602-1607.
179. L. R. Allen, D. Y. Jeter, A. W. Cordes, B. Durham, Inorg. Chem. 27 (1988) 3880-3885.
180. R. Hage, A. H. J. Dijkhuis, J. G. Haasnoot, R. Prins, J. Reedijk, B. E. Buchanan, J. G. Vos, Inorg. Chem. 27 (1988) 2185-2189.
181. M. R. M. Bruce, E. Megehee, B. P. Sullivan, H. Thorp, T. R. O'Toole, A. Downard, T. J. Meyer, Organometallics 7 (1988) 238-240.
182. M. T. Indelli, C. A. Bignozzi, A. Marconi, F. Scandola, J. Am. Chem. Soc. 110 (1988) 7381-7386.
183. V. Palaniappan, S. Sathiah, H. D. Bist, V. C. Agarwala, J. Am. Chem. Soc. 110 (1988) 6403-6410.
184. J. C. Dobson, B. P. Sullivan, P. Doppelt, T. J. Meyer, Inorg. Chem. 27 (1988) 3863-3866.
185. P. Liska, N. Vlachopoulos, M. K. Nazeeruddin, P. Comie, M. Gratzel, J. Am. Chem. Soc. 110 (1988) 3686-3687.
186. D. J. Stufkens, Th. L. Snoeck, A. B. P. Lever, Inorg. Chem. 27 (1988) 953-956.
187. C. V. Kumar, J. K. Barton, I. R. Gould, N. J. Turro, J. Van Houten, Inorg. Chem. 27 (1988) 648-651.

188. R. Kroener, M. J. Heeg, E. Deutsch, Inorg. Chem. 27 (1988) 558-566.
189. M. T. Stershic, L. K. Keefar, B. P. Sullivan, T. J. Meyer, J. Am. Chem. Soc. 110 (1988) 6884-6885.
190. K. R. Bargawi, A. Llobet, T. J. Meyer, J. Am. Chem. Soc. 110 (1988) 7751-7759.
192. L. De Cola, F. Barigelletti, M. J. Cook, Helv. Chim. Acta 71 (1988) 733-741.
192. R. H. Schmelz, R. A. Auerbach, W. F. Wacholts, J. Phys. Chem. 92 (1988) 6202-6026.
193. T. B. Hadda, H. Le Bozec, Polyhedron 7 (1988) 575-577.
194. A. Juris, V. Balzani, F. Barigelletti, S. Campagna, P. Belser, A. von Zelewsky, Coord. Chem. Rev. 84 (1988) 85-277.
195. C. A. Bignozzi, C. Paradisi, S. Roffia, F. Scandola, Inorg. Chem. 27 (1988) 408-414.
196. N. E. Katz, C. Creutz, N. Sutin, Inorg. Chem. 27 (1988) 1687-1694.
197. A. Basu, T. G. Kasar, N. Y. Sapre, Inorg. Chem. 27 (1988) 4539-4542.
198. S. Tachiyashiki, N. Nagao, K. Mizumachi, Chem. Lett. (1988) 1001-1004.
199. A. J. Blake, A. Mca Marr, D. W. H. Rankin, M. Schroder, Acta Cryst. C44 (1988) 935-936.
200. G. DeMunno, G. Denti, G. De Rosa, G. Bruno, Acta Cryst. C44 (1988) 1193-1196.
201. T. S. Akasheh, D. Marji, Z. M. Al-Ahmed, Inorg. Chim. Acta 141 (1988) 125-130.
202. N. C. Thomas, J. Cox, Polyhedron 7 (1988) 731-735.
203. N. Kitamura, M. Sato, H. B. Kim, R. Obata, S. Tazuke, Inorg. Chem. 27 (1988) 651-658.
204. A. Kirsch-De Mesmaeker, L. Jacquet, J. Nasielski, Inorg. Chem. 27 (1988) 4451-4458.
205. N. C. Thomas, B. L. Foley, A. L. Rheingold, Inorg. Chem. 27 (1988) 3426-3429.
206. A. Llobet, P. Doppelt, T. J. Meyer, Inorg. Chem. 27 (1988) 514-520.
207. C. W. Lee, J. Guyang, A. J. Bard, J. Electroanal. Chem. Interfacial Electrochem. 244 (1988) 319-324.
208. A. B. P. Lever, P. Seymour, P. R. Auburn, Inorg. Chim. Acta 145 (1988) 43-48.
209. A. Mills, E. Dodsworth, G. Williams, Inorg. Chim. Acta 138 (1988) 101-106.
210. G. Mulazzani, M. Vencuri, M. E. Hurlman, Radiat. Phys. Chem. 32 (1988) 71-78.
211. J. Gonzalez-Velasco, J. Phys. Chem. 92 (1988) 2202-2207.
212. R. E. Toma, P. S. Santos, A. B. P. Lever, Inorg. Chem. 27 (1988) 3850-3853.
213. R. L. Blackburn, J. T. Rupp, J. Phys. Chem. 92 (1988) 2817-2820.
214. S. S. Isled, A. Vassilian, J. F. Wishart, C. Creutz, H. A. Schwarz, N. Sutin, J. Am. Chem. Soc. 110 (1988) 635-637.
215. R. A. Leising, K. J. Takeuchi, J. Am. Chem. Soc. 110 (1988) 4079-4080.
216. M. R. Torres, A. Perales, J. Ros, Organometallics 7 (1988) 1223-1224.
217. V. Guerschais, C. Lapinte, J. Y. Thepot, L. Toupet, Organometallics 7 (1988) 604-612.
218. M. I. Bruce, G. A. Koutsantonis, E. R. T. Tiekink, Acta Cryst. C44 (1988) 1130-1131.
219. H. Lehmkühl, M. Bellenbaum, J. Grundke, H. Mauermann, C. Kruger, Chem. Ber. 121 (1988) 1719-1728.
220. L. J. Johnston, M. C. Baird, J. Organomet. Chem. 358 (1988) 405-409.

221. L. J. Johnston, M. C. Barid, Organometallics 7 (1988) 2469-2475.
222. K. E. Howard, T. B. Rauchfuss, S. R. Wilson, Inorg. Chem. 27 (1988) 1710-1716.
223. J. Amarasekera, T. B. Rauchfuss, S. R. Wilson, J. Am. Chem. Soc. 110 (1988) 2332-2334.
224. B. K. Campion, R. H. Heyn, T. D. Tilley, J. Am. Chem. Soc. 110 (1988) 7558-7560.
225. A. M. Z. Slawin, D. J. Williams, J. Crosby, J. A. Ramsden, C. White, J. Chem. Soc., Dalton Trans. (1988) 2491-2494.
226. A. W. Cordes, M. Draganjac, Acta Cryst. C44 (1988) 363-364.
227. R. M. Moriarty, Y. Y. Ku, U. S. Gill, Organometallics 7 (1988) 660-665.
228. P. G. Gassman, C. H. Winter, J. Am. Chem. Soc. 110 (1988) 6130-6135.
229. R. P. Hughes, J. Robbins, D. J. Robinson, A. L. Rheingold, Organometallics 7 (1988) 2413-2415.
230. M. Wenzel, Y. Wu, J. Labelled Compd. Radiopharm. 25 (1988) 53-61.
231. M. Wenzel, D. Preiss, G. Gunther, J. Labelled Compd. Radiopharm. 25 (1988) 121-131.
232. S. C. Hockett, L. L. Miller, R. A. Jacobson, R. J. Angelici, Organometallics 7 (1988) 686-691.
233. S. C. Hockett, R. J. Angelici, Organometallics 7 (1988) 1491-1500.
234. X. Hu, J. Duchowski, R. K. Pomeroy, J. Chem. Soc., Chem. Commun. (1988) 362-364.
235. W. Klau, E. Buchholz, Angew. Chem. Int. Ed Engl. 27 (1988) 580-581.
236. W. Klau, E. Buchholz, Inorg. Chem. 27 (1988) 3500-3506.
237. T. D. Kim, T. J. McNeese, A. L. Rheingold, Inorg. Chem. 27 (1988) 2554-2555.
238. F. B. McCormick, W. B. Gleason, Acta Cryst. C44 (1988) 603-605.
239. K. Zenkert, H. Werner, Chem. Ber. 121 (1988) 811-813.
240. M. Stebler-Rothlisberger, W. Hummel, P. A. Pittet, H. B. Burgi, A. Ludi, A. E. Merbach, Inorg. Chem. 27 (1988) 1358-1363.
241. R. J. H. Clark, A. J. Hempleman, D. A. Tocher, J. Am. Chem. Soc. 110 (1988) 5968-5972.
242. F. A. Cotton, M. Matusz, Inorg. Chim. Acta 143 (1988) 45-53.
243. R. J. H. Clark, A. J. Hempleman, J. Chem. Soc., Dalton Trans. (1988) 2601-2606.
244. A. J. Deeming, N. P. Randle, P. A. Bates, M. B. Hursthouse, J. Chem. Soc., Dalton Trans. (1988) 2753-2757.
245. V. M. Miskowski, H. B. Gray, Inorg. Chem. 27 (1988) 2501-2506.
246. V. M. Miskowski, T. M. Loehr, H. B. Gray, Inorg. Chem. 27 (1988) 4708-4712.
247. F. A. Cotton, M. Matusz, B. Zhang, Inorg. Chem. 27 (1988) 4368-4372.
248. P. Higgins, G. M. McCann, J. Chem. Soc., Dalton Trans. (1988) 661-667.
249. B. K. Das, A. R. Chakravarty, Polyhedron 7 (1988) 685-687.
250. P. Neubold, K. Wieghardt, B. Nuber, J. Weiss, Angew. Chem. Int. Ed. Engl. 27 (1988) 933-935.
251. S. J. Sherlock, M. Cowie, E. Singleton, M. M. de V. Steyn, Organometallics 7 (1988) 1663-1666.
252. M. Casarin, A. Vittadini, K. Kriese, F. Muller, G. Granozzi, R. Bertocello, J. Am. Chem. Soc. 110 (1988) 1775-1781.
253. A. A. Cherkas, L. H. Randall, S. A. MacLaughlin, G. N. Mott, N. J. Taylor, A. J. Carty, Organometallics 7 (1988) 969-977.

254. A. A. Cherkas, G. N. Mott, R. Granby, S. A. MacLaughlin, J. E. Yule, N. J. Taylor, A. J. Carty, Organometallics 7 (1988) 1115-1121.
255. D. Osella, M. Botta, R. Gobetto, F. Laschi, P. Zanello, Organometallics 7 (1988) 283-288.
256. F. A. Cotton, M. Matusz, J. Am. Chem. Soc. 110 (1988) 5761-5764.
257. S. Gopinathan, S. S. Deshpande, C. Gopinathan, Indian J. Chem. Sect. 27A (1988) 126-128
258. K. L. Lu, Y. C. Lin, M. C. Cheng, Y. Wang, Acta Cryst. C44 (1988) 979-981.
259. R. M. Bullock, R. T. Hembre, J. R. Norton, J. Am. Chem. Soc. 110 (1988) 7868-7870.
260. W. A. Herrmann, E. Herdtweck, A. Schafer, Chem. Ber. 121 (1988) 1907-1911.
261. R. Tannenbaum, Inorg. Chim. Acta 148 (1988) 199-202.
262. A. E. Ogilvy, T. B. Rauchfuss, Organometallics 7 (1988) 1884-1885.
263. H. Suzuki, H. Omori, D. H. Lee, Y. Yoshida, Y. Moro-Oka, Organometallics 7 (1988) 2243-2245.
264. H. Suzuki, H. Omori, Y. Moro-Oka, Organometallics 7 (1988) 2579-2581.
265. C. Hampton, T. W. Dekleva, B. R. James, W. R. Cullen, Inorg. Chim. Acta 145 (1988) 165-166.
266. C. Hampton, W. R. Cullen, B. R. James, J. P. Charland, J. Am. Chem. Soc. 110 (1988) 6918-6919.
267. M. R. Gagne, J. Takats, Organometallics 7 (1988) 561-563.
268. S. Aime, M. Botta, R. Gobetto, D. Osella, J. Chem. Soc., Dalton Trans. (1988) 791-792.
269. S. Aime, M. Botta, R. Gobetto, D. Osella, L. Milone, Inorg. Chim. Acta 146 (1988) 151-152.
270. A. J. Arce, P. A. Bates, S. P. Best, R. J. H. Clark, A. J. Deeming, M. B. Hursthouse, R. C. S. McQueen, N. I. Powell, J. Chem. Soc., Chem. Commun. (1988) 478-480.
271. W. R. Cullen, S. T. Chacon, M. I. Bruce, F. W. B. Einstein, R. H. Jones, Organometallics 7 (1988) 2273-2278.
272. V. V. Krivykh, T. Asunta, O. V. Gusev, M. I. Rybinskaya, J. Organomet. Chem. 338 (1988) 55-58.
273. S. H. Han, G. L. Geoffroy, B. D. Dombek, A. L. Rheingold, Inorg. Chem. 27 (1988) 4355-4361.
274. J. A. Partin, M. G. Richmond, J. Organomet. Chem. 353 (1988) C13-C16.
275. R. Khattar, B. F. G. Johnson, J. Lewis, J. Organomet. Chem. 354 (1988) 221-225.
276. R. Guläner, B. F. G. Johnson, J. Lewis, J. Organomet. Chem. 355 (1988) 419-425.
277. R. A. Kridas, G. R. Kinas, F. V. Petrovskii, W. E. Koldovsk, Y. T. Struchkov, A. I. Yanovsky, J. Organomet. Chem. 338 (1988) 81-87.
278. S. L. Mullen, A. G. Marshall, J. Am. Chem. Soc. 110 (1988) 1766-1774.
279. P. D. Alexiev, J. Evans, A. C. Street, B. Webster, Acta Cryst. C44 (1988) 1186-1189.
280. H. J. Kneuper, D. S. Strickland, J. R. Shapley, Inorg. Chem. 27 (1988) 1110-1111.
281. D. S. Strickland, S. R. Wilson, J. R. Shapley, Organometallics 7 (1988) 1674-1676.
282. J. R. Werner, B. P. Jan, P. D. Getman, R. Moker, S. G. Shore, Inorg. Chem. 27 (1988) 4274-4276.
283. C. E. Housecroft, S. M. Owen, Organometallics 7 (1988) 1385-1390.
284. R. Zoet, G. van Koten, K. Vrieze, J. Jansen, K. Goubitz, C. H. Stam, Organometallics 7 (1988) 1565-1572.

285. D. C. Pribich, E. Rosenberg, Organometallics 7 (1988) 1741-1745.
286. D. M. Skinner, E. Rosenberg, J. Bracker-Novak, S. Aime, D. Osella, R. Gobetto, L. Milone, Organometallics 7 (1988) 856-858.
287. M. J. Sailor, M. Sabat, D. F. Shriver, Organometallics 7 (1988) 728-736.
288. M. J. Sailor, M. J. Went, D. F. Shriver, Inorg. Chem. 27 (1988) 2666-2672.
289. D. F. Shriver, M. J. Sailor, Acc. Chem. Res. 21 (1988) 374-379.
290. R. D. Adams, J. E. Babin, J. Tanner, Organometallics 7 (1988) 765-772.
291. R. D. Adams, J. E. Babin, Organometallics 7 (1988) 963-969.
292. R. D. Adams, J. T. Tanner, Organometallics 7 (1988) 2241-2243.
293. R. D. Adams, J. E. Babin, Organometallics 7 (1988) 2300-2306.
294. K. L. Lu, J. L. Chen, Y. C. Lin, S. M. Peng, Inorg. Chem. 27 (1988) 1726-1730.
295. J. K. Shen, Y. L. Shi, Y. C. Gao, Q. Z. Shi, F. Basolo, J. Am. Chem. Soc. 110 (1988) 2414-2418.
296. J. K. Shen, Y. C. Gao, Q. Z. Shi, F. Basolo, Inorg. Chem. 27 (1988) 4236-4239.
297. M. I. Bruce, M. J. Liddell, C. A. Hughes, B. W. Skelton, A. H. White, J. Organomet. Chem. 347 (1988) 157-180.
298. M. I. Bruce, M. J. Liddell, C. A. Hughes, J. M. Patrick, B. W. Skelton, A. H. White, J. Organomet. Chem. 347 (1988) 181-205.
299. M. I. Bruce, M. J. Liddell, O. bin Shawkataly, C. A. Hughes, B. W. Skelton, A. H. White, J. Organomet. Chem. 347 (1988) 207-235.
300. T. Chin-Choy, N. L. Keder, G. D. Stucky, P. C. Ford, J. Organomet. Chem. 346 (1988) 225-236.
301. M. M. Harding, S. J. Maginn, A. K. Smith, Acta Cryst. C44 (1988) 237-239.
302. W. Radecka-Paryzek, R. J. Puddephatt, Inorg. Chim. Acta 147 (1988) 207-209.
303. D. W. Engel, K. G. Moodley, L. Subramony, R. J. Haines, J. Organomet. Chem. 349 (1988) 393-403.
304. M. Herberhold, K. Schamel, G. Herrmann, A. Gieren, C. Ruiz-Perez, T. Huber, Z. Anorg. Allg. Chem. 562 (1988) 49-61.
305. N. M. J. Brodie, A. J. Poe, Inorg. Chem. 27 (1988) 3156-3159.
306. N. Luqan, J. J. Bonnet, J. A. Ibers, Organometallics 7 (1988) 1538-1545.
307. N. Luqan, G. Lavigne, J. J. Bonnet, R. Reau, D. Neibecker, I. Tkatchenko, J. Am. Chem. Soc. 110 (1988) 5369-5376.
308. A. M. Arif, T. A. Bright, R. A. Jones, C. M. Nunn, J. Am. Chem. Soc. 110 (1988) 6894-6895.
309. J. S. Field, R. J. Haines, D. N. Smit, J. Chem. Soc., Dalton Trans. (1988) 1315-1330.
310. G. Predieri, A. Tiripicchio, C. Vignali, E. Sappa, J. Organomet. Chem. 342 (1988) C33-C37.
311. D. Nucciarone, S. A. MacLaughlin, N. J. Taylor, A. J. Carty, Organometallics 7 (1988) 106-117.
312. D. Nucciarone, N. J. Taylor, A. J. Carty, A. Tiripicchio, M. T. Camellini, E. Sappa, Organometallics 7 (1988) 118-126.
313. D. Nucciarone, N. J. Taylor, A. J. Carty, Organometallics 7 (1988) 127-137.
314. M. A. Gallop, B. F. G. Johnson, J. Lewis, A. McCamley, R. N. Perutz, J. Chem. Soc., Chem. Commun. (1988) 1071-1073.
315. S. J. Wang, R. J. Angelici, Inorg. Chem. 27 (1988) 3233-3235.
316. A. J. Deeming, S. Donovan-Mtunzi, K. I. Hardcastle, S. E. Kabir, K. Henrick, M. McPartlin, J. Chem. Soc., Dalton Trans. (1988) 579-586.

317. A. J. Deeming, K. I. Hardcastle, S. E. Kabir, J. Chem. Soc., Dalton Trans. (1988) 827-831.
318. A. J. Deeming, S. E. Kabir, J. Organomet. Chem. 340 (1988) 359-366.
319. R. A. Bartlett, C. J. Cardin, D. J. Cardin, G. A. Lawless, J. M. Power, P. P. Power, J. Chem. Soc., Chem. Commun. (1988) 312-313.
320. S. H. Han, S. T. Nguyen, G. L. Geoffroy, A. L. Rheingold, Organometallics 7 (1988) 2034-2038.
321. J. A. Cabeza, L. A. Ono, A. Tiripicchio, M. Tiripicchio-Camellini, J. Chem. Soc., Dalton Trans. (1988) 1437-1444.
322. A. J. Arce, C. Acuna, A. J. Deeming, J. Organomet. Chem. 356 (1988) C47-C49.
323. R. Zoet, J. T. B. H. Jastrzebski, G. van Koten, T. Mahabiersing, K. Vrieze, D. Heijdenrijk, C. H. Stam, Organometallics 7 (1988) 2108-2117.
324. R. Zoet, G. van Koten, D. J. Stufkens, K. Vrieze, C. H. Stam, Organometallics 7 (1988) 2118-2123.
325. R. D. Adams, J. E. Babin, M. Tasi, Organometallics 7 (1988) 503-513.
326. G. L. Griewe, M. B. Hall, Inorg. Chem. 27 (1988) 2250-2255.
327. S. S. Kristjansdottir, A. E. Moody, R. T. Weberg, J. R. Norton, Organometallics 7 (1988) 1983-1987.
328. L. H. Polm, W. P. Mul, C. J. Elsevier, K. Vrieze, M. J. N. Christophersen, C. H. Stam, Organometallics 7 (1988) 423-429.
329. J. T. Jaeger, J. S. Field, D. Collison, G. P. Speck, B. M. Peake, J. Hahnle, H. Vahrenkamp, Organometallics 7 (1988) 1753-1760.
330. G. Hogarth, J. A. Phillips, F. van Gestel, N. J. Taylor, T. B. Marder, A. J. Carty, J. Chem. Soc., Chem. Commun. (1988) 1570-1572.
331. L. R. Martin, F. W. B. Einstein, R. K. Pomeroy, Organometallics 7 (1988) 294-304.
332. V. J. Johnston, F. W. B. Einstein, R. K. Pomeroy, Organometallics 7 (1988) 1867-1869.
333. L. R. Martin, F. W. B. Einstein, R. K. Pomeroy, Inorg. Chem. 27 (1988) 2986-2989.
334. J. Puga, A. Arce, R. A. Sanchez-Delgado, J. Ascanio, A. Andriollo, D. Braga, F. Grepioni, J. Chem. Soc., Dalton Trans. (1988) 913-923.
335. S. B. Colbran, B. F. G. Johnson, F. J. Lahoz, J. Lewis, P. R. Raithby, J. Chem. Soc., Dalton Trans. (1988) 1199-1204.
336. R. D. Adams, J. E. Babin, M. Tasi, T. A. Wolfe, J. Am. Chem. Soc. 110 (1988) 7093-7097.
337. S. B. Colbran, F. J. Lahoz, P. R. Raithby, J. Lewis, B. F. G. Johnson, C. J. Cardin, J. Chem. Soc., Dalton Trans. (1988) 173-181.
338. B. F. G. Johnson, R. A. Kamarudin, F. J. Lahoz, J. Lewis, P. R. Raithby, J. Chem. Soc., Dalton Trans. (1988) 1205-1211.
339. L. J. Farrugia, Acta Cryst. C44 (1988) 997-998.
340. R. D. Adams, J. E. Babin, J. T. Tanner, Organometallics 7 (1988) 2027-2033.
341. S. R. Drake, M. H. Barley, B. F. G. Johnson, J. Lewis, Organometallics 7 (1988) 806-812.
342. M. H. Barley, C. E. Ansur, B. F. G. Johnson, J. Lewis, J. Organomet. Chem. 339 (1988) 151-157.
343. S. R. Drake, B. F. G. Johnson, J. Lewis, J. Organomet. Chem. 346 (1988) 105-109.
344. S. R. Drake, B. F. G. Johnson, J. Lewis, J. Chem. Soc., Dalton Trans. (1988) 1517-1522.
345. J. C. Malin, J. D. Boyin, A. Pettford-Long, D. J. Smith, G. Schmid, N. Klein, Angew. Chem. Int. Ed. Engl. 27 (1988) 555-558.

346. C. M. Hay, B. F. G. Johnson, J. Lewis, P. R. Raithby, A. J. Whitton, J. Chem. Soc., Dalton Trans. (1988) 2091-2097.
347. B. F. G. Johnson, J. Lewis, P. R. Raithby, A. J. Whitton, J. Chem. Soc., Chem. Commun. (1988) 401-402.
348. E. Rosenberg, J. Wang, R. W. Gellert, Organometallics 7 (1988) 1093-1100.
349. M. Cazanoue, N. Lugan, J. J. Bonnet, R. Mathieu, Organometallics 7 (1988) 2480-2486.
350. R. D. Adams, J. E. Babin, M. Tasi, Organometallics 7 (1988) 219-227.
351. R. D. Adams, J. E. Babin, M. Tasi, J. G. Wang, Organometallics 7 (1988) 755-764.
352. R. D. Adams, J. E. Babin, M. Tasi, Inorg. Chem. 27 (1988) 2618-2625.
353. H. Bantel, W. Bernhardt, A. K. Powell, H. Vahrenkamp, Chem. Ber. 121 (1988) 1247-1256.
354. H. Matsuzaka, T. Kodama, Y. Uchida, M. Hidai, Organometallics 7 (1988) 1608-1613.
355. L. J. Farrugia, Acta Cryst. C44 (1988) 219-221.
356. W. E. Lindsell, K. J. McCullough, J. Organomet. Chem. 346 (1988) 425-431.
357. P. Sundberg, B. F. G. Johnson, J. Lewis, P. R. Raithby, J. Organomet. Chem. 354 (1988) 131-137.
358. W. E. Lindsell, N. M. Walker, A. S. Boyd, J. Chem. Soc., Dalton Trans. (1988) 675-683.
359. S. S. D. Brown, I. D. Slater, L. Toupet, J. Chem. Soc., Dalton Trans. (1988) 757-767.
360. T. Adatia, P. J. McCarthy, M. McPartlin, M. Rizza, I. D. Salter, J. Chem. Soc., Chem. Commun. (1988) 1106-1108.
361. P. J. McCarthy, I. D. Salter, V. Sik, J. Organomet. Chem. 344 (1988) 411-417.
362. S. S. D. Brown, I. D. Salter, D. B. Dyson, R. V. Parish, P. A. Bates, M. B. Hursthouse, J. Chem. Soc., Dalton Trans. (1988) 1795-1801.
363. S. S. D. Brown, I. D. Salter, V. Sik, I. J. Colquhoun, W. McFarlane, P. A. Bates, M. B. Hursthouse, M. Murray, J. Chem. Soc., Dalton Trans. (1988) 2177-2185.
364. T. Adatia, M. McPartlin, I. D. Salter, J. Chem. Soc., Dalton Trans. (1988) 751-755.
365. B. D. Alexander, M. P. Gomez-Sal, P. R. Gannon, C. A. Blaine, P. D. Boyle, A. M. Mueting, L. H. Pignolet, Inorg. Chem. 27 (1988) 3301-3308.
366. J. B. Keister, C. C. O. Onyeso, Organometallics 7 (1988) 2364-2372.
367. H. B. Davis, F. W. B. Einstein, V. J. Johnston, R. K. Pomeroy, J. Am. Chem. Soc. 110 (1988) 4451-4453.
368. J. T. Park, J. R. Shapley, C. Bueno, J. W. Ziller, M. R. Churchill, Organometallics 7 (1988) 2307-2316.
369. M. R. Churchill, J. C. Fettinger, F. J. Hollander, R. A. Lashewycz-Rubycz, J. Organomet. Chem. 340 (1988) 367-376.
370. R. Shojai, J. D. Atwood, Inorg. Chem. 27 (1988) 2558-2560.
371. P. Ewing, L. J. Farrugia, D. S. Rycroft, Organometallics 7 (1988) 859-870.
372. P. Ewing, L. J. Farrugia, Organometallics 7 (1988) 871-878.
373. L. J. Farrugia, Acta Cryst. C44 (1988) 818-820.
374. L. J. Farrugia, Acta Cryst. C44 (1988) 1307-1309.
375. S. R. Drake, B. F. G. Johnson, J. Lewis, J. Organomet. Chem. 340 (1988) C31-C36.
376. G. C. Bruce, S. R. Stobart, Inorg. Chem. 27 (1988) 3897-3880.
377. J. Stoch, D. Q. Ho, T. Czeppe, Bull. Pol. Acad. Sci., Chem. 36 (1988) 387-391.

378. M. J. Albarelli, J. H. White, G. M. Bommarito, M. McMillan, H. D. Abruna, J. Electroanal. Chem., Interfacial Electrochem. 248 (1988) 77-86.
379. S. Alerasool, D. Boecker, G. Bahman, D. Richard, G. Del Angel, M. Azamosa, R. Gomez, Langmuir 4 (1988) 1083-1090.
380. T. Mizushima, K. Tohji, Y. Udagawa, J. Am. Chem. Soc. 110 (1988) 4459-4460.
381. T. K. Sham, T. Ohta, T. Yokoyama, Y. Kitajima, M. Funabashi, N. Kosugi, H. Kuroda, J. Chem. Phys. 88 (1988) 475-477.
382. Z. Lin, T. Okuhara, M. Misono, J. Chem. Phys. 92 (1988) 723-729.
383. G. C. Grunewald, R. S. Drago, J. Chem. Soc., Chem. Commun. (1988) 1206-1208.
384. L. D'Ornelas, A. Theolier, A. Choplin, J. M. Basset, Inorg. Chem. 27 (1988) 1261-1265.
385. A. Beck, S. Dobos, L. Gucci, Inorg. Chem. 27 (1988) 3220-3226.
386. K. Asakura, Y. Iwasawa, J. Chem. Soc., Faraday Trans. 1 84 (1988) 2445-2456.
387. S. Dobos, I. Boszormenyi, J. Mink, L. Gucci, Inorg. Chim. Acta 144 (1988) 37-45.
388. J. J. Bergmeister, III, B. E. Hanson, J. Organomet. Chem. 352 (1988) 367-372.
389. S. Uchiyama, B. C. Gates, Inorg. Chim. Acta (1988) 65-70.
390. A. S. Fung, P. A. Tooley, M. J. Kelly, B. C. Gates, J. Chem. Soc., Chem. Commun. (1988) 371-372.
391. C. Dossi, A. Fusi, E. Grilli, R. Psaro, R. Ugo, R. Zannoni, Catal. Today 2 (1988) 585-594.
392. J. J. Venter, M. A. Vannice, Appl. Spectrosc. 42 (1988) 1096-1103.
393. Y. Fu, L. Kraus, M. I. Zaki, C. Kappenstein, B. Tesche, H. Knozinger, J. Mol. Catal. 44 (1988) 295-311.
394. L. Hasselbring, J. Puga, C. Dybowski, B. C. Gates, J. Phys. Chem. 92 (1988) 3934-3936.
395. T. H. Walter, G. R. Frauenhoff, J. R. Shapley, E. Oldfield, Inorg. Chem. 27 (1988) 2561-2563.
396. A. Choplin, B. Besson, L. D'Ornelas, R. Sanchez-Delgado, J. M. Basset, J. Am. Chem. Soc. 110 (1988) 2783-2787.
397. F. A. Carter, W. A. Goddard, III, Organometallics 7 (1988) 675-686.
398. D. P. Summers, N. W. Frese, Jr., J. Electrochem. Soc. 135 (1988) 264-265.
399. G. Jenner, J. Organomet. Chem. 345 (1988) 237-252.
400. H. Ishida, K. Tanaka, T. Tanaka, Chem. Lett. (1988) 339-342.
401. D. P. Summers, K. W. Frese, Jr., Langmuir 4 (1988) 51-57.
402. S. Perrier, J. K. Kochi, Inorg. Chem. 27 (1988) 4165-4173.
403. A. M. El-Hendawy, W. P. Griffith, B. Piggott, D. J. Williams, J. Chem. Soc., Dalton Trans. (1988) 1983-1988.
404. M. M. T. Khan, S. A. Mirza, P. A. Rao, C. Sreelatha, J. Mol. Catal. 44 (1988) 107-115.
405. M. Kaneko, R. Ramaraj, A. Kira, Bull. Chem. Soc. Jpn. 61 (1988) 417-421.
406. T. C. Lau, C. M. Che, W. O. Lee, C. K. Poon, J. Chem. Soc., Chem. Commun. (1988) 1406-1407.
407. J. M. Madurro, G. Chiericato, Jr., W. F. DeGiovani, J. R. Romero, Tett. Lett. 29 (1988) 765-768.
408. J. C. Dobson, T. J. Meyer, Inorg. Chem. 27 (1988) 3283-3291.
409. S. J. Raven, T. J. Meyer, Inorg. Chem. 27 (1988) 4478-4483.
410. M. E. Marnion, K. J. Takeuchi, J. Am. Chem. Soc. 110 (1988) 1472-1480.
411. S. A. Kubow, M. E. Marnion, K. J. Takeuchi, Inorg. Chem. 27 (1988) 2761-2767.
412. S. Davis, R. S. Drago, Inorg. Chem. 27 (1988) 4759-4760.

413. M. Bressan, A. Morvillo, J. Chem. Soc., Chem. Commun. (1988) 650-651.
414. J. M. Wallis, J. K. Kochi, J. Org. Chem. 53 (1988) 1679-1686.
415. J. M. Wallis, J. K. Kochi, J. Am. Chem. Soc. 110 (1988) 8207-8223.
416. T. Hayashi, Z. H. Gu, T. Sakakura, M. Tanaka, J. Organomet. Chem. 352 (1988) 373-378.
417. E. P. Giannelis, E. G. Rightor, T. J. Pinnavaia, J. Am. Chem. Soc. 110 (1988) 3880-3885.
418. M. Kleijn, H. P. Van Leeuwen, J. Electroanal. Chem., Interfacial Electrochem. 247 (1988) 253-263.
419. W. Nussbaumer, H. Gruber, G. F. Greber, Monatsh. Chem. 119 (1988) 1-15.
420. J. M. Kleijn, E. Rouwendal, H. P. Van Leeuwen, J. Lyklema, J. Photochem. Photobiol. 44A (1988) 29-50.
421. D. Morton, D. J. Cole-Hamilton, J. Chem. Soc., Chem. Commun. (1988) 1154-1156.